CHARACTERIZATION OF THE NOVEL ROLE OF PARKIN IN GLIOMAGENESIS

YEO WEE SING

M. Sc, NUS

A THESIS SUBMITTED

FOR THE DEGREE OF DOCTOR OF PHILOSOPHY

DEPARTMENT OF PHYSIOLOGY

YONG LOO LIN SCHOOL OF MEDICINE

NATIONAL UNIVERSITY OF SINGAPORE

2011

ACKNOWLEDGEMENTS

My thanks to God for His love so that I could complete this project.

My many sincere thanks, utmost gratitude and appreciation to my supervisor, Associate Professor Lim Kah Leong for his great patience, invaluable guidance, encouragements and wisdom throughout the course my Ph.D. studies, his passion and love for science had greatly changed my view of how difficult but yet satisfying the pursue of science can be.

My thanks to Associate Professor Ang Beng Ti, Dr Carol Tang, for their endless guidance and encouragements in the various aspects of my project particularly the animal work component.

Many thanks to Associate Professor Lim Tit Meng for his many encouragements and support towards my Ph.D. work.

My thanks to the Singapore Millennium Foundation for awarding me a SMF Ph.D. scholarship for my Ph.D. study.

My thanks to Felicia Ng for the tremendously amount of support she has given me for the analysis of the microarray and bioinformatics data.

My thanks to Miss Katherine Chew for all the technical advices and artworks in my thesis.

My thanks to my family, especially my dad and mum for all the encouragements and support they have given me.

My thanks to my church friends and DG friends, Vivian, Yin, Luke, Pei Theng, Wei San, Audrey, Jackie, Karen, Aileen, Ling Hong, David, Evon for the countless encouragements and support.

Many thanks to my past and present labmates (Jeanne, Chee Hoe, Huiyi, Chai Chou Esther, Eugenia, Shiam Peng, Eugenia, Xiao Hui, Hui Mei, Grace, Cheng Wu, Melissa, Saheen, Cherlyn, Zhengshui) and colleagues (Hanchi, Priya, Irene, Alex, Kok Poh, Dr Liao Ping, Lydiana, Tan Boon, Yuk Kien, Lynette, Charlene, Geraldine, Esther, Kimberly, Joan, Bryce, Zhirong) at the National Neuroscience Institute for all the encouragements, support, wonderful discussions and meals we had together.

Yeo Wee Sing, Calvin
2011
"Trust in the LORD with all your heart
and lean not on your own understanding;
in all your ways submit to him,
and he will make your paths straight." Proverbs 3:5-6

TABLE OF CONTENTS

LIST OF FIGURES

LIST OF TABLES

A**BBREVIATIONS**

ATP	Adenosine Triphosphate
CDK	Cyclin-dependent kinase
CSF	Cerebral-spinal fluid
DMEM	Dulbecco's Modified Eagle's Medium
DMSO	Dimethyl sulfoxide
EGFR	Epidermal growth factor receptor
ERK	Extracellular signal-regulated kinase
FAK	Focal adhesion kinase
FGFR	Fibroblast growth factor receptor
GBM	Glioblastoma multiforme
GFAP	Glial fibrillary acidic protein
HNRNPK	Heterogeneous nuclear ribonucleoprotein K
HSP	Heat Shock Protein
JMY	Junction-mediating and regulatory protein
LPS	Lipopolysaccharide
MAPK	Mitogen-activated protein kinase
MMP	Matrix metalloproteinases
MRI	Magnetic resonance imaging
OLIG2	Oligodendrocyte transcription factor 2
PDCD4	Programmed cell death 4
PDGFR	Platelet-derived growth factor receptor
PTEN	Phosphatase and tensin homolog
RB	Retinoblastoma
RING	Really Interesting New Gene
RTK	Receptor tyrosine kinase

SDS-PAGE	Sodium dodecyl sulfate polyacrylamide gel electrophoresis
TP53BP2	Tumor protein p53 binding protein 2
TPM1	Tropomyosin 1
VEGFR	Vascular endothelial growth factor receptor

SUMMARY

Parkin was originally discovered as a gene whose mutations are causative of familial parkinsonism. However, numerous subsequent evidences suggest that parkin also plays a role in the progression and development of a variety of cancer.

In this thesis, I investigated the potential role of parkin in gliomagenesis and showed that parkin expression is dramatically reduced in glioma cells. I further showed that restoration of parkin expression in these cells promotes their arrest at G1 phase and significantly mitigates their proliferation rate both in vitro and in vivo. Notably, the level of cyclin D1, but not cyclin E, is reduced in parkin-expressing glioma cells. Moreover, parkin expression also leads to a selective downregulation of Akt serine-473 phosphorylation and VEGF receptor 2 levels. Supporting this, cells derived from parkin null mouse exhibit increased levels of cyclin D1, VEGF receptor 2 and Akt phosphorylation and divide significantly faster compared to their wild type counterparts, all of which are suppressed following the re-introduction of parkin into these cells. However, parkin-mediated effects on these components is dependent on its catalytic competency as a catalytically null parkin mutant failed to influence the expression of cyclin D1, phospho-Akt and VEGF receptor. Interestingly, parkin expression also leads to the downregulation of two oncogenic microRNAs namely miR-21 and miR-155. Importantly, analysis of parkin pathway activation revealed its predictive power for survival outcome of glioma patients.

Taken together, my study provides a mechanism by which parkin exerts its tumor suppressor function and a signature pathway of parkin that is of potential prognostic value.

CHAPTER 1

INTRODUCTION

1.1 Gliomas

Gliomas are cancer of the glial cells and are among the most difficult cancers to treat because of the limited selection of anticancer drugs that could permeate through the blood brain barrier to reach the tumors. Although gliomas are considered as a rare disease with an incidence rate of about 1-2% as compared to other types of cancer, there is a high rate of recurrence even after complete surgical removal of the tumor. In addition to this, the median rate of survival of malignant glioma is usually about 12 months (Maher et al., 2001). Thus, it is important to understand the disease better in order to treat it more effectively. Broadly, gliomas include astrocytomas, ependymomas, medulloblastomas, meningiomas, oligodendrogliomas and pituitary adenomas. Astrocytomas are glial tumors derived from the star-shaped glial cells that are normally involved in several vital processes including neurotransmitter uptake and release, vasomodulation, and modulation of synaptic transmission (Kanu et al., 2009). Ependymomas are derived from cuboidal ependymal cells which line the cerebrospinal fluid (CSF)-filled ventricles in the brain and the central canal of the spinal cord (Gilbert et al., 2010), whereas oligodendrogliomas are derived from myelin forming cells of the central nervous system (Wen et al., 2008). Medulloblastomas are usually located around the region from the cerebellum to brain stem and they represent about 20% pediatric and adult brain tumors. Meningiomas are tumors that develop in the meninges covering the central

nervous system and it accounts for about 25% of all primary brain tumors. Finally, pituitary adenomas are usually benign tumors of the pituitary gland and they represent about 10% of all primary brain tumors.

1.2 Glioma Prevalence and Epidemiology

The annual incidence of malignant gliomas is approximately 5 cases per 100,000 people (Louis et al., 2007). Malignant gliomas refers to the metastatic gliomas which are the WHO classified grade III and IV gliomas. The most malignant type of glioma, glioblastoma multiforme (GBM) accounts for about 50% of malignant gliomas. Other forms of malignant gliomas include astrocytomas and oligodendrogliomas, which together account for about 34% of all gliomas. The remaining 5-10% consists of less common tumors such as anaplastic ependymomas and gangliogliomas (Louis et al., 2007) (Fig. 1.1). The word "anaplastic" refers to dedifferentiation which is a distinctive feature as the cancer progresses to a more advanced stage.

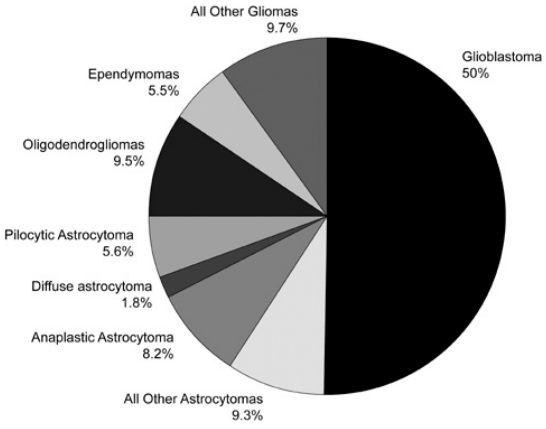

Figure 1.1 Distribution of the different types of gliomas (Graph from Central Brain Tumor Registry of the United States, CBTRUS)

The recorded incidence of gliomas has increased slightly over the past two decades as a result of advances in diagnostic imaging techniques (Fisher et al., 2007). The incidence of malignant gliomas is 40% more common in men as

compared to women and twice as common in Caucasians compared to African populations. The median age of onset in patients at the time of diagnosis is 64 years of age in the case of GBM and 45 years of age in the case of anaplastic gliomas (Fisher et al., 2007). About 5% of patients with malignant gliomas exhibit a family history of gliomas and a portion of these familial cases are associated with rare genetic syndromes, such as Turcot's syndrome, neurofibromatosis type 1 and 2 and the Li-Fraumeni syndrome (Farrell et al., 2007).

1.3 Glioma Clinical Presentation and Imaging

Patients with malignant gliomas may present with a variety of symptoms including headaches, nausea, vomiting, confusion, seizures, memory loss, focal neurological deficits and personality changes. Classical headaches observed in glioma patients are indicative of increased intracranial pressure and are most severe in the morning and may potentially cause insomnia for these patients.

The medical diagnosis of gliomas is usually confirmed by magnetic resonance imaging (MRI) or computed tomography. These glioma imaging studies conventionally show a heterogeneously enhanced mass with edema in the surrounding cavity. In the case of GBMs, there are necrotic regions in the central areas of the tumors and more extensive peritumoral edema compared to anaplastic astrocytomas (Fig. 1.2) (Cha, 2006).

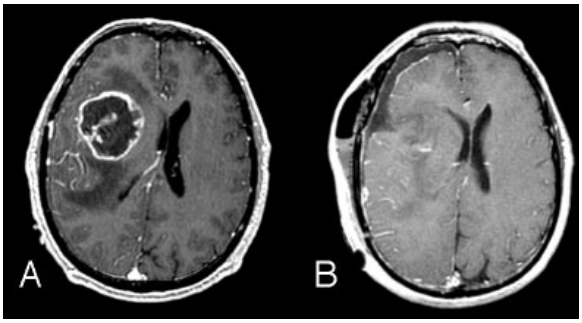

Figure 1.2 MRI scan of a 51-year old man with frontal glioblastoma multiforme which shows a centrally necrotic frontal lobe mass with edema. (A) Pre-operation MRI image. (B) Post-operation MRI image. (Image from Cha, 2006)

MRI techniques like diffusion-weighted imaging (DWI) for tumor grade assessment, dynamic contrast-enhanced MRI to measure blood vessel permeability, perfusion-weighted imaging to measure relative cerebral blood volume are used more frequently as diagnostic aids and for monitoring of response to therapies (Young, 2007). DWI-MRI uses the principle that water diffusivity within the extracellular compartment is inversely related to the cellularity within the extracellular space. The basic principle of DWI-MRI measurement is as follows: the higher the level of cellularity, the lower the water diffusivity through the intracellular spaces between cells and hence a lower apparent diffusion coefficient (ADC). Based on this, DWI-MRI is commonly used to assess tumor grade (Fig. 1.3) and cellularity, post-operative injury, peritumoral edema and integrity of the white matter tract.

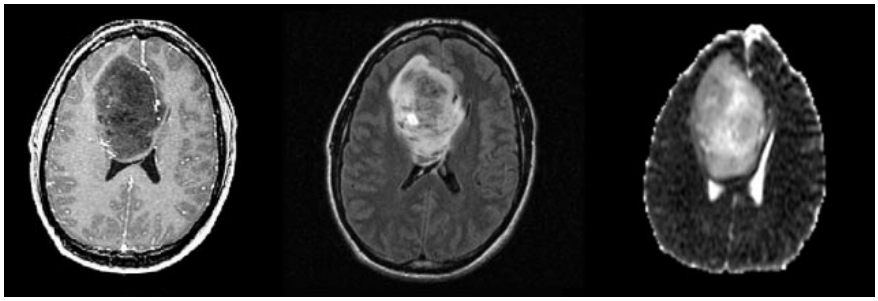

Figure 1.3 DWI scans of different WHO grades astrocytomas. (Left) WHO grade II, Middle) WHO grade III, (Right) WHO grade IV astrocytomas (Image from Cha, 2006).

There is also the use of proton magnetic resonance spectroscopy (^{1}H-MRS) to assist in the detection of the levels of metabolites and that could help to differentiate proliferating tumors from benign and necrotic lesions. For this imaging technique, samples from malignant glioma would show an increase in the choline peak and a decrease in the N-acetyl aspartate peak as compared to unaffected areas of the brain (Fig. 1.4A). These metabolites level changes have

moderate to high sensitivity (64%-95%) and high specificity (82%-100%) for identifying actively dividing tumors. In addition, the corresponding increase in lactate, an end-product of nonoxidative glycolysis in regions of tumors may correlate with hypoxia within the tumor tissues. However, this technique is not able to distinguish between malignant and benign tumors (Fig. 1.4B) (Allen, 1972).

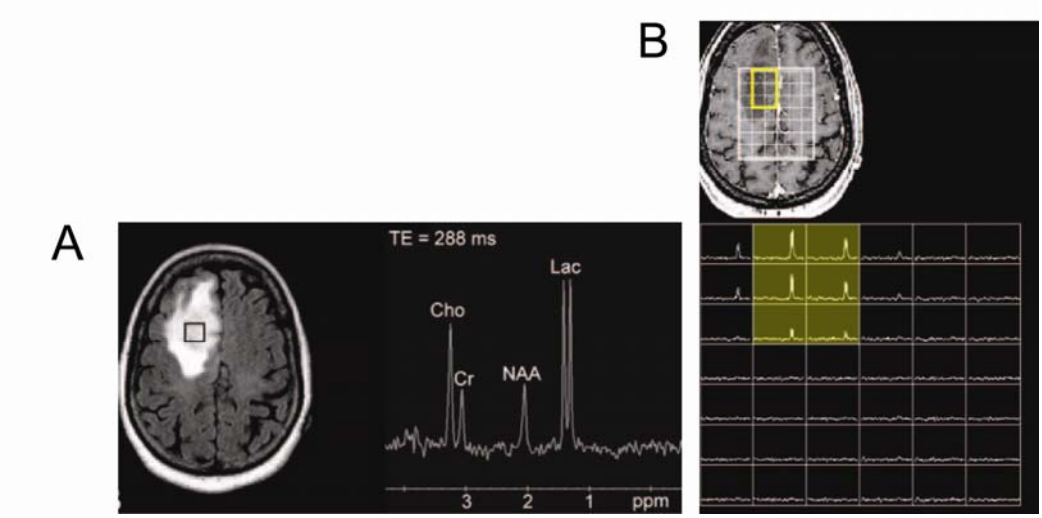

Figure 1.4 ^{1}H-MRS imaging of 59 year-old woman with superior frontal anaplastic astrocytomas. (A) The centre of tumor mass reveals a marked increase in lactate (Lac), choline (Cho) and a decrease in N-acetyl aspartate (NAA) metabolite**.** (B) Corresponding lactate metabolite peaks detected within the tumor regions. (Image from Cha, 2006).

1.4 Glioma Classification and Grading

Gliomas are classified and sub-categorized on the basis of histopathological manifestations and clinical presentations. They are graded on a World Health Organization (WHO) consensus-derived scale of I to IV according to the degree of malignancy as determined by various histological features and genetic alterations (Louis et al., 2007).

According to WHO classification, Grade I gliomas are considered as biologically benign and can be completely eradicated by surgical resection. Grade II gliomas are low-grade malignant tumors that could potentially infiltrate surrounding brain tissues rendering them incurable by surgery. The mean survival rate for this group of patients is around 5 to 10 years. Grade III gliomas demonstrate much enhanced proliferation, anaplasia and angiogenic responses over grade II glioma with a mean survival rate of about 2 to 3 years. Finally, grade IV glioma which is the most prevalent and biologically aggressive is defined by hallmarks of unrestrained cellular proliferation, diffuse infiltration, increased angiogenesis, propensity for necrosis, resistance to apoptosis and rampant genomic instability. Grade IV gliomas are usually quite recalcitrant to radiotherapy and chemotherapy. Patients with Grade IV gliomas have a mean survival rate of around 9 to 14 months (Furnari et al., 2008). GBM (WHO grade IV) is one of the most common and malignant type of brain tumor that accounts for 50% of all incident cases of astrocytic and oligodendroglial tumors. Despite advances in surgery, chemotherapy and radiation therapy, the median survival rate remains dismal (about 12 months) (Bansal et al., 2006).

1.5 Glioma Databases

Towards better understanding and treatment of gliomas, a number of databases that capture and integrate data associated with glioma studies have been developed in recent years. Two of such glioma databases, Rembrandt and TGCA, are briefly described below.

1.5.1 REMBRANDT

REpository for Molecular BRAin Neoplasia DaTa (REMBRANDT) is clinical glioma patients' genomics database that leverages data warehousing technology to host and integrate clinical and functional genomics data from clinical trials involving patients suffering from gliomas. The knowledge framework can be used to provide researchers with the ability to perform ad hoc querying and reporting across multiple data domains, such as gene expression, chromosomal aberrations and clinical data. To date, Rembrandt contains data generated through the glioma diagnostic initiative from 1018 glioma specimens comprising of 568 gene expression arrays and 920 copy number arrays.

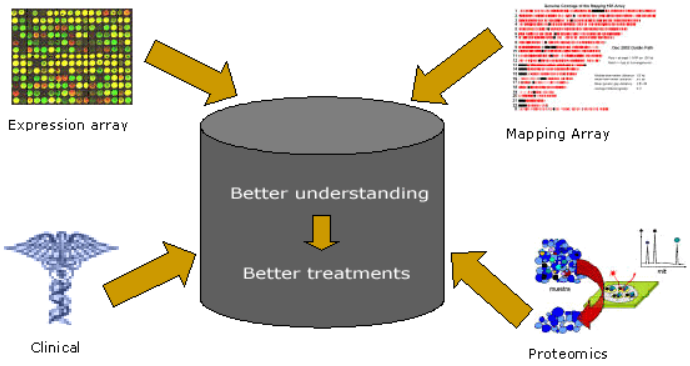

Fig. 1.5 REMBRANDT knowledge database (from http://caintegrator-info.nci.nih.gov/rembrandt**)**

Through the use of Rembrandt, one is able to trace the expression level of a gene of interest in the various grades of glioma patients and its correlation with survival rate. And at the same time, the database also provides a platform for validation of gene signature derived from cellular or animal model studies.

1.5.2 TCGA (The Cancer Genome Atlas)

The Cancer Genome Atlas (TCGA) is another comprehensive and coordinated effort by cancer researchers to accelerate the understanding of the

molecular basis of cancer through the application of genome analysis technologies and large-scale genome sequencing. As a public resource, all TCGA data are deposited at the Data Coordinting Center for public access (http://cancergenome.nih.gov/). The first cancer that was studied by TCGA is glioblastoma and this database provides a network view of the pathways altered in the development of glioblastoma. Importantly, TCGA is able to integrate analysis of DNA copy number, gene expression and DNA aberration data to come out with a more defined core signaling pathways in glioblastoma in which we can compare against in our own studies. The only caveat is that TCGA at this moment comprises mainly GBM specimens and has thus less molecular heterogeneity than Rembrandt, which contains information on gliomas at different stages.

1.6 Intervention and Treatment of Glioma

The care for glioma patients revolves around the management of common set of problems faced by brain tumor patients which include seizures, venous thromboembolism, cognitive dysfunction, fatigue and peritumoral edema (Wen et al., 2006). The standard therapy for the treatment of malignant gliomas involves radiotherapy, surgical resection and chemotherapy (Table 1).

Types of Tumors	Therpeutic Intervention
Glioblastomas (WHO grade IV)	Maximal surgical resection, plus radiotherapy, plus concomitant adjuvant TMZ or carmustine wafers (Gliadel)
Anaplastic astrocytomas (WHO grade III)	Maximal surgical resection, with radiotherapy, plus concomitant and adjuvant TMZ or TMZ alone
Anaplastic oligodendroglioma and anaplastic oligoastrocytomas (WHO grade II)	Maximal surgical resection with radiotherapy alone, TMZ or PCV with or without radiotherapy afterward, radiotherapy plus concomitant and adjuvant TMZ, or radiotherapy plus adjuvant TMZ
Recurrent tumors	Reoperation in selected patients, carmustine wafers (Gliadel), conventional chemotherapy (e.g. lomustine, PCV, carmustine, irinotecan, etoposide), bevacizumab plus irinotecan.

Table 1. Overview of current treatments for malignant gliomas (From Wen et al., 2008) temozolomide (TMZ), procarbazine (PCV), lomustine (CCNU).

1.6.1 Radiotherapy

Radiotherapy is the mainstream treatment of malignant gliomas and is usually used in combination with surgery to increase the survival among glioma patients from about 3 to 4 months to 7 to 12 months (Stupp et al., 2005). A typical radiotherapy regime consists of 60 Gy of partial-field external-beam irradiation delivered 5 days per week in portions of 1.8 to 2.0 Gy, which represents the standard treatment for glioma patients after resection. Age appears to be an important factor in determining the effectiveness of radiotherapy. Radiotherapy performed on glioma patients who are 70 years of age or older produces only a modest benefit in median survival of about 29.1 weeks as compared to supportive care with a median survival of 16.9 weeks and elderly glioma patients generally have a worse prognosis than their younger counterparts (Keime-Guibert et al., 2007).

1.6.2 Surgical Resection

Surgical resection is the most common initial therapeutic approach for obtaining tissues for diagnosis and for "tumor debulking" (i.e. surgical removal of as much tumor tissues as possible) provided that neurological function is not compromised. Although glioma patients undergo maximal surgical resection whenever possible, malignant gliomas are usually infiltrative by nature and cannot be completely eliminated surgically. The benefits of surgical debulking include reduction of intracranial pressure that could result from the mass effect of the

tumor and provides tumor tissues for molecular studies and histological diagnosis. Advances in surgical technologies such as MRI-guided neuro-navigation, intraoperative mapping (Asthagiri et al., 2007) and fluorescence-guided surgery (Stummer et al., 2006) have increased the efficacy of surgical resection and improved the safety of surgery.

1.6.3 Chemotherapy

Chemotherapy is gaining importance in the treatment of gliomas and is frequently used in combination with radiotherapy. One of the more commonly used chemotherapeutic drugs against gliomas is temozolomide. Temozolomide is a DNA alkylating agent that is approved for use in adult patients with anaplastic astrocytoma that failed to respond to other drug treatments. It is also approved for use during and after radiation therapy for patients newly diagnosed with GBM. The current first-line treatment for patients with glioblastoma is combined radiotherapy and temozolomide, followed by monthly doses of temozolomide after radiation treatment ends. The treatment of malignant gliomas using a combination radiotherapy plus temozolomide as compared with radiotherapy alone significantly increased the median survival from 12.1 months to about 14.6 months (Stupp et al., 2005). Further to this, the survival rate at 2 years among the glioma patients who received radiotherapy and temozolomide is 16.1% greater than the survival rate among patients who received radiotherapy alone (Stupp et al., 2005).

Another chemotherapeutic drug, carmustine is commonly being used to treat many types of brain tumors, including GBM, medulloblastoma, and anaplastic astrocytoma. Carmustine or bis-chloronitrosourea is a mustard gas-

related α-chloro-nitrosourea compound used as a DNA alkylating agent in chemotherapy. It is usually administered into the vein via IV but can also be delivered through a wafer implant (Gliadel), which is surgically placed into the brain cavity after tumor removal. An interesting chemotherapeutic approach involves the implantation of biodegradable polymers containing carmustine (Gliadel Wafers, MGI Pharma) into the tumor bed to gradually kill off the residual tumor cells after the resection of the tumor. The use of these carmustine-containing polymers in patients with malignant gliomas in a randomized, placebo-controlled trial was shown to significantly increase their median survival from 11.6 months to 13.9 months (Westphal et al., 2003).

Currently, anaplastic astrocytomas are treated with radiotherapy and either concurrent with adjuvant temozolomide or with temozolomide alone in the case of GBMs. However, despite optimal treatment, almost all malignant gliomas recur with a median time of progression time of 6.9 months after treatment with radiotherapy and temozolomide (Stupp et al., 2005). Despite intensive efforts in research for novel therapies, there remains a need for improvements in the treatment strategies of malignant gliomas.

1.6.4 Targeted Molecular Therapy

The increasing understanding of the molecular pathogenesis of malignant glioma has produced a more directed use of targeted molecular therapies. The main focus has been on inhibitors that target receptor tyrosine kinases like EGFR (Rich et al., 2004), VEGFR (Batchelor et al., 2007) and PDGFR (Wen et al., 2006) as well as inhibitors targeting intracellular signaling components such as the PI3K/Akt signaling pathway. Interestingly, these inhibitors when used as a single

agent often only exhibit modest activity with patient response rate of about 0 to 15% (Chi et al., 2007). This response to single tyrosine kinase inhibitor could be attributed to coactivation of multiple tyrosine kinases together with redundant signaling pathways thereby limiting the activity of single inhibitors (Stommel et al., 2007).

As mentioned earlier, malignant gliomas are among the most vascularized human tumors and thus making them ideal targets for angiogenesis inhibitors (Jain et al., 2007). Irinotecan, one of the more common topoisomerase I inhibitor used is activated by its hydrolysis to SN-38 and this leads to the inhibition of both DNA replication and transcription. Bevacizumab, on the other hand, is a humanized monoclonal antibody that binds to vascular endothelial growth factor A to block angiogenesis, commonly used in a variety of cancers. A positive effect was observed in one of the angiogenesis inhibitor studies when the treatment of malignant gliomas using a combination of bevacizumab and irinotecan had lowered the incidence of haemorrhage. This combined regimen also increased the 6 month rate of progression free survival from 21% to 46% as compared to patients who were already receiving temozolomide treatment.

With the increasing understanding of the molecular pathogenesis of gliomas, it may be possible in the future to select the most appropriate therapies on the basis of the patient's tumor genotype. In the sections below, I shall provide an update on our current understanding regarding the molecular events surrounding gliomagenesis.

1.7 Glioma Pathogenesis and Signaling Pathways

Three major signaling pathways have been identified to contribute significantly towards the onset of gliomagenesis (Funari et al., 2008): 1) cell cycle signaling pathways, 2) growth factor-regulated signaling pathways and 3) mitogenic signaling pathways. Cell cycle signaling pathways relevant to gliomagenesis consist of the retinoblastoma and p53 signaling pathways which are involved in the regulation of cell cycle progression in tumor cells. In the growth factor-regulated signaling pathways, extracellular growth factors are involved in the cellular signaling of cell proliferation and signaling pathways implicated in promoting glioma development include those mediated by epidermal growth factor (EGF), platelet-derived growth factor (PDGF), fibroblast growth factor (FGF) and vascular endothelial growth factor (VEGF). And for mitogenic signaling pathways involved in gliomagenesis, the mitogen-activated protein kinase signaling pathway and the PI3K/PTEN/Akt signaling pathway are two major downstream effectors that shall be discussed herein.

1.7.1 Cell Cycle Signaling pathways

The mammalian cell cycle is a highly conserved mechanism which is conventionally divided into 4 phases: G1 (first gap phase), S (DNA synthesis phase), G2 (second gap phase) and M (mitosis phase) (Murray et al., 1993). The progression through the cell cycle is regulated by sequential expression, activation and inhibition of cyclins, cyclin-dependent kinases (CDKs) and cyclin-dependent kinase inhibitors (CDKIs). In proliferating cells, there are certain checkpoints which functions as molecular switches that ensure certain critical events in the respective phases are completed before entry into the next phase. If the cells were

arrested at any of these checkpoints, they will either return back to G_0, resting phase, re-differentiate or die by apoptosis so as to ensure that the non-repairable DNA are not passed onto the next progeny of a mutated cell (Fig. 1.6) (Nagy, 2000).

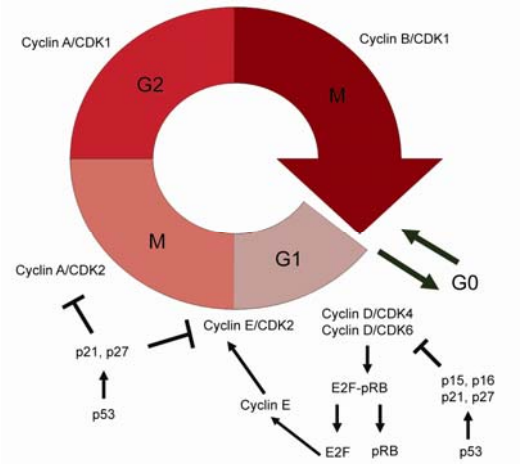

Figure 1.6 Stages of the cell cycle with the various regulators. Progression through cell cycles is tightly regulated by cyclin/CDK complexes and their inhibitors.

The activation of the cell cycle proceeds after mitogenic stimulation. This requires the synthesis of cyclin D, which binds to and activates CDK4 and CDK6 to allow the progression of the G1 phase of the cell cycle. The retinoblastoma protein (Rb) (which normally binds and inactivates E2F) is then phosphorylated by the active cyclin D-CDK4 or cyclin D-CDK6 complexes on serine residues at positions 788 together with 795. Upon its phosphorylation, Rb is released from the E2F transcription factor which results in trans-activation and de-repression of E2F transcription factor-target genes required for S-phase entry (Liu et al., 2001). This allows for the transcription of cyclin E by the E2F family members. Cyclin E then interacts with and binds to CDK2 towards the end of the G1 phase to form an active complex which further phosphorylates the Rb protein on threonine residues

at position 821 and 826 resulting in the full activation of E2F due to further dissociation of free E2F. The cyclin E-CDK2 complex is necessary for transition from the G1 phase into the S-phase through phosphorylation of NPAT (nuclear protein mapped to the AT locus). NPAT is associated with histone gene clusters and activates histone gene transcription which increases the expression of histones necessary for the assembly of newly synthesized DNA into chromatin (Ma et al., 2000). The cyclin E-CDK2 complex also promotes centromere duplication via phosphorylation of the centrosomal proteins NPM (nucleophosmin)/B23, which results in its dissociation from the centrosome to trigger centriole duplication. This event is important for chromosomal segregation (Lacey et al., 1999). The progression of the cell cycle through the S-phase is regulated by cyclin A-CDK2 complex and subsequently, by cyclin A- CDK1 complex when the DNA replication is completed, which drives the cell through G2 phase. The cyclin A-CDK1 complex phosphorylates the ORC (origin recognition complex) subunit Orc1 during mitosis to prevent its interaction with chromatin in order to prevent further DNA replication (Li et al., 2004). At the G2/M transition phase, cyclin A is degraded and CDK1 associates with the newly synthesized cyclin B for progression through mitosis. In the late stages of mitosis, the cyclin B-CDK1 complex is disassembled due to the degradation of cyclin B by the anaphase-promoting complex (APC), an E3-ubiquitin ligase (Harper et al., 2002).

Abnormalities in the cell cycle machinery that alter the ability of the cell to arrest itself at the G1 or G2 phase of the cell cycle would result in unrestrained cellular proliferation and promote tumorigenesis. For example, loss of Rb activity promotes unregulated G1-S phase transition and increases cell cycle progression. Similarly, p53, a tumor suppressor, is also frequently mutated or deleted in human

tumors and is often found mutated or lost early in glioma formation (Nozaki et al, 1999). Clearly, aberrant Rb- and p53-mediated signaling can contribute to gliomagenesis, as discussed below.

1.7.2 Retinoblastoma (RB) Signaling pathway in gliomagenesis

Supporting a role for Rb in gliomagenesis, the *Rb1* gene that is mapped to chromosome 13q14 is mutated in 25% of known high grade astrocytomas. Further to this, the allelic loss of 13q arm typifies the transition from a lower to intermediate grade gliomas (Henson et al., 1994). In addition, the cell cycle machinery proteins CDK4 and CDK6 (Fig. 1.6 and 1.7) that phosphorylate Rb are found to be frequently amplified and are responsible for the functional inactivation of Rb in 10% to 15% of high-grade gliomas (Reifenberger et al., 1994, Costello et al., 1997). This CDK4/6-mediated Rb downregulation is further promoted by the inactivation of critical negative regulators of both CDK4 and CDK6, namely $p16^{Ink4a}$ and $p14^{ARF}$ (Serrano et al., 1993). Notably, both $p16^{Ink4a}$ and $p14^{ARF}$ can be inactivated by hypermethylation at CpG positions (Costello et al., 1996) or by allelic loss, which occur in 50% to 70% of high grade gliomas and about 90% of cultured glioma cell lines (Fueyo et al., 1996).

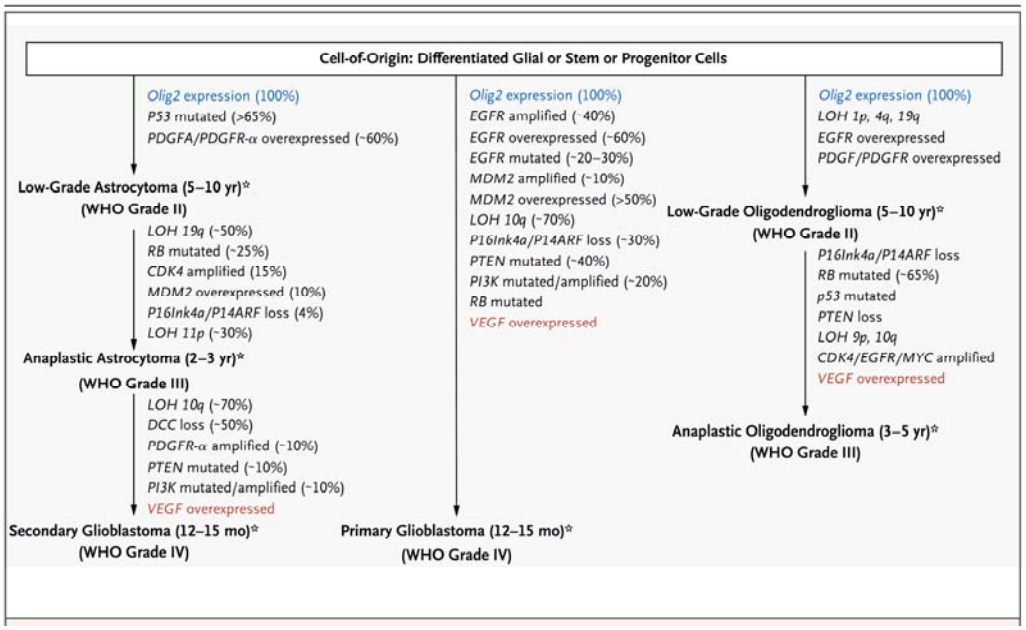

Figure 1.7 Altered signaling pathways in the development of malignant gliomas (From Wen et al., 2008)

1.7.3 p53 Signaling pathway

Besides Rb, p53 represents another tumor suppressor that is often dysregulated in gliomas. The transcription factor p53 is widely regarded as a "guardian of the genome", whose chief function is to prevent the proliferation of cells with unstable genomes primarily through the halting the cell cycle at the G1 phase (Vousden et al., 2002). When needed, p53 can also activate apoptosis. Upon its post-translational modification by various cytotoxic and genotoxic stress-sensing proteins, p53 becomes stabilized and binds transcriptionally to promoters of over 2500 effectors genes (Levine et al., 2006). One of the best characterized p53 effector genes is the CDNK1A which encodes for the CDK2 inhibitor, p21 (Harper et al., 1993). The inhibition of CDK2 prevents its association with cyclin E which is necessary for G1 phase to S phase transition. The loss of p53 function either through point mutations or the loss of chromosome 17 where the gene resides is a frequent event in the cellular progression of secondary gliomas (Louis,

1994). The importance of the p53 pathway in gliomagenesis is further emphasized by the increased incidence of gliomas in Li-Fraumeni syndrome, a familial cancer-predisposition syndrome associated with germline p53 mutations (Srivastava et al., 1990).

1.7.4 Growth Factor-Regulated Signaling Pathway

Aside from promoting cell cycle dysregulation, gliomas may potentially activate growth factor receptor-driven pathways to augment its growth by a combination of mechanisms such as overexpression of both of the ligands and the receptors, amplification or mutation of the growth receptor leading to constitutive activation of the downstream signaling pathway in the absence of ligand. The EGF, PDGF, FGF and VEGF signaling pathways in particular play important roles in the development of the central nervous system (CNS) as well as in gliomagenesis. Notably, directed therapy against these potentially critical signaling pathways is currently in progression (Kanu et al, 2009).

1.7.5 EGF Receptor Signaling Pathway

Epidermal growth factor receptor (EGFR) is a transmembrane protein belonging to the erbB/HER family of receptor tyrosine kinases (RTKs) which includes four members defined as ErbB-1/EGFR/HER1, ErbB-2/HER2/neu, ErbB-3/HER3 and ErbB-4/HER4 (Citri et al., 2006). The EGFR gene encodes a protein containing 1186 amino acids, 621 residues of which comprise the extra-cellular region. After EGFR dimerization, multiple residues of the cytoplasmic kinase domain are autophosphorylated and several downstream adaptors protein

are recruited under the plasma membrane, including Grb2, Shc or Dok-R for activation of the different signal transduction pathways.

EGFR gene amplification occurs in about 40% of all GBM and the amplified gene is frequently rearranged (Wong et al., 1992). One of the most common EGFR mutations is the mutation found between exons 2-7 previously known as EGFRvIII, △EGFR, or EGFR* with an occurrence of about 20%-30% in all GBM and about 50%-60% out of those that have amplified wild-type EGFR (Frederick et al., 2000). EGFRvIII is an important glioma target as shown by the capacity of this mutant to enhance the tumorigenic behavior of human GBM cells by reducing apoptosis, increasing cellular proliferation (Narita et al., 2002). In a similar manner, EGFRvIII mutations was similarly shown to malignantly transform murine *Ink4a/Arf*-null neural stem cells (NSCs) or primary astrocytes obtained from mouse brains (Bachoo et al., 2002).

1.7.6 PDGF Receptor Signaling Pathway

The PDGF family consists of five isoforms that are homodimers of A-, B-, C-, and D polypeptide chains, i.e. PDGF-AA, -BB, -CC, and -DD, and a heterodimer PDGF-AB (Heldin et al., 2002). The A- and B-chains are synthesized as inactive precursors, but are cleaved during secretion from the producer cell and are present extracellularly in active forms. The PDGF isoforms exert their cellular effects by binding to structurally similar α- and β- PDGF receptor (PDGFR) tyrosine kinases. Each PDGFR contains five extracellular Ig-like domains and an intracellular tyrosine kinase domain to which PDGF bind and activate by ligand-induced receptor dimerization. The PDGF α- and β-receptor homo- and heterodimers induce similar but not identical cellular effects. Almost all dimeric

receptor complexes mediate potent mitogenic effects with the exception of αα heterodimers and ββ homodimers, which mediate chemotaxis of smooth muscle cells and fibroblasts (Eriksson et al., 1992).

PDGFs and PDGFRs are frequently overexpressed in glioma tumor cell lines and surgical resection samples, and their expression levels appear to correlate with tumor grade (Hermanson et al., 1992). The expression of PDGFRs especially PDGFRα and its activating ligand PDGF-A and PDGF-B are particularly enhanced in high-grade gliomas while high expression of PDGFRβ occurs in proliferating endothelial cells in GBM (Di Rocco et al., 1998). In comparison to EGFR, the amplification or rearrangement of PDGFR is less common but a rare oncogenic deletion mutation in exon 8 and 9 of PDGFRα has been described to be constitutively active and enhances tumorigenicity (Clarke et al., 2003). PDGF-C and PDGF-D which require proteolytic cleavage for activity are also found to contribute to gliomagenesis (Lokker et al., 2002). The elevated coexpression of the various PDGFs and PDGFRs could potentially activate the range of autocrine and paracrine loops for activation of the downstream survival signaling pathway. The secretion of PDGF-B was also shown to enhance glioma angiogenesis through the stimulation of endothelial cells expression PDGFRβ to express vascular endothelial growth factor (VEGF) (Guo et al., 2003).

In addition to glial cell precursor, PDGFα and PDGFR have been shown to be able to stimulate NSCs in the adult subventricular zone of mouse brains to generate glioma-like lesions (Jackson et al., 2006). Further, transgenic mice over-expressing PDGF-B exhibit increased tendency to form oligodendrogliomas (Dai et al., 2001) and increased overall incidence of tumor formation (Shih et al., 2004).

1.7.7 FGF Receptor Signaling Pathway

In addition to both EGFRs and PDGFRs, FGF receptor (FGFR) pathway is also implicated in the progression of gliomagenesis. The expression of both FGF and FGFR1 is significantly increased in GBM (Morrison et al., 1994). Interestingly, lower-grade astrocytomas expressed higher levels of FGFR2 and as these tumors progressed to higher grade gliomas, they switched expression from FGFR2 to FGFR1 (Yamaguchi et al., 1994).

1.7.8 VEGF Receptor Signaling Pathway

Vascular endothelial growth factor (VEGFs) ligands and receptors (VEGFRs) regulate a wide variety of physiological events which include vascular development, lymphangiogenesis and angiogenesis. VEGF consists of a family of homodimeric glycoproteins which are essential for the embryonic development of the blood vascular system (vasculogenesis), lymphatic system (lymphangiogenesis) and formation of new blood vessels from pre-existing blood vessels (angiogenesis). In the mammalian system, there are a total of 5 members in the VEGF family namely VEGF-A, VEGF-B, VEGF-C, VEGF-D and placenta growth factor (PLGF). In humans, VEGF-A_{165} is the most abundant and catalytically active form and is expressed as a 46kDa homodimer composed of two 23 kDa subunits and is produced by a range of cells including vascular smooth muscle cells, tumor cells and macrophages (Berse et al., 1992). These VEGF ligands bind to three different but structurally similar VEGFR tyrosine kinases namely VEGFR-1, VEGFR-2 and VEGFR-3.

VEGFR-1 (Flt-1) is expressed on monocytes, vascular endothelial cells, macrophages, haematopoietic stem cells and is important for development of

haematopoietic stem cells. VEGFR-2 (Flk-1/KDR) is essential for the development of vascular endothelial cells and is expressed mainly on lymphatic and vascular endothelial cells. VEGFR-3 on the other hand is needed for lymphatic endothelial cells development and is expressed mainly on lymphatic endothelial cells (Holmes et al., 2007). Although predominantly found on endothelial cells, VEGFR have also been detected on cancer cells including gliomas (Zhang et al., 2008), suggesting a possible autocrine effect on their growth.

VEGF plays a key role in the vascularization process of a growing tumor. During the development of the tumor, cells within the expanding mass of the tumor are frequently deprived of oxygen because of their great distance from the nearest blood vessels. As a consequence, regions rich in hypoxia begin to form and it increases the transcription rate and the stability of the messenger RNAs of the VEGF (Shinkaruk et al., 2003). As a tumor increases in size, there is a demand for an increase in density in the network of blood vessels to provide sufficient oxygen and nutrients to the growing tumor, and hence the VEGF signaling pathway plays an important role in the growth of the tumor. Malignant glioma like GBMs are among the most highly vascularized of all solid tumors and microvascular hyperplasia is a common feature of transition from a low-grade glioma (anaplastic astrocytomas) to high-grade malignant glioma (GBMs) (Maher et al., 2006). The levels of VEGF mRNA and protein are highly expressed in glioma cells with malignant GBMs producing more VEGF than low grade anaplastic astrocytomas (Chaudhry et al., 2001). The inhibition of VEGFR kinase using the small molecule inhibitor of Raf, AAL881 leads to inhibition of glioma xenograft growth (Sathornsumetee et al., 2006).

1.7.9 Mitogenic Signaling Pathways

Under normal conditions, the stimulation of cellular proliferation requires the regulated activation of mitogenic signal transduction pathways through growth factor binding, contact with extracellular matrix (ECM) or cell-cell adhesion. In gliomas, many of the mitogen-specific membrane receptors are however present in a constitutively active form, which concomitantly leads to enhanced activation of downstream effector pathways. Genomic alterations in gliomas that amplify these signaling pathways thus greatly reduce their dependency on exogenous growth factor signaling, and as a result, encourage their uncontrolled cell division, survival and motility. Two important downstream pathways that are of particular relevance to gliomagenesis are the mitogen-activated protein kinase (MAPK) signaling pathway and the PI3K/PTEN/Akt signaling pathway, which are discussed in more detail below.

1.7.10 MAPK Signaling Pathway

Cell surface signals for the mitogen-activated protein kinase (MAPK) pathway can be transduced by both the receptor tyrosine kinases (RTKs) and integrins. Integrins are membrane-bound ECM receptors that facilitate the interaction between the ECM and the cytoskeleton. Integrins bind to cytoplasmic anchor proteins to synchronize the association of integrins with actin filaments to create a focal adhesion complex upon contact adhesion to ECM. Following this, numerous molecules of focal adhesion kinase (FAK) cluster at these complexes and become activated by cross phosphorylation, which in turn, activates a signaling cascade that leads to the phosphorylation of extracellular signal-regulated kinase (ERK) through the activation of Ras. This activation of Ras is

facilitated by the recruitment of the adaptor protein Grb2 and the Ras guanine nucleotide exchange factor SOS to phosphorylate FAK at the plasma membrane or through Src-dependent phosphorylation of p130Cas (Fig. 1.8) (Schlaepfer et al., 1997).

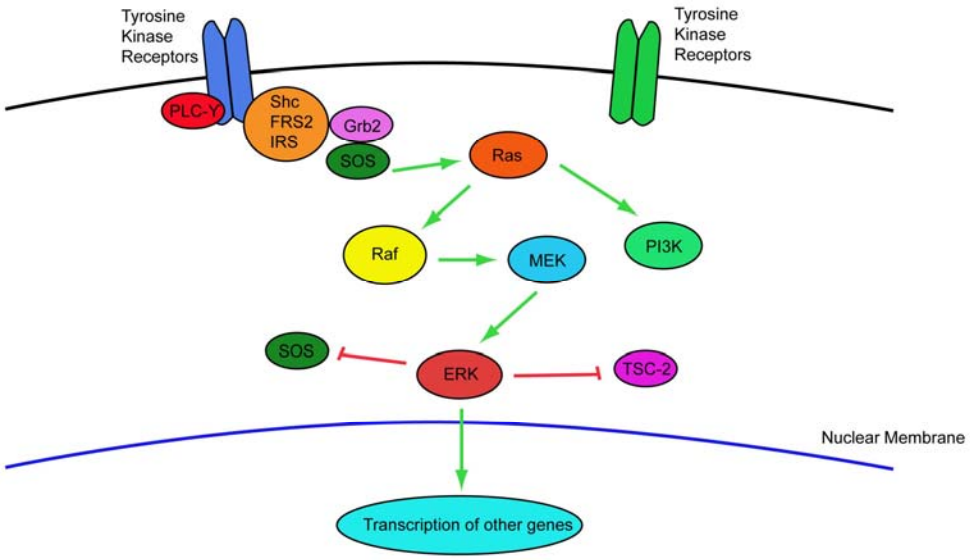

Figure 1.8 MAPK signaling pathway in growth and differentiation. (Adapted from www.cellsignal.com).

Similarly, RTKs are able to activate the MAPK pathway through growth factor signaling. The binding of growth factors to their cognate receptors results in receptor dimerization and trans-phosphorylation that create binding sites for adaptor protein complexes such as Grb2/SOS. The recruitment of Grb2/Sos to the activated receptor is important for the activation of Ras. Once the Ras-GTPase is activated, it phosphorylates Raf kinase (or MAPKKK) which in turn phosphorylates MEK. MEK is a dual specific kinase that is responsible for the phosphorylation of ERK. The activated ERK then enters the nucleus and phosphorylates a number of transcription factors that regulate the expression of genes promoting cell cycle progression, like for example cyclin D1.

1.7.11 PI3K/PTEN/Akt Signaling Pathway

The class 1A family of phosphoinositide 3-kinases (PI3K) are heterodimers recruited to activated RTKs and adaptor proteins through their regulatory subunit in which there is a total of 5 isoforms namely p85α, p55α, p50α (*PIK3R1*), p85β (*PIK3R2*); and p55γ (*PIK3R3*). These isoforms are encoded by 3 genes shown within parenthesis (i.e. *PIK3R1-3*). The PI3K are currently grouped according to the catalytic isoform present namely: p110α, p110β and p110γ which are encoded by *PIK3CA*, *PIK3CB* and *PIK3CD* genes respectively (Hawkins et al., 2006). *PIK3CA* gain-of-function point mutants have been identified in a variety of tumors including GBMs and the frequency of mutation is as high as 15% (Gallia et al., 2006). Further, elevated expression of *PIK3CD* gene has also been found in GBMs (Kang et al., 2006).

Upon activation, PI3K phosphorylates its lipid substrate phosphatidylinositol 4,5-biphosphate [PtdIns(4,5)P_2] to form phosphatidylinositol 3,4,5-triphosphate [PtdIns(3,4,5)P_3], an intracellular lipid second messenger (Hawkins et al., 2006). This process is opposed by the tumor suppressor, PTEN (phosphatase and tensin homolog) located on chromosome 10 which functions as a lipid phosphatase that dephosphorylates PtdIns(3,4,5)P_3 (Di Cristofano et al., 2000). Notably, PTEN is frequently mutated or deleted in human cancers including gliomas (Vivanco et al., 2002). The tumor suppressor is inactivated in 50% of malignant gliomas by mutations or epigenetic mechanisms resulting in unrestrained PI3K signaling in these tumors (Knobbe et al., 2003). The genomic loss of PTEN would result in the accumulation of high levels of PtdIns(3,4,5)P_3 and would potentially lead to the constitutive activation of the PI3K pathway. Interestingly, PTEN inactivation was also found to be associated with an increase

in angiogenesis which coincides with the progression of malignant tumors (Xiao et al., 2005). In quiescent and differentiated cells with high levels of PTEN, the phosphatase was shown to fulfill essential roles in the maintenance of genomic integrity mainly through centromere stabilization and DNA repair (Shen et al., 2007). Genetic studies in familial cancer predisposition syndromes have shown that a number of PTEN point mutants have mutations located within the PTEN localization domain. This resulted in the aberrant sequestration of PTEN into either the cytoplasm or nucleus, and the resultant mislocalization of PTEN contributes to the loss of its tumor suppressor function (Denning et al., 2007).

Among the numerous signaling proteins recruited to the membrane and activated by PtdIns(3,4,5)P_3 is protein kinase B (PKB) or Akt. PtdIns (3,4,5)P_3 recruits and anchors Akt to the plasma membrane via association with its pleckstrin homology (PH) domain. The kinase then undergoes a conformation change that allows its phosphorylation and activation by PDK1 and PDK2. The complete activation of Akt requires phosphorylation of its 2 regulatory residues, i.e. threonine 308 (Thr 308) on the kinase domain and serine 473 (Ser 473) on the hydrophobic domain, by PDK1 and PDK2 respectively (Sarbassov et al., 2005). The phosphorylation of Akt on Ser 473 by PDK2 (thought to be composed of mTOR/Rictor/GβL and mSin1 complex) augments the Akt activity by about 10-fold. It is noteworthy that 85% of the diffuse glioma patient samples have increased Akt activity as compared to controls (Wang et al., 2004). Further, an Akt phosphatase, PHLPP (PH domain leucine-rich repeat protein phosphatase) which dephosphorylates Akt at Ser 473 position is under-expressed in GBM cells lines. These modifications would result in a constitutively activated Akt environment that would enhance cellular proliferation.

Taken together, it is apparent a cancer cell (like a glioma cell) can exploit multiple strategies that subvert normal cell cycle regulation to promote its growth. Besides the components and pathways mentioned above, it is perhaps noteworthy to highlight that the ubiquitination pathway, normally associated with protein degradation and quality control, also has important roles to play in cancer.

1.7.12 MicroRNAs

MicroRNAs (miRNAs) are a recently discovered class of evolutionarily conserved single-stranded non-coding RNA molecules of about 18-25 nucleotides that regulate gene expression at the post-transcriptional level through binding to target mRNA. The miRNA are derive from the processing of long RNA transcripts encoded by *miR* genes and are involved in numerous cellular processes including proliferation, differentiation, apoptosis and metabolism (Bartel, 2004). The miRNAs have been predicted to target and control the expression of at least 30% of the mammalian genome (Filipowicz et al., 2008) and deregulation of miRNAs can potentially be involved in different human pathological diseases including cancer.

The generation of miRNA is multi-step process which includes numerous post-transcriptional modifications. In the initial step, the RNA polymerase II transcribes the *miR* genes to generate the pri-miRNA transcripts. A nuclear microprocessor which contains the RNase III enzyme, Drosha and a double stranded RNA-binding protein, DGCR8 (Digeorge syndrome critical region gene 8) converts the pri-miRNA into ~70 nucleotide miRNA precursor, pre-miRNA. The pre-miRNA stem-loop structures are then transported to the cytoplasm through the exportin 5 complex (Denli et al., 2004). Dicer, a cytoplasmic

endonuclease together with its co-factors TRBP (TAR RNA binding protein) and PACT (PKR-activating protein) would cleave the pre-miRNA stem loop forming a 21-24 bp duplex miRNA. The miRNA is then loaded onto the RNA induced silencing complex (RISC) containing argonaute (AGO) proteins and degradation of the target mRNA would occur only when the miRNA and the target mRNA is a complementary match to each other (Diederichs et al., 2007).

An estimation of more than 1000 miRNA has been identified and are involved in a wide variety of diseases including cancer. miR-15a and miR-16 are found frequently deleted in chronic lymphocytic leukemia (CLL) (Calin et al., 2002) interestingly more than 50% of the current known *miR* genes were found to be located among common fragile sites or chromosomal regions showing amplification, translocation or deletions in cancer (Calin et., 2004). Several other tumor types which include colon, breast and lung cancer have been associated with deregulation of miRNA expression (Lu et al., 2005).

1.7.12.1 MicroRNA-21 (miR-21)

miR-21 was initially discovered to be highly elevated in all high grade glioma samples from patient tissues and early passage from GBM cultures (Chan et al., 2005). In a large-scale study of miRNA expression in 540 human samples derived from 6 solid tumor types, miR-21 was the only miRNA upregulated in all tumor types analysed which includes the breast, lung stomach, colon, pancreas and prostate (Volinia et al., 2006). A number of other independent studies have also shown elevated levels of miR-21 in ovarian cancer (Nam et al., 2008), cervical carcinoma (Lui et al., 2007), papillary thyroid carcinoma (Tetzlaff et al 2007), hepatocellular carcinoma (Kutay et al., 2006) and numerous head and neck

cancer cell lines (Tran et al., 2007). Further to this, miR-21 was also found to be upregulated in leukemic cancers and its expression is dramatically higher by about 10-folds in patients with chronic lymphocytic leukemia (CLL) as compared to normal lymphocytes (Fulci et al., 2007).

miR-21 was found to be overexpressed in even low grade gliomas such as astrocytomas (WHO Grade II) (Conti et al., 2009) that is characterized by slower proliferation rate as compared to GBM. Interestingly, miR-21 was described to regulate the expression of two tumor suppressor genes, PTEN (phosphatase and tensin homolog) (Meng et al., 2007) and TPM1 (Tropomyosin 1) (Zhu et al., 2008). miR-21 has been shown to target various signaling pathways of p53, TGF-β and mitochondrial apoptosis pathways (Papagiannakopoulos et al., 2008). The direct targets of miR-21 that have been identified are p63, p53 activators JMY (Junction-mediating and regulatory protein), TOPORS (an E3 ubiquitin protein ligase), TP53BP2 (Tumor protein p53 binding protein 2), HNRNPK (Heterogeneous nuclear ribonucleoprotein K) and DAXX (Death domain associated protein) which serve as p53 stabilizers by interfering with MDM2 or serve as co-factors in assisting p53 in the activation of genes that induces growth arrest and apoptosis. These array of proteins are essential for the proper functioning of p53 and by targeting these genes, miR-21 can impair p53 response to stimuli such as DNA damage.

miR-21 also regulates the TGF-β pathway by direct targeting of the TGFBR2 and TGFBR3 receptors and DAXX can mediate TGF-β apoptosis (Papagiannakopoulos et al., 2008). miR-21 also helps to maintain the invasiveness of glioma cells by targeting inhibitors of MMPs (matrix metalloproteinases). MMPs are a group of zinc-dependent endopeptidases involved in the degradation

of the extracellular matrix and their levels are usually significantly upregulated in correlation with invasiveness in gliomas (Nakada et al., 2003). miR-21 supposedly regulates the activity of MMPs through their inhibitors RECK and TIMP3 (Gabriely et al., 2008).

PDCD4 (programmed cell death 4) was previously described as a target of miR-21 in glioblastoma cell line (Chen et al., 2008) and in colorectal cancer (Asangani et al., 2008). PDCD4 could potentially inhibit translation through its interaction with a factor that initiates translation of eIF4A and eIF4G and also inhibits cellular proliferation through activation of p21 (Göke et al 2004).

1.7.12.2 MicroRNA-155 (miR-155)

miR-155 is processed from an exon of a non-coding RNA transcribed from the B-cell Integration Cluster (BIC) located on chromosome 21 and has been found to be involved in a variety of cellular processes including inflammation, immunity and haematopoiesis. The deregulation of miR-155 has been shown to be implicated in different kinds of diseases like cancer, viral infections and cardiovascular diseases. miR-155 has been designated as a component of the primary macrophage response to different types of inflammatory mediators such as the induction of miR-155 by a bacterial lipopolysaccharide (LPS) in a human monocytic cell line (O'Connell et al., 2007).

miR-155 was found to be responsible for the suppression of apoptosis in human T-cell leukemia, Jurkat cell line and in MDA-MB-453 breast cancer cell line through mitigation of caspase-3 activity (Ovcharenko et al., 2007). The overexpression of miR-155 was shown to decrease the levels of TP53INP1 (tumor protein 53-induced nuclear protein 1 which is a nuclear protein that is able to

induce cell cycle arrest and apoptosis through caspase-3 activation (Gironella et al., 2007). There was observed high expression level of miR-155 in Reed-Sternberg cells of Hogkin's Lymphoma and also in the lymphocytic and histiocytic cells of the variant nodular lymphocyte-predominant Hogkin's Lymphoma (Kluiver et al., 2005).

In addition, miR-155 was found to be overexpressed in several solid tumors such as breast cancer (Volinia et al., 2006), thyroid carcinoma (Nikiforova et al., 2008), lung carcinoma (Volinia et al., 2006), pancreatic ductal adenocarcinoma (Lee et al., 2007) and colon cancer (Volinia et al., 2006).

1.8 Ubiquitin and E3 ligases in Cancer

The timely synthesis and degradation of the multitude of cell cycle regulatory proteins via ubiquitin modification by various ubiquitin ligases (E3) is another layer of control that the cell has over its division cycle. Accordingly, dysfunction in the ubiquitin-proteasome pathway that disrupts the delicate maintenance of protein homeostasis in the cell could result in the accumulation of unwanted oncogenic proteins or accelerated degradation of tumor suppressors leading to the potential onset of oncogenesis.

Ubiquitin is a small 76 amino acid modifier that tags target proteins in a highly specific manner through a highly conserved process known as ubiquitination. Similar to phosphorylation, the modification of proteins with ubiquitin is common in normal as well as in pathological cellular processes. Ubiquitination was initially described as the process that labels proteins for degradation through the ubiquitin-proteasome degradation pathway (Hershko et al., 1998). However with time, a number of distinct ubiquitin-mediated functions

have evolved such as regulation of protein trafficking, enzyme activity regulation and assembly of protein signaling complex that may or may not involve substrate degradation (Mukhopadhyay et al., 2007). The mechanism of ubiquitination involves the attachment of ubiquitin to the substrate through the sequential action of 3 consecutive enzymes (Fig. 1.9). The first step involves the activation of ubiquitin by the formation of thioester bond with the ubiquitin-activating enzyme, E1 and this is followed by the E1 delivering the activated ubiquitin to the E2 ubiquitin-conjugating enzyme. The final step involves the transfer of ubiquitin from E2 to a lysine residue in the protein substrate catalyzed by E3 ligases which determine the substrate specificity. The ubiquitin molecule contains seven lysine residues at positions 6, 11, 27, 29, 33, 48 and 63, and polyubiquitination can occur at any of these lysine residues (Pickart, 2000). Monoubiquitination of proteins can also occur. Notably, both monoubiquitination and K63-linked polyubiquitination are not typically associated with proteasome-mediated degradation. Thus, the process of ubiquitin conjugation can result in ubiquitin chains of different length, topologies and functional outcomes (Ikeda et al., 2008). There are many proteins known to be regulated by the ubiquitination process and these proteins include those that control cellular processes such as cell cycle progression, gene transcription, receptor downregulation and apoptosis.

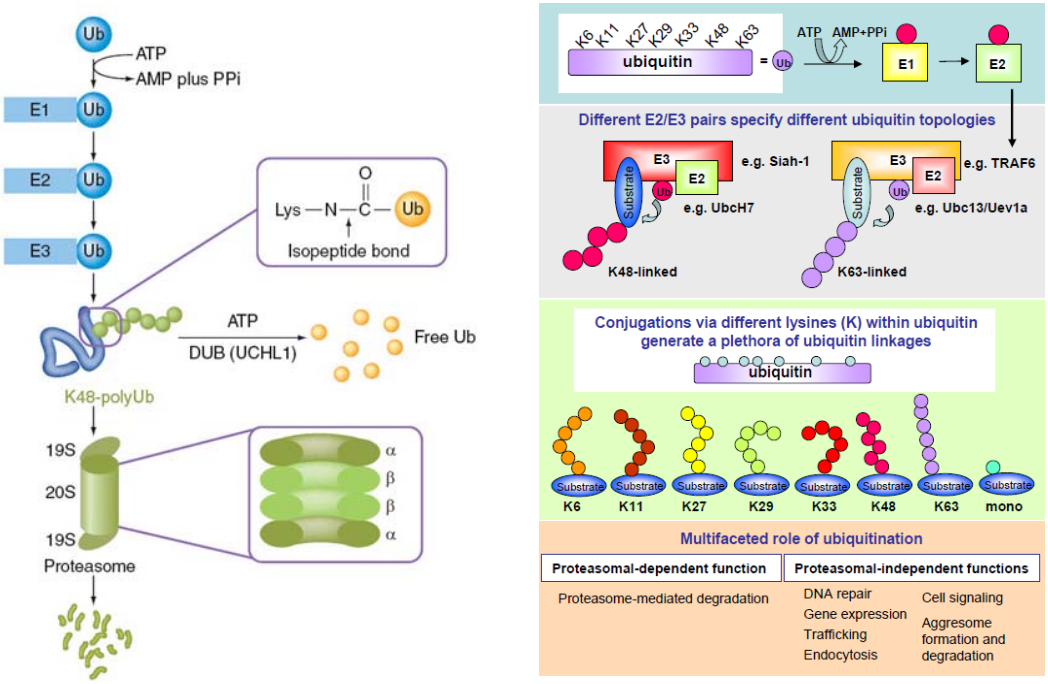

Fig. 1.9 Protein Ubiquitination. (Left) Ubiquitin-proteasome system. (Right) Ubiquitination topologies and their roles (adapted from Lim KL, 2007 and Tan et al., 2009).

E3 ubiquitin ligases are considered one of the most important aspects of the ubiquitin conjugation machinery as they are the ones that bind directly to their target that determine substrate specificity. The numerous ubiquitin ligases are classified according to different categories dependent upon their structural configuration and mechanism of action. They are often grouped according to the presence of either U-box, HECT or RING domain (Nakayama et al., 2006). In certain cases, the core of the ubiquitin ligase consist of several proteins like in SCF complex composed of several proteins like RBX, SKP1, CUL1 and a variable substrate specific F-box protein to form a multi-subunit ubiquitin ligase. There are several examples of E3 ligases that have been linked to the development of cancer. Depending on its substrate specificity; an E3 can either function as a tumor suppressor or promoter (Nakayama et al., 2006). Examples of E3 ligases

that function as tumor suppressors include the Elongin B/C-CUL2-VHL E3 ligase complex and BRCA1 (breast cancer suspceptibility gene 1). The Elongin B/C-CUL2-VHL E3 ligase complex suppresses tumor vascularization through degradation of HIF (hypoxia-inducible factor) via interaction with VHL (von Hippel-Lindau) protein in the complex (Kaelin, 2007). This degradation of HIF prevents the activation of hypoxia-inducible genes such as VEGF which is responsible for tumor vascularization. BRCA1 on the other hand is responsible for the formation of nuclear foci, essential for the repair of damaged DNA (Bennett et al., 2008). The expression of truncated or inactive BRCA1 protein is strongly linked to the development of ovarian and breast cancer (Hashizume et al., 2001). On the other hand, examples of E3 ligases which have oncogenic capacity include Hdm2 (human double minute 2) and HECT-type E3 ligase Nedd4-1. Under normal cellular conditions, the activation of Hdm2 allows it to bind and target p53 for degradation, which represses the p53 signaling pathway leading to faster cell cycle progression (Vousden et al., 2005). Nedd4-1, a similar oncogenic E3 ligase was reported to mediate both monoubiquitination and polyubiquitination-dependent proteasomal removal of PTEN (a tumor suppressor involved in the suppression of PI3K/Akt signaling pathway) *in vitro* (Fouladkou et al., 2008). Surprisingly, an E3 ligase known as parkin that was originally associated with Parkinson's disease (PD) has recently emerged as a new player in cancer. That two disparate diseases such as PD and cancer may share common mechanism is as intriguing as it is fascinating. In the section below, I shall briefly discuss the salient features of PD and its potential relationship with cancer.

1.9 Parkinson's Disease (PD) and Cancer

PD is a major neurodegenerative disorder characterized principally by a rather selective loss of melanin-positive, dopaminergic neurons in the *substantia nigra pars compacta* (SNpc) of the midbrain and the frequent presence of intraneuronal protein aggregates known as Lewy bodies (LBs) that are composed predominantly of fibrillar α-synuclein. On the other hand, cancer is a group of diseases that is characterized by two main features: i) uncontrolled growth of the cells in the human body and ii) the ability of these cells to migrate from the original site and spread to distant sites (metastasis), which can result in death if not controlled. Notably, both PD and cancer are thought to arise from gene-environment interaction with age as the singular most important risk factor (Migliore et al., 2002). Even though the exact mechanisms of aging remains incompletely defined, the aging process is likely to bring about cellular changes that would play an important role in linking the two disorders.

As disparate as PD and cancer might appear to be at first glance, emerging evidence suggests interesting relationship between the two disorders. For example, Doshay noted as early as nearly six decades ago that "for reasons as yet unclear, cancer is phenomenally rare in paralyses agitans (old name for PD)" (25). We now know from numerous reported epidemiological studies that most cancer rates are lower in patients with PD compared with those in the general population and that the risk of dying from cancer is lower in PD patients than in the general population, indicating that PD might provide some form of "biologic protection" against several types of cancers. For example, in a large population cohort study involving 10,322 parkinsonian patients, there was an overall reduction in cancer mortality in both smoking and non-smoking related cancers (Vanacore et al.,

1999). This trend is essentially observed in another related study involving more than 14 000 patients with a primary diagnosis of PD.

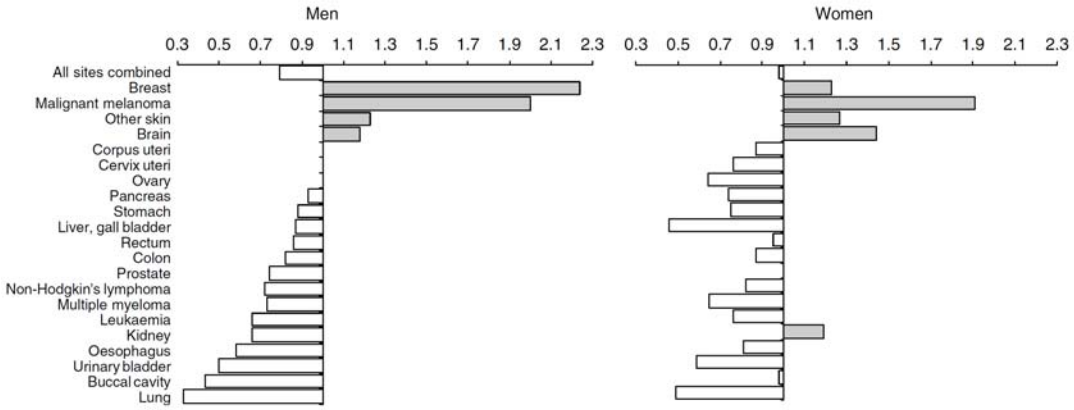

Figure 1.10 The Relative Risk of Cancer from various sites in both men and women with Parkinson's Disease. (Figure from Olsen et al., 2005)

However, it is important to recognize that a few types of cancer occur much more frequently in PD patients compared with controls. Indeed, there was a statistically significant overall increase in the risk for cancer in both men and women for breast cancer, malignant melanoma, brain cancer and other types of skin cancers (Fig. 1.10) (Olsen et al., 2005). Thus, although it is attractive to speculate that a specific genetic background that predispose an individual to neurodegeneration in PD can protect the same individual from cancer, it may also be true in some cases that certain PD-linked genes when dysfunctional may trigger cell death in post-mitotic neurons and paradoxically also promote de-regulated proliferation in dividing somatic cells. It has become increasingly clear recently that *parkin* may be one of such genes.

1.10 Parkin

Parkin is a 52kDa E3 ubiquitin ligase whose mutations were originally linked to autosomal recessive juvenile parkinsonism (ARJP) (Kitada et al., 1998), an inherited form of PD that usually afflicts individuals before 40 years of age. The parkin gene was assigned the PARK2 locus in the original report and thereafter. Accordingly, much of the interest in characterizing the function of the parkin gene has been directed towards understanding its role in PD neurodegeneration. However, aberrant parkin function has also been linked to several other disorders like leprosy (Mira et al., 2004) and transient focal cerebral ischemia (Mengesdorf et al., 2002), amongst which, to the development of several types of cancers (Cesari et al., 2003). Comparatively, the role of parkin in these disorders is less well characterized. Here, I shall provide a brief overview of our current understanding of parkin function and its rather unexpected role in cancer.

1.10.1 Genetic Organization and Regulation of Parkin

The *parkin* gene (also known as PARK2) spans an impressive length of 1.43 Mb on human chromosome 6. It contains 12 exons that are each flanked by introns of massive size averaging 100 kb each. Not surprisingly, *parkin* is one of the largest human gene after *dystrophin* in the human genome. *Parkin* shares a common 204 bp bidirectional promoter with an adjacent gene, *PACRG* which spans a genomic size of only about 0.6 Mb and contains about 5 exons encoding a protein of about 257 amino acids. Perhaps because of its enormous gene size that is accompanied by a paradoxically tiny upstream region, the regulatory elements of parkin remains relatively poorly understood although several studies have indicated that parkin can be regulated under a variety of conditions. N-myc, a

transcription factor involved in neuronal development has been shown to be able to bind to the parkin promoter and negatively regulate parkin through reduction of its promoter activity (West et al., 2004b). Supporting this, several high N-myc expressing neuroblastoma cell lines are characterized by low levels of parkin (West et al., 2004b). Like the action of N-myc, the presence of biallelic hypermethylation on CpG island positions in the promoter region of parkin also leads to the downregulation of parkin transcript levels as evident in acute lymphoblastic leukemia and chronic myeloid leukemia patients (Agirre et al., 2006).

1.10.2 Distribution and Expression of Parkin

Parkin is ubiquitously expressed and distributed in a wide range of organs, tissues and glands which include the brain, heart, skeletal muscles, stomach, colon, kidney, testis, ovary, thyroid and adrenal glands with a much higher expression level in the heart and the skeletal muscles (Kitada et al., 1998). In the brain, the expression of parkin is not solely confined to the SNpc but also present in many other regions such as the cerebral cortex, cerebellum, thalamus, amygdala, corpus callosum, hippocampus and subthalamic nucleus. (Kitada et al., 1998). At the cellular level, parkin is usually uniformly localized throughout the cytosol and can be found in the endoplasmic reticulum, Golgi apparatus and mitochondrial membrane. Although the nucleus was thought to be devoid of parkin, recent evidence suggests that parkin may translocate to the nucleus under certain conditions. For example, Kao showed that parkin translocates to the nucleus following DNA damage (Kao, 2009a), apparently to assist in DNA repair (Kao, 2009b). In a separate study, de Costa and colleagues demonstrated that

endogenous parkin could regulate p53 expression in the nucleus of mammalian cell (Alves da Costa et al., 2009). However, since parkin lacks a defined nucleus localization signal, precisely how the translocation of parkin occurs under different conditions remains to be elucidated.

1.10.3 Structure and Function of Parkin

Structurally, the 465 amino acid-containing parkin protein is composed of several modular domains. At the N-terminal of parkin, there is an UBL (ubiquitin-like) domain, a unique central sequence connecting the UBL to the two RING (Really-Interesting-New-Gene) finger domains (Fig. 1.3) (Shimura et al., 2000). The two RING finger domains (RING1 and RING2) are further separated by a cysteine-rich IBR (In-Between-Ring) domain. Together, the RING-IBR-RING domain constitutes the catalytic box of parkin. However, the RING2 domain appears to be the essential domain for parkin's catalytic activity as the majority of the missense mutations that occur on outside parkin's RING2 domain retain much of their catalytic activity (Wang et al., 2005, Sriram et al., 2005, Matsuda et al., 2006). Recently, a region on parkin which resides between the UBL and RING1 domains of parkin was proposed to contain a new RING domain (designated RING0). Like RING1 and 2, RING0 was found to co-ordinate Zn^{2+} ion and this property of RING0 is apparently important in maintaining the three-dimensional structure of parkin and thereby its enzymatic activity (Hristova et al., 2009). The UBL domain shares 60% homology to ubiquitin (Kitada et al 1998) and was demonstrated to bind to Rpn10, a subunit of the 26S proteasome which could serve to target K48 polyubiquitinated substrates of parkin to the 26S proteasome for degradation (Sakata et al., 2003).

Soon after the discovery of parkin as a PD-linked gene, several groups showed that parkin-mediated ubiquitination is linked to protein degradation and that disease-associated parkin mutations compromise its E3 ligase activity (Imai et al., 2000, Zhang et al. 2000, Shimura et al., 2000). However, it is now clear that parkin is a unique, multifunctional enzyme that is capable of performing multiple forms of ubiquitin modifications including monoubiquitination and lysine 63 (K63) polyubiquitination (Tan et al., 2007; Moore 2006). Notably, both monoubiquitination and K63-linked polyubiquitination are typically uncoupled from the proteasome and are often considered as "non-proteolytic" in nature (Lim et al., 2005, Hampe et al., 2006, Matsuda et al., 2006). Instead, both forms of ubiquitin modification by parkin may participate in cellular signaling. Supporting this, Fallon and colleagues demonstrated that parkin-mediated monoubiquitination of the adaptor protein Eps15 inhibits its ability to initiate receptor down-regulation and leads to enhanced EGF receptor signaling as well as downstream EGF-induced Akt signaling (Fallon et al., 2006). Separately, parkin-mediated K63-linked ubiquitination was proposed by our lab to be involved in cargo diversion during proteasomal stress and accordingly, in the biogenesis of inclusion bodies associated with various neurodegenerative diseases (Lim 2006). Consistent with this, our lab and others have shown that parkin-mediated K63 polyubiquitination of proteins (synphilin-1 and misfolded DJ-1) promotes their sequestration to aggresome-like inclusion bodies (Lim et al., 2005, Olzmann et al 2007). Related to this, our lab has also identified K63-linked polyubiquitin as a novel cargo selection signal for macroautophagy-mediated clearance of aggresomes (Tan et al., 2008, Tan et al., 2008 Autophagy). Thus, parkin appears to be capable of performing multiple roles in the cell.

1.10.4 Mutations in Parkin

Mutations in parkin were originally identified in Japan more than a decade ago to be causative of ARJP (Kitada et al., 1998). Following this discovery, several ethnically diverse individuals with early-onset PD (age < 45 years) in other parts of the world were also found to carry parkin mutations, which occur at a frequency of about 10-20% and 50% in sporadic and familial early-onset cases respectively (Lucking et al., 2000; Mata et al., 2004; Periquet et al., 2003). To date, more than 100 different parkin mutations have been described with over 50 of these being missense/nonsense substitutions (Fig. 1.11). Although most of the missense mutations occur within the RING1-IBR-RING2 catalytic moiety, many of them are also found along the length of the protein outside this region. Further, exonic mutations are also frequently observed with deletion of exon 3 and/or 4 being the most common (Hedrich et al., 2004). Notwithstanding the heterogeneity, there is no observable difference in the clinical signs and symptoms among PD patients carrying different parkin mutations. The probability of having a parkin mutation correlates inversely with age and is likely to be as high as 50% in patients with parkinsonism less than 25 years of age (Lücking et al., 2000). A large proportion of the missense parkin mutations are attributed to a common founder whereas exon rearrangements like deletions and duplications tends to be *de novo* (Lincoln et al., 2003).

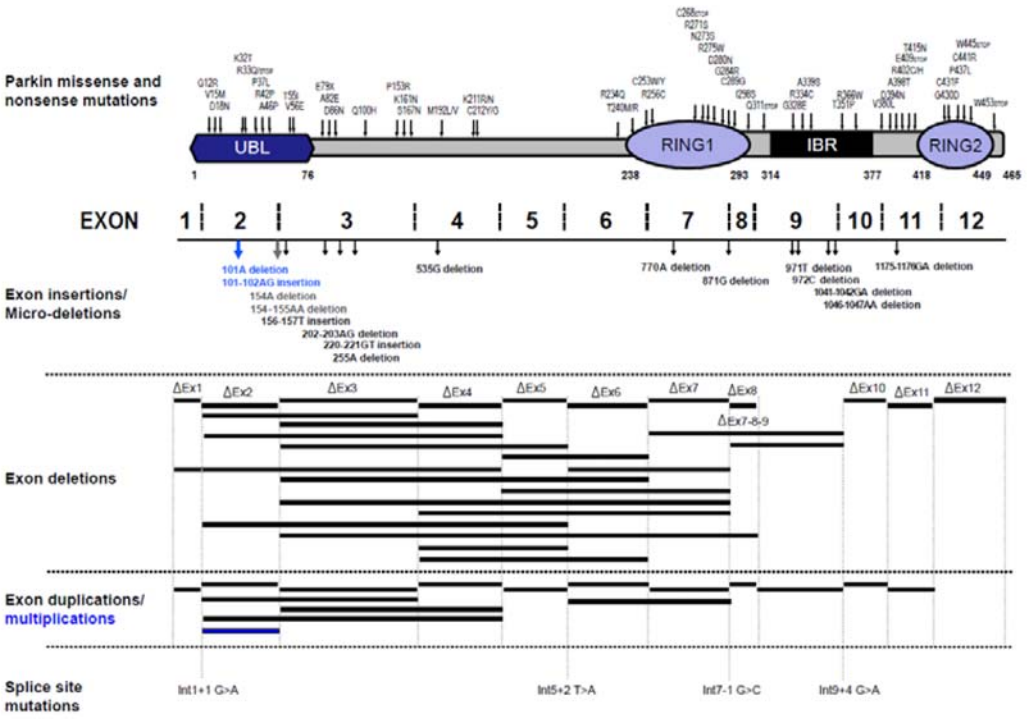

Figure 1.11 Parkin exon structure and various mutations. Parkin protein structure and indication of the various domains including UBL, RING1, IBR and RING2 (upper panel). Various PD-linked parkin muations which included micro-insertions, exon deletions, duplications and multiplications on various regions located on parkin exons (lower panel) (Image from Tay et al., 2011).

The mutations found in parkin were originally thought to abolish its catalytic properties, but several studies have showed that many disease-associated parkin mutants still preserve significant ubiquitination activity (Zhang et al., 2000, Imai et al., 2000). Instead, misfolding of parkin triggered by these mutations appears to be the major mechanism underlying parkin inactivation. Notably, missense parkin mutations frequently alter the protein solubility and concomitantly promote its aggregation into inclusion bodies (Ardley et al., 2003; Cookson et al., 2003; Gu et al., 2003; Hampe et al., 2006; Muqit et al., 2004; Sriram et al., 2005; Wang et al., 2005b) These missense mutations in parkin seem to inactivate parkin's activity through altering the protein's solubility and concomitantly promote its aggregation into inclusion bodies (Wang et al, 2005).

Other mutations of parkin compromise its function by destabilizing the protein and increase its rate of degradation via the proteasome (Schlehe et al., 2008).

1.11 Parkin and Cancer

Although a role for parkin in cancers may come as a surprise to many, the 1.4Mb parkin gene is located within the common fragile site (CFS), FRA6E, a mutational hotspot on chromosome 6 that is frequently deleted in several tumor types including breast, ovarian, kidney and liver cancers (Smith 1998). Indeed, parkin bears genomic similarities to two other large tumor-suppressor genes that also resides within CFS regions *FHIT*/FRA3B (Druck et al., 1998) and *WWOX*/FRA16D (Bednarek et al., 2001). In a recent study, parkin was found to be frequently affected by homozygous and hemizygous deletions (Fig. 1.12) (Bignell et al., 2010). In a related study, high-resolution analyses of somatic copy-number alterations (SCNAs) from 3,131 cancer specimens comprising of 26 histological types revealed that parkin (*PARK2*) is frequently deleted in a variety of cancer cell types (Fig. 1.13) (Beroukhim et al., 2010).

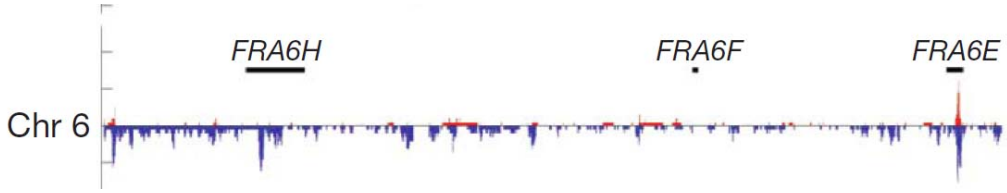

Figure 1.12 Genomic Deletion Profile of human chromosome 6 from a panel of 746 cancer cell lines. Homozygous deletions are indicated in red and hemizygous deletions are indicated in blue. Each tick-mark on the vertical axis denotes ten deletions and the horizontal axis represents p-telomere to q-telomere. (Image from Bignell et al., 2010)

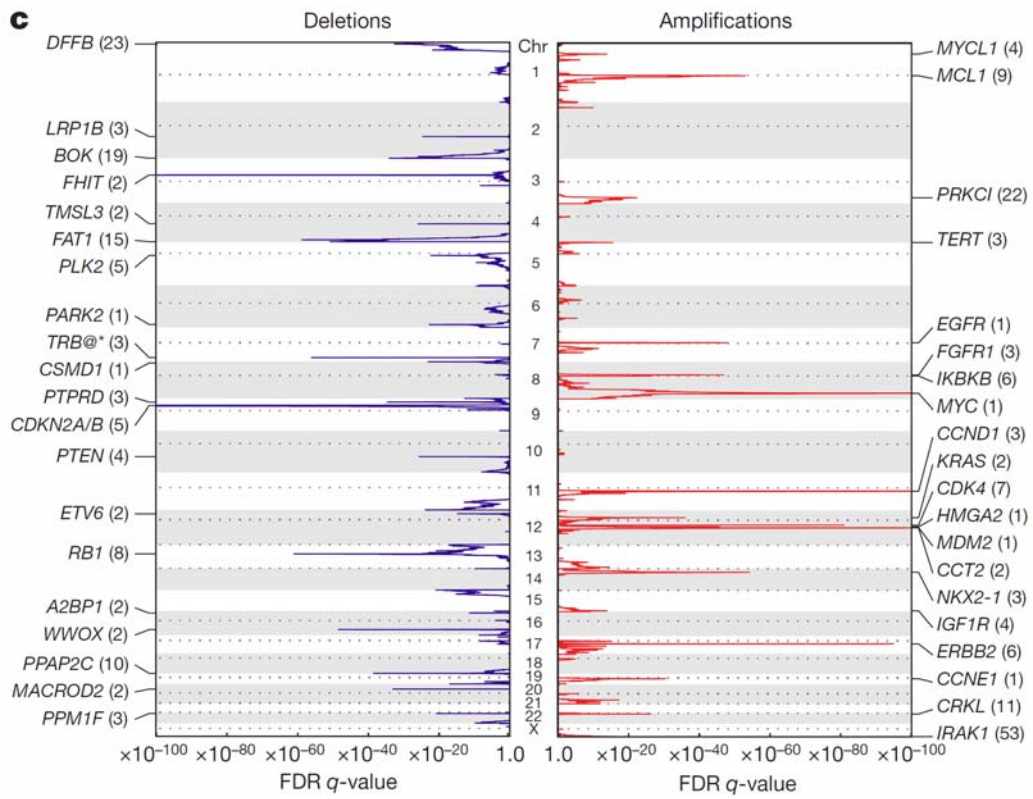

Figure 1.13 The Identification of significant arm-level and focal SCNAs across the panel of cancers. Deletions are in blue and amplifications of the respective genes are in red. Parkin is denoted by *PARK2*. (Image from Beroukhim et al., 2010)

Further to this, parkin gene alterations and expression variability were discovered in a variety of tumor biopsies and cell lines representing a wide range of cancers including ovarian (Denison et al., 2003), breast (Cesari et al., 2003), lung (Picchio et al., 2004), liver (Wang et al., 2004), colorectal (Ikeuchi et al., 2009) (Poulogiannis et al., 2010) cancers, lymphomas (Gaidano et al., 1992), melanomas (Millikin et al., 1991; Guan et al., 2002) and leukemias (Agirre et al., 2006). There is frequent diminished or absence of parkin expression in these cancers which implicate parkin as a putative tumor suppressor. Supporting this, microcell-mediated transfer of human chromosome 6 (where parkin resides) into 2 breast cancer cell lines (Negrini et al., 1994) and BKV-transformed mouse pRPcT1ss1 cells (Gualandi et al., 1994) result in reduced tumorigenicity and

restoration of the ability of these cells to undergo senescence. Further evidence supporting a tumor suppressor role for parkin came from a parkin null mice model, which exhibit enhanced hepatocyte proliferation and development of macroscopic hepatic tumors with the characteristics of hepatocellular carcinoma (Fujiwara et al., 2008). Mechanistically, how does parkin dysfunction contribute to cancer remain relatively not well understood, although the accumulation of certain substrates in the absence of functional parkin expression may hold the key to unlock the pathways involved.

1.12 Cyclin E – A link between parkin, cancer and neurodegeneration?

Among the laundry list of parkin substrates or putative substrates that has been identified to date (Table 2), the cell cycle regulator cyclin E is perhaps the most relevant one in connecting parkin function to cancer.

Substrates	Ub Type	Elevated in			Reference
		KO mice	ARJP Brain	PD brain	
CDCrel-1	-	Yes/No	Yes/No	-	(Ko et al., 2005)
CDCrel-2a	-	-	Yes	-	(Choi et al., 2003)
Synaptotagmin XI	-	Yes/No	-	-	(Periquet et al., 2005)
Synphilin-1	K63	No	No		Chung et al., 2001; Ko et al., 2005; Lim et al., 2005)
P38/AIMP2	Multiple Mono	Yes	Yes	Yes	(Corti et al., 2003; Hampe et al., 2006; Ko et al., 2005; Periquet et al., 2005)
FBP1	-	Yes	Yes	Yes	(Ko et al., 2006)
PARIS (ZNF746)	K48	Yes	Yes	Yes	(Shin et al., 2011)
Cyclin E	-	No	Yes/No	Yes	(Ko et al., 2005; Staropoli et al., 2003)
PDCP2-1	-	-	Yes	Yes	(Fukae et al., 2009)
Pael-R	-	No	Yes/No	-	(Ko et al., 2005)
α/β tubulin	-	Yes/No	No	-	(Ko et al., 2005; Ren et al., 2003)
Hsp70	Multiple Mono	No	No	Yes	(Moore et al., 2008)
PICK1	Mono	No	-	-	(Joch et al., 2007)
VDAC1	K27, Mono	Yes	-	-	(Geisler et al., 2010; Narendra et al.; Periquet et al., 2005)
Ataxin-2	-	Yes	-	-	(Huynh et al., 2007)
O-glycosylated α-synuclein	-	-	Yes	-	(Shimura et al., 2001)
RanB2	-	-	-	-	(Um et al., 2006)
LIM Kinase	-	-	-	-	(Lim et al., 2007)
Eps15	Mono	-	-	-	(Fallon et al., 2006)
DJ-1 L166P	K63	-	-	-	(Olzmann et al., 2007)
Bcl-2	Mono	-	-	-	(Chen et al., 2010)
Drp1	K48	-	-	-	(Wang et al., 2011)
Mitofusin	-	-	-	-	(Poole et al., 2010; Ziviani et al., 2010)
Dopamine Transporter	-	-	-	-	(Jiang et al., 2004)
Phospholipase Cγ1	-	Yes	-	-	(Dehvari et al., 2009)
Ataxin3 polyQ79	-	-	-	-	(Tsai et al., 2003)

Table 2 List of parkin substrates/ putative substrates (Adapted from Tay et al., 2011)

The elucidation of cyclin E, an interactor of hSel-10, as a parkin degradation-associated substrate led to the proposal that parkin may operate as part of a multiprotein ubiquitin ligase complex that comprises also of Cullin (Staropoli et al., 2003). As discussed above, ubiquitination and degradation of phosphorylated cyclin E by the $SCF^{hSel-10}$ complex underlies the regulation of cell cycle entry into S phase. Accordingly, accumulation of cyclin E upon parkin dysfunction could promote aberrant cellular proliferation. Supporting this, recent studies have demonstrated defects in cyclin E proteolysis in colon and brain

cancer cells harboring dysfunctional parkin (Ikeuchi et al., 2009, Veeriah et al., 2010). In postmitotic neurons, cyclins accumulation has been implicated in triggering apoptosis. Not surprisingly, the regulation of cyclin E levels by parkin has apparent effects on cellular apoptosis. Primary neuronal cultures rendered deficient in parkin by RNA interference displayed increased accumulation of cyclin E that correlates with increased cleaved poly (ADP-ribose) polymerase, a marker of apoptosis. Furthermore, cyclin E also accumulates in SN extracts from parkin-deficient PD brains, suggesting its involvement in PD pathogenesis (Staropoli et al., 2003). It is therefore attractive to suggest that altered cyclin E proteolysis in parkin-deficient cancer and neuronal cells may underlie their respective susceptibility to undergo cell division and degeneration. However, a caveat is that parkin-cyclin E relationship is not universally observed (Tay et al., 2010).

Interestingly, parkin also exhibits an apparent E3-independent function in the control of gene transcription. Amongst the genes regulated by parkin is the *p53* tumor suppressor, whose expression is repressed by functional parkin (Alves da Costa et al., 2009). This is rather surprising, as the elevation of p53 levels in parkin-deficient cells should in theory retard (instead of promote) cell division. Other genes whose expression is also regulated by parkin are *follistatin*, *CDK6* and *Eg5*. Whereas the level of follistatin increases in parkin-deficient cells, the reverse is true for CDK6 (Fujiwara et al., 2008, Tay et el., 2010). Both events are however thought to promote carcinogenesis (Fujiwara et al., 2008, Tay et el., 2010). Accumulation of Eg5, a member of the kinesin family, can lead to genome instability in transgenic mice and is associated with leukemia (Liu et al., 2008). Liu and colleagues demonstrated that parkin represses the expression of Eg5 via

inactivation of JNK signaling pathway, suggesting a novel mechanism by which parkin can exert its tumor suppressor function (Liu et al., 2008).

1.13 Other PD-linked Genes and Cancer

Although my thesis topic is primarily focused on the role of parkin in gliomagenesis, it is noteworthy to highlight that besides parkin, there are at least 4 other PD-linked that are suspected to also play a role in cancer development namely α-synuclein, PINK1, DJ-1 and LRRK2 (Table 3), which I will briefly discuss below.

Gene	Function	Role in Neurodegeneration	Role in Cancer
α-synuclein (*PARK1/4*)	Unclear	Gain of function leads to PD, component of Lewy bodies in PD.	Aberrantly expressed and methylated in cancer.
PINK1 (*PARK6*)	Kinase	Loss of function leads to mitochondrial defects and PD.	Somatic mutation in cancer (COSMIC website) putative tumor suppressor induced by PTEN?
DJ-1 (*PARK7*)	Unclear	Loss of function leads to PD, might act as an oxidative stress sensor.	Oncogene, negative regulates PTEN and overexpressed in several tumors.
LRRK2 (*PARK8*)	Kinase, GTPase	Gain of function leads to PD.	Somatic mutation in cancer (COSMIC website) Putative Oncogene?
ATP13A2 (*PARK9*)	ATPase	Loss of function leads to PD, may alter autophagic lysosomal function.	Role in cancer?

Table 3. Genetic Determinants at the interface of neurodegeneration and cancer. (Adapted from Plun-Favreau et al., 2010)

α-synuclein is a small (140 amino acid) presynaptically-enriched protein of largely unknown function. Like parkin, mutations of α-synuclein, which can occur as substitution (A53T, A30P and E46K) or gene duplication/triplication, were originally associated with familial parkinsonism (Kumar et al., 2009). More recently, α-synuclein was shown to be highly expressed in human melanoma cell lines but is undetectable in non-melanoma cell lines, suggesting a potential link between abnormal α-synuclein expression and skin cancer. Specifically, α-

synuclein was positively detected in 86% of the primary and 85% of the metastatic melanoma sections and was undetectable in non-melanocytic cutaneous carcinoma and normal skin (Matsuo et al., 2010).

PINK1 is a 581 mitochondrial-localized serine/threonine kinase whose mutations cause autosomal recessive PD. PINK1 is otherwise known as PTEN-Induced Kinase, which immediately suggest its relationship with the tumor suppressor and hence cancer. Indeed, the restoration of PTEN in PTEN-deficient cancer cells enhanced the expression of PINK1 indicating its regulation by PTEN. (Matsushima-Nishiu et al., 2001). By virtue of its positive association with PTEN, it is attractive to speculate that PINK1 may have a tumor suppressing role.

Unlike most other PD-linked genes, DJ-1 was originally identified as a novel oncogene with the ability of transforming mouse NIH3T3 cells in cooperation with H-ras (Nagakubo et al., 1997). The downregulation of DJ-1 using siRNA was observed to enhance apoptosis by oxidative stress, proteasome inhibition and endoplasmic reticulum stress (Yokota et al., 2003). Importantly, DJ-1 deficiency results in decreased phosphorylation of Akt, whereas its overexpression leads to Akt hyperphosphorylation and increased cellular proliferation. In primary breast cancer samples, DJ-1 expression correlates negatively with PTEN immunoreactivity and positively with Akt hyperphosphorylation which implicates DJ-1 as a negative regulator of the tumor suppressor, PTEN (Kim et al., 2005). More recently, DJ-1 was found to enhance cell survival through interaction with cezanne, a deubiquitination enzyme that inhibits NF-κB activity and further microarray profiling revealed that DJ-1 and Cezanne could regulate IL-8 and ICAM-1 expression (McNally et al., 2010). In another study, elevated levels of circulating DJ-1 and anti-DJ-1 autoantibodies

have been detected in breast cancer patients as compared to normal healthy control individuals (Le Naour et al., 2001). All these evidences support DJ-1 function as an oncogene.

LRRK2 is a 2527 amino acid large GTP-regulated serine/threonine kinase consisting of several structural and functional domains which include ankyrin repeat region (ANK), leucine-rich repeat domain (LRR), Ras of complex proteins domain (ROC), COR (carboxy terminal of ROC) domain, kinase domain (consisting of mitogen activated protein kinase kinase kinase) and WD40 domain. Structurally, it is apparent that LRRK2 contain many motifs that are typically involved in mitogenic signaling. LRRK2 apparently interacts with the C-terminal RING2 finger domain of parkin through the COR domain (Smith et al., 2005). Currently, mutations of LRRK2 are presumed to cause PD through a toxic gain of function mechanism that elevates its kinase activity. For example, several disease-associated LRRK2 mutations such as G2019S and I2020T exhibit enhanced kinase activity (Moore, 2008). A recent study showed that there is an increased risk of non-skin cancers in LRRK2 G2019S mutation carriers, which may be related to toxic gain of function of mutated LRRK2 (Saunders-Pullman et al., 2010). LRRK2 was amplified and overexpressed in papillary renal and thyroid carcinomas, subsequent downregulation of LRRK2 in cultured papillary renal and thyroid carcinoma cells was observed to compromise MET activation and selectively reduces downstream MET signaling of mTOR and STAT3 (Looyenga et al., 2011). This would eventually lead to the loss of important mitogenic pathways which induces cell cycle arrest and cell death due to loss of ATP production. Thus, MET and LRRK2 could potentially cooperate to promote efficient cancer cell growth and proliferation.

1.15 A role for parkin in gliomagenesis – Project Aims and Rationales

At the start of my project, a definite role for parkin in gliomagenesis has yet to be established, let alone the mechanism underlying the potential effects of parkin on glioma growth. Given the importance in understanding the molecular mechanism underlying the formation of glial tumors, I was interested to pursue this novel topic. Furthermore, brain cancer is one of the few cancer types that are over-represented in the PD population. One of the first questions that I have therefore asked myself was if there were any evidence at all that might implicate the involvement of parkin in gliomagenesis. Shortly after my project has started formally, I found a paper by Mulholland and colleagues who showed by means of high resolution microarray comparative genomic hybridization and molecular cytogenetic characterization techniques that parkin was deleted in 2 out of 10 GBM patients' tumor samples and 4 out of 10 glioblastoma cell lines (Mulholland et al., 2006). The finding by Mulholland et al has given me some confidence that I was not on a wrong track altogether. Along the way, I have gathered increasing evidence that supports the involvement of parkin in gliomagenesis. Moreover, a related paper by McLendon and colleagues was published who demonstrated in three microarray platforms (each analyzed with multiple analytical algorithms) that significantly recurrent focal alterations involving homozygous deletions of parkin were detected in 206 glioblastomas (McLendon et al., 2008). Together, the reported findings as well as my own findings suggest that parkin acts as a putative tumor suppressor gene in gliomagenesis. My project directions therefore become progressively clearer during the course of my Ph.D. work and I found myself probing deeper and deeper into the topic.

In sum, the chronological objectives (with the benefit of hindsight) regarding the role of parkin in gliomagenesis that I have pursued during the course of my Ph.D. work can be summarized as follows:

I. To characterize the expression of parkin in glioma cells and examine the effects of parkin over-expression on the rate of glioma cell proliferation both *in vitro* and *in vivo*.

II. To dissect the mechanism underlying parkin-mediated tumor suppression (of glioma growth).

III. To validate the results obtained (from above aims) in human biopsy samples and/or glioma databases.

At the end of my Ph.D. work, I was able to make the following discoveries regarding the role of parkin in gliomagenesis, which I believe are of significance.

1. Firstly, I have found that parkin expression is highly deficient in glioma cells both at the transcript and protein level. By means of both *in vitro* cancer cell assays and an intracranial glioma *in vivo* model. I demonstrated that restoration of parkin expression in parkin-deficient glioma cells significantly mitigates their growth

2. I found that parkin expression in otherwise parkin-deficient glioma cells promote their arrest at the G1 cell cycle phase and have identified cyclin D1 and Akt signaling as key factors regulated by parkin that influence cell cycle progression in glioma cells.

3. Finally, with help from an in-house bioinformatician, I have identified a signature pathway of parkin as an independent predictor of glioma disease progression and survival that predicted survival outcome in glioma patients better than histology alone. My findings here therefore have potential prognostic value.

Taken together, the main finding of my thesis work is that **parkin pathway activation mitigates glioma cell proliferation and predicts survival outcome for patients**.

CHAPTER 2

MATERIALS AND METHODS

2.1 Materials

2.1.1 cDNAs

The FLAG-tagged parkin expression construct was a kind gift from Professor R. Takahashi (Kyoto University). The FLAG-tagged T415N catalytically null parkin mutant was constructed through site-directed mutagenesis by means of the QuickChangeTM method (Stratagene, La Jolla, CA, USA) as previously described by our lab (Wang et al., 2005).

2.1.2 Antibodies

The following antibodies were used: mouse monoclonal anti-β-actin (Sigma), rhodamine-conjugated anti-mouse and anti-rabbit IgG (Molecular Probes, Eugene, OR, USA), fluorescein-conjugated anti-mouse IgG (Jackson ImmunoResearch Laboratories, West Grove, PA, USA), fluorescein-conjugated anti-rabbitIgG (BD Biosciences), mouse monoclonal anti-parkin (clone PRK8) (Covance), phospho-Akt (Ser 473) (Cell Signaling, USA), phospho-Akt (Thr 308) (Cell Signaling, USA), phospho-PDK1 (Cell Signaling, USA), PDK1 (Cell Signaling, USA), Akt (Cell Signaling, USA), cyclin D1 (Cell Signaling, USA), Hsp70 (BD Biosciences Pharmingen, USA), Hsp90 (BD Transduction Laboratories, USA).

2.1.3 Cell lines

HEK293 cells (from ATCC, catalog no. CRL-1573), MCF7 (kind gift from Associate Professor Bay Boon Huat, National University of Singapore), U87MG (kind gift from Dr Carol Tang, National Neuroscience Institute). Immortalized wild type and parkin null mouse embryonic fibroblasts (derived from parkin exon 3 knockout mice) were kind gifts from Professor R. Takahashi (Kyoto University).

2.2 Methods

2.2.1 Cell Culture

Human Embryonic Kidney (HEK) 293 and MCF-7 cells were grown in Dulbecco's modified Eagle's medium (DMEM) containing 10% foetal bovine serum (FBS) supplemented with 100units/ml of penicillin/streptomycin in a 5% CO_2 atmosphere at 37°C. The various glioma cell lines used in the study, i.e. U-87MG, U-373MG, U-251MG, A-172 and T-98G cells were also grown in DMEM containing 10% FBS containing supplemented with 100units/ml of penicillin/streptomycin, but including 0.1mM MEM non-essential amino acids (Invitrogen, USA) and 1mM MEM sodium pyruvate (Invitrogen, USA) in a 5% CO_2 atmosphere at 37°C. Primary mouse embryonic fibroblasts (MEFs) (see section below for preparation) were maintained in DMEM containing 10% FBS supplemented with 100units/ml of penicillin/streptomycin, 2mM glutamine and 55μM β-Mercaptoethanol in a 5% CO_2 atmosphere at 37°C. The cells were maintained on round 10-cm tissue culture plates (Corning, USA) and were passaged every two to three days or whenever they are confluent in a 5% CO_2

atmosphere at 37°C. Generally, primary MEFs at low passage number (between 2-4) were used for analysis.

2.2.2 Preparation of primary MEFs

From wild type and parkin KO mice, the fetuses were extracted from embryonic day 14 were removed and place in a sterile 10-cm tissue culture plate (Corning, USA) containing 1x PBS. The head, spinal cord and the internal organs of the fetus was removed and the remaining body parts were dissected into fine pieces. The pieces were transferred to a centrifuge tube containing 12ml of trypsin and were stored at 4^{o}C overnight. The next day, the centrifuge tube containing the embryonic parts were incubated at 37^{o}C for 15 minutes and were vigorously titrated with 8ml of MEF medium before the supernatant was collected and the cells pelleted at 1,000 rpm for 5 minutes. The supernatant was discarded and the cell pellet was resuspended in MEF medium before it was plated out onto 10-cm tissue culture plate.

2.2.3 Cryopreservation of cells

The cultured cells were cryopreserved in cryopreservation medium containing 50% FBS, 40% DMEM and 10% dimethyl sulfoxide (DMSO) for long-term storage in liquid nitrogen. The cells were trypsinized using 2ml of trypsin for one to two minutes before the equal volume of culture medium was added to it to stop trypsin activity. The cells were then transferred into a 15ml centrifuge tube and spun at 1,000 rpm for 5 minutes. The supernatant was then removed and the cell pellet was resuspended in an appropriate volume of cryopreservation medium at 4^{o}C to make up to a concentration of 1×10^{6} cells/ml

in cryovials. The cryovials were then left in -20^{o}C for 2 hours before it is transferred to -80^{o}C for overnight and finally transferred to liquid nitrogen the next day.

2.2.4 Thawing of cryopreserved cells

The cryovial was quickly removed from the liquid nitrogen and thawed in a clean 37^{o}C water-bath. The cryopreservation medium in the cryovial is thawed until there is a tiny shard of ice left before it was transferred into 9 ml of ice-cold DMEM or culture medium in a 15ml centrifuge tube. The centrifuge tube was then spun at 1,000 rpm for 5min (Eppendorf Centrifuge 5810, USA). The supernatant was then removed and the cell pellet was resuspended in 10ml of culture medium in a 10-cm tissue culture plate. The used medium in the 10-cm tissue culture plate was replaced with fresh culture medium on the next day to remove trace amount of DMSO.

2.2.5 Transfection of U-87MG using Invitrogen Plus™ and lipofectamine™ reagents

The required amount of plasmid was aliquoted out into a 1.0 ml microcentrifuge tube (0.5µg of plasmid for 6-well tissue culture plate and 1.0µg of plasmid for 10cm tissue culture plate) and topped up with 100µl Opti-MEM (Invitrogen, USA) or serum-free DMEM. 6ul of PLUS reagent (Invitrogen, USA) was added to the microcentrifuge tube and the tube was mixed well by pipetting up and down, briefly spun down and labeled as tube A. Tube A was then incubated at room temperature for 15 minutes. After 15 minutes of incubation at room temperature, tube B containing 4µl of lipofectamine topped up with 100µl of

Opti-MEM or serum-free DMEM were added to tube A and incubated for another 15 minutes at room temperature. The medium from the cells in 6-well tissue culture plate were aspirated and replaced with 800µl of either Opti-MEM or serum-free DMEM medium. The transfection reagents containing the plasmid were added dropwise to the well and the well was swirled gently to allow even mixing of the transfection reagents and plasmid with the cells. The cells in the well were seeded at a concentration of $1x10^5$cells/well for at least 24 hours prior to transfection. The transfection medium with the cells in the 6-well plate were incubated in a 5% CO_2 atmosphere at 37°C for 4 hours before the transfection medium was aspirated and replaced with 3ml of fresh culture medium. The cells were then incubated in a 5% CO_2 atmosphere at 37°C for another 48 hours for the episomal replication of the plasmid and expression of the protein in the cells.

2.2.6 Preparation of electrocompetent cells for electroporation

A sterile inoculating loop was used to streak out single bacteria colonies on a Luria-Bertani (LB) plate from a bacteria stock tube stored at -80^{o}C and was incubated overnight in a 37^{o}C bacteria incubator. The following day, a single bacterial colony was picked from the LB plate, inoculated into 3ml of LB broth and incubated overnight at 37^{o}C, shaken at 220 rpm. The next day, the 3ml overnight culture of bacteria was transferred into 200ml of LB broth kept at 37^{o}C, shaken at 220 rpm until it reached at OD_{600} of 0.8 to 0.9. The bacterial culture was chilled on ice for 30 minutes once it reached the desired OD_{600} and after this, the bacteria culture was aliquoted into a clean telfon centrifuge tube and spun at 4,000 rpm for 15 minutes at 4^{o}C with the supernatant decanted after centrifugation. The bacterial cell pellet was thoroughly resuspended in 200ml of sterile, ice-cold 10%

glycerol and spun at 4,000 rpm for 15 minutes at 4^{o}C with the supernatant decanted after centrifugation. The bacterial cell pellet was further resuspended in a lesser volume of 100ml of sterile, ice-cold 10% glycerol and again spun at 4,000 rpm for 15 minutes at 4^{o}C with the supernatant decanted after centrifugation. The remaining bacterial cell pellet was resuspended in 10ml of sterile, ice-cold 10% glycerol before it was transferred into a 50ml centrifuge tube. The bacterial cells were centrifuged at 3,500 rpm for 15 minutes at 4^{o}C with the supernatant removed after centrifugation. Finally, the bacterial cell pellet was resuspended in 1ml of sterile, ice-cold 10% glycerol before it was aliquoted in volumes of 50µl into each microcentrifuge tube and stored at -80^{o}C prior to use.

2.2.7 Electroporation of electrocompetent cells

0.1µg of desired plasmid was added into a tube of freshly thawed out electrocompetent cells and mixed thoroughly before it was transferred into a sterile electroporation curvette that was pre-chilled on ice. The electroporation curvette was gently tapped a few times to bring the competent cells down to the bottom of the tube and was then placed into the electroporation machine (Bio-Rad, USA). The bacterial cells were then electroporated according to the manufacturer's instructions on the electroporation machine (Bio-Rad, USA) at 2.5kV. After the electroporation step, 1ml of sterile LB broth was added into the curvette and mixed thoroughly after which it was then pipetted out and transferred into a bacterial culture tube and shaken at 220rpm, 37^{o}C for an hour for the recovery of the electroporated bacterial cells. After the incubation, 20µl of the bacterial culture was plated onto a LB agar plate with ampicillin and the plate was

incubated overnight in a bacterial incubator at 37^{o}C for isolation of single colonies.

2.2.8 Extraction of plasmid

For mini-plasmid preparation, a single plasmid-containing bacteria colony was inoculated into 3ml of LB broth in a bacterial culture tube and was incubated at 37^{o}C, 220 rpm overnight. plasmid was extracted using the Axygen plasmid miniprep kit according to the manufacturer's instructions. For the preparation of larger amount of plasmid, the Invitrogen plasmid maxiprep kit was used. In this case, the overnight 3ml bacteria culture was added into 400ml of LB broth and was allowed to grow at 37^{o}C, 220 rpm for another 24 hours.

2.2.9 Creation of vector control, human wild type parkin and mutant parkin, T415N stables in U-87MG glioma cell line

The cells were first transfected with the relevant plasmids (empty pCDNA3 plasmid vector, pCDNA3-FLAG- wild type parkin, pCDNA3-T415N mutant parkin) using the Invitrogen Plus^{TM} and lipofectamine^{TM} reagent transfection protocol and the cells were then incubated in a 5% CO_2 atmosphere at 37°C for 48 hours. Transfected cells were then harvested using trypsinization and re-seeded at a concentration of 1 x 10^5 cells into each round 10-cm tissue culture plates. After 24 hours in culture, the used culture medium was replaced with fresh culture medium containing 1000µg/ml of geneticin (G418). Before this, a kill curve was established for U-87MG cell line using various concentration of geneticin (0µg/ml, 200µg/ml, 400µg/ml, 600µg/ml, 800µg/ml, 1000µg/ml) and the optimum concentration of geneticin (i.e. 1000µg/ml) was determined as the

concentration that was able to kill off 95-100% of the cells on the day 05 of the culture. The cells were incubated in a 5% CO_2 atmosphere at 37°C for 5 days to allow for the isolation of single cells that contained the desired transfected plasmid in them. The concentration of geneticin in the culture medium was then lowered to 200µg/ml and sterile cloning cylinders (Sigma, USA) were placed around each isolated single cells after 5 days to allow for the formation of single colonies on the 10-cm tissue culture plate. After 2-3 weeks, the colonies formed were picked off from the 10-cm tissue culture plate using 15µl of 37°C pre-warm trypsin in a yellow pipette tip pipetted up and down vigorously for 20-30 times in order to allow the colonies to be dislodged from the plate. The picked colonies were then transferred into a 96-well flat-bottomed tissue culture plate with each well containing 200µl of culture medium. The cells were monitored daily for confluency and were transferred to a 24-well tissue culture plate upon reaching confluency. The confluent cells in the 24-well tissue culture plate were then transferred into 6-well tissue culture plate and upon reaching its confluency, they were sub-divided into two 6-well tissue culture plates, one was used for the checking of expression using parkin monoclonal antibodies (prk8 clone) in immunoblotting and the other for the maintenance in passage. Once the identification of the positive clones have been established at least 3 times, the parkin-positive cells were expanded in 10-cm tissue culture plates and a proportion of them were cryopreserved down for future experiments.

2.2.10 Total RNA extraction using Qiagen RNeasy® Mini Kit (Qiagen, Singapore)

U-87MG cells were grown on 10-cm tissue culture plate 24 hours prior to the harvesting of total RNA. The culture medium was aspirated from each 10-cm tissue culture plate and the plates were washed once with ice-cold PBS, pH 7.4 before 600µl of Buffer RLT containing β-Mercaptoethanol was added to the plate and the cells on the plate were lysed and scraped using a cell scraper. The lysate was then transferred to a RNase-free 1.5ml microcentrifuge tube and was subsequently homogenized by passing the lysate through a 23G gauge needle 10 times using a RNase-free 1.0ml syringe. The lysate was then centrifuged in a microcentrifuge at 13,000 rpm for 3 minutes before the supernatant was removed and transferred to a new 1.5ml microcentrifuge tube. 600µl of 70% ethanol was added to the supernatant and was mixed immediately by pipetting up and down for a 5 times before the mixture was transferred to a RNeasy spin column placed in a 2ml collection tube and was spun at 13,000 rpm for 15 seconds. The flowthrough was discarded and following after this, 700µl of Buffer RW1 was added to the spin column and centrifuged at 13,000 rpm for 15 seconds. After the flowthrough was removed, 500µl of Buffer RPE was added into the spin column and centrifuged at 13,000 rpm for 2 minutes. The procedure was repeated again before the RNeasy spin column was placed in a new 1.5ml microcentrifuge tube. 40µl of pre-warmed RNase-free water was added to the centre of the RNeasy spin column and centrifuged at 13,000 rpm for 1 minute to elute out the RNA. The concentration of total RNA was determined by using the NanoDrop ND-1000 machine (Thermo Scientific, USA).

2.2.11 Reverse-transcription of total RNA using Invitrogen SuperScript™ II Reverse Transcriptase

15µg of total RNA, 3µl of random primers, 3µl of dNTP mix (10mM each) were added into a nuclease-free microcentrifuge tube and sterile, nanopure water was added to top up the volume to 36µl. The mixture was heated to 65^{o}C for 5 minutes and chilled on ice before the addition of 12µl of 5X First-Strand Buffer, 6µl of 0.1M dithiothreitol (DTT) and 3µl of RNaseOUT (40units/µl) to make up the volume to 57µl. The contents of the tube were mixed gently before it was incubated at 25^{o}C for 2 minutes. After the incubation, 3µl of SuperScript™ II reverse transcriptase was added into the tube before the tube was incubated at 25^{o}C for 10 minutes followed by 42^{o}C for 50 minutes and heat inactivated at 70^{o}C for 15 minutes.

2.2.12 Real-Time Polymerase Chain Reaction (Real-Time PCR)

After total RNA were extracted from various glioma cells, 100ng of the cDNA reverse transcribed from the RNA was used for each Real-Time PCR reaction. The Real-Time PCR reaction was performed in a Light Cycler (Roche) using the FastStart DNA Master Plus Sybergreen I system (Roche, USA) according to manufacturer's protocol. The primers were designed specific to our genes of interest were generated as follows: parkin-specific primers (Forward: 5'-GGAAGTCCAGCAGGTAGATCA; Reverse: 5'-ACCCTGGGTCAAGGTGAG), Concurrently, Real-Time PCR with a primer pair specific to GAPDH (Forward: 5'- GAAGGTGAAGGTCGGAGTCAACG; Reverse: 5'-TGCCATGGGTGGAATCATATTGG) was also included in the same set of

experiments as a housekeeping gene. The evaluation of statistical significance was done using Student's paired t-test for all comparisons (*$P < 0.05$, **$P < 0.01$).

The Real-Time PCR cycling parameters are as followed:

Pre-incubation Step: 95°C, 10 minutes, temperature transition rate 20°C/second

Amplification Step: 95°C, 10 seconds, 20°C/second }

60°C, 10 seconds, 20°C/second } 40 cycles

72°C, 5 seconds, 20°C/second, Single acquisition }

Melting curve Step: 95°C, 0 second, 20°C/second

65°C, 15 seconds, 20°C/second

95°C, 0 second, 0.10°C/second, Continuous acquisition

Cooling Step: 40°C, 30 second, 20°C/second

The specificity of the transcript amplification for Real-time PCR was determined through presence of a single peak on the melt curve analysis and a single, specific band seen from the separation of Real-time PCR product on an agarose gel electrophoresis.

2.2.13 Assessment of cellular proliferation using simple cell count by haemocytometer

2×10^4 cells in 3 ml of culture medium were seeded into each well of a 6-well tissue culture plate in 5 sets of triplicates. The cells were incubated in a humidified, 37°C, 5.0% CO_2 atmosphere incubator and were harvested daily by means of trypsinization using 0.5ml of trypsin on each well. The various cells were harvested and resuspended in an appropriate volume of culture medium and their cell number were determined using the haemocytometer and the formula:

{[(A+B+C+D)] / 4}x dilution factor x 10^4 cells per ml, where A, B, C, D is the number of cells in each of the 16 squares quadrant and their numbers need to fall within the range of 7-70 cells for an accurate estimation of the concentration of cells. The number of the various cell types were determined daily and statistical significance was done using Student's paired t-test for all comparisons (*$P < 0.05$, **$P < 0.01$).

2.2.14 Assessment of cellular proliferation using Roche Cell proliferation Kit I (MTT)

1 x 10^4 cells in 100µl of culture medium were seeded into each well of a flat-bottomed 96-well tissue culture plate in 5 sets of triplicates. The cells were incubated in a humidified, 37^{o}C, 5.0% CO_2 atmosphere incubator for 24 hours before 10µl of the 3-(4,5-dimethylthiazol-2-yl)-2,5-diphenyltetrazolium bromide (MTT) labeling reagent was added into each well and incubated at 37^{o}C, 5.0% CO_2 atmosphere incubator for 4 hours. After the 4 hours of incubation, 100µl of solubilization reagent was added into each well and the plate was again incubated in a humidified, 37^{o}C, 5.0% CO_2 atmosphere incubator for 16 hours. The absorbance in each well of the 96-well tissue culture plate was evaluated and determined with the use of an ELISA plate reader at a wavelength of 550nm and a reference wavelength of 690nm. The MTT assay was performed on various flat-bottomed 96-well tissue plates daily in order to establish the rate of cellular proliferation over a period of 5 days.

2.2.15 Assessment of cellular proliferation using Roche 5-Bromo-2'-deoxy-uridine Labeling and Detection Kit I (BrdU)

3 x 10^4 of the various cell types in 1ml of culture medium were seeded into 24-well tissue culture plate containing poly-D-lysine coated sterile 13mm round coverslips incubated in a humidified, 37^{o}C, 5.0% CO_2 atmosphere incubator. After 24 hours, the cell culture medium was aspirated and replaced with fresh BrdU labeling medium (1:1000) and incubated at 37^{o}C in 5.0% CO_2 atmosphere for an hour. After incubation, the BrdU labeling medium was aspirated away and the coverslips were washed 3 times in the washing buffer. The cells on the coverslips were fixed using the designated ethanol fixative (30ml of 50mM glycine and 70ml of absolute ethanol, pH2.0) for 30 minutes at -20^{o}C. After fixation, the coverslips were again washed 3 times in the washing buffer and 50µl of diluted anti-BrdU working solution (1:10 with incubation buffer) was used to cover each coverslip for 30 minutes at 37^{o}C after which the coverslips were washed 3 times in the washing buffer. The coverslips were then covered with 50µl of anti-mouse-Ig-fluorescein working solution (1:10 with PBS, pH7.2) for another 30 minutes at 37^{o}C and were counterstained with 4',6-diamidino-2-phenylindole (DAPI) for about 10 minutes a in moist chamber at room temperature before they were again washed 3 times in the washing buffer. The coverslips were then mounted onto glass slides using FluorSave Reagent (Calbiochem, USA). The immunofluorescent images were then acquired using an Olympus confocal microscope.

2.2.16 Soft-Agar colony formation assay

100ml of sterile 1% agar was mixed well together with 100ml of sterile culture medium and was dispensed in aliquots of 3ml in each well of a 6-well tissue culture plate as a 0.5% agar (basal/underlay agar). The plates are allowed to cool and set for about 30 minutes before they are kept at 4^{o}C for up to 2 weeks prior to use. The 0.5% basal agar plates are pre-warmed at 37^{o}C in a 5.0% CO_2 incubator for 30 minutes before the start of the experiment. The cells were harvested by trypsinization and centrifuged at 1,000 rpm for 5 minutes. The supernatant was removed with the cell pellet was resuspended in an appropriate volume of culture medium and the concentration of cells were determined using a haemocytometer. 3 x 10^4 cells were mixed thoroughly with 3ml of cooled molten 0.3% plating overlay agar that was previously maintained at a temperature of 42^{o}C by pipetting gently up and down, taking care to avoid air bubbles. 1ml of this mixture was overlaid onto each 0.5% basal agar well and was allowed to cool and solidified. The plates were then incubated at 37^{o}C in a 5.0% CO_2 incubator for 28 days, monitored daily under a dissecting microscope and images of their growth were taken every 3 days until the end of the experimental period, i.e. 28 days (colonies are sometimes stained with crystal violet or MTT to enhance their visibility).

2.2.17 Cell cycle analysis via DNA content analysis using propidium iodide

The cells were seeded at a concentration of 5 x 10^5cells in 10ml of culture medium in 10-cm tissue culture plate and incubated at 37^{o}C in a 5.0% CO_2 incubator. After 24 hours, the culture medium was aspirated and the cells were rinsed 3 times with serum-free culture medium replaced with 10ml of serum-free

culture medium for 24 hours at 37°C in a 5.0% CO_2 incubator to synchronize the cell cycle of the cells at G_0 resting phase. After 24 hours in the serum-free culture medium, quiscient cells were harvested by trypsinization and the cell pellet was collected in a 1.5ml microcentrifuge tube. The cell pellet was resuspended in 1ml of 70% ethanol (for fixation) kept at -20°C for 2 hours before it was centrifuged at 3,000 rpm for 5 minutes in a microcentrifuge. The supernatant was removed and the cell pellet was washed in 1ml of PBS containing 5mM ethylenediaminetetraacetic acid (EDTA) (divalent metal cation chelating agent to prevent cell to cell adhesion) before it was centrifuged again at 3,000 rpm for 5 minutes. The supernatant was discarded and the cell pellet was resuspended in 1ml of propidium iodide (PI)/RNase A staining solution (10ml of 0.1µg/µl of PI, 50µl of 20mg/ml RNase A) and incubated in the dark at room temperature for 3 hours. The cells were then analyzed by fluorescence activated cell sorting (FACS) at 20,000 events using DNA content analysis via histogram plot on a flow cytometry (Calibur) (Becton Dickinson, USA).

2.2.18 Immunocytochemistry and confocal microscopy

3 x 10^4 of U-87MG, U-373MG, U-251MG and T-98G cells were seeded onto poly-D-lysine coated sterile 13mm round coverslips in a 24-well tissue culture plate for at least 24 hours prior to transfection. After 48 hours post-transfection, the cells were rinsed once with phosphate buffer saline (PBS) and fixed with 1.0ml of 2.5% of paraformaldehyde (w/v) at pH 7.4 for overnight at 4°C. After the overnight fixation of the cells, they were washed three times in cold PBS before permeabilisation with 0.1% Triton X-100 (v/v) in PBS for 2 minutes at room temperature. After the permeabilisation step, 60µl of diluted anti-parkin

antibodies (prk8, Covance, USA) at a concentration of 0.2µg per coverslip, in blocking reagent which contained 5% fetal bovine serum (FBS), 1% horse serum and 1% bovine serum albumin (BSA) were added and incubated in a moist chamber overnight at 4^{o}C. The next day, the coverslips were washed six times with cold PBS before incubating in secondary antibodies at a concentration 0.2ug per coverslip, in blocking reagent in a moist chamber for 1 hour at room temperature covered with aluminium foil in the dark. The secondary antibodies reagent was removed and the nuclei of cells were stained with 4',6-diamidino-2-phenylindole (DAPI) for about 10 minutes a in moist chamber at room temperature. The glass coverslips with cells were then washed six times with cold PBS before the coverslips were mounted onto glass slides using FluorSave Reagent (Calbiochem, USA). The immunofluorescent images were then acquired using an Olympus confocal microscope.

2.2.19 Cell lysis, western blotting and immunoblotting

The cells were grown on 10-cm tissue culture plate before they were lysed with 200µl of 1% triton X-100 in phosphate buffer saline (PBS) lysis buffer containing 10µg/ml aprotinin and 1mM PMSF in PBS with phosphatase inhibitor cocktail 1 (for inhibition of Serine/Threonine Protein Phosphatases and L-Isozymes of Alkaline Phosphatases) (Sigma, USA) and phosphatase inhibitor cocktail 2 (for inhibition of Tyrosine Protein Phosphatases, Acid and Alkaline Phosphatases) (Sigma, USA). The protein lysate is then transferred into a 1.5ml ultracentrifuge tube and centrifuged at 55,000 rpm for 15 minutes at 4^{o}C. The supernatant was collected and transferred to a clean 1.5ml microcentrifuge tube and protein quantification was done using the Bradford assay at absorbance OD_{595} (Bio-Rad,

USA). Before the quantification of protein lysate, bovine serum albumin (BSA) of amount 1µg to 6µg was used to determine their respective absorbance and elucidate a standard curve for a range of protein concentration. 2µl of each protein lysate was pipetted into a disposable curvette and 1ml of diluted Coomassie® Brilliant Blue G-250 dye (1:4) was added into each curvette and the absorbance was determined by a spectrophotometer. Approximately 30µg to 70µg of total proteins was used for each western blot. The protein bands were separated on 6% to 15% resolving SDS-PAGE gel depending on the size of the protein band that was being detected at a voltage of 70V to 150V. The transfer of the protein bands on the SDS-PAGE gel to the nitrocellulose membrane was usually transferred at 30V for 15 hours or 100V for 2 hours depending on the size of the protein band being analyzed. After the transfer of protein bands onto the nitrocellulose membrane, the membrane was blocked with 5% fat-free milk in TBST (50 mM Tris.HCl, pH 7.4, 150 mM NaCl, 0.1% Tween 20) for an hour. After the blocking step, the membrane is incubated with the desired diluted primary (1:1000) antibody in 5% fat-free milk in TBST for overnight at 4^{o}C. The next day, the membrane was washed 3 times, 10 minutes each wash using TBST before it was incubated with the diluted secondary (1:1000) antibody conjugated to horseradish peroxidase (HRP) for 2 hours at room temperature. The membrane was then washed 3 times again, 10 minutes each wash using TBST and after this, the various protein bands were analyzed by means using enhanced chemiluminescence (ECL) detection reagents (Pierce, USA) (Amersham, USA).

2.2.20 Cell cycle analysis via BrdU

The cells were similarly seeded at a concentration of 5 x 10^5cells in 10ml of culture medium in 10-cm tissue culture plate and incubated at 37^{o}C in a 5.0% CO_2 incubator. After 24 hours, the culture medium was aspirated and the cells were rinsed 3 times with serum-free culture medium replaced with 10ml of serum-free culture medium for 24 hours at 37^{o}C in a 5.0% CO_2 incubator to synchronize the cell cycle of the cells at G_0 resting phase. The next day, 100µl of diluted BrdU solution (1mM) were added to the 10-cm tissue culture plate and incubated for an hour at 37^{o}C in a 5.0% CO_2 incubator. The cells harvested as a cell pellet in 1.5ml microcentrifuge tube were resuspended with 100µl of BD Cytofix/Cytoperm Buffer and incubated on ice for 30 minutes. The cells were washed once with 1ml of 1x BD Perm/Wash Buffer with the supernatant removed and subsequently, the cell pellet was resuspended in 100µl of Cytoperm Plus Buffer and incubated on ice for 10 minutes. The wash was repeated again with 1ml of 1x BD Perm/Wash Buffer and resuspended in 100µl of Cytofix/Cytoperm Buffer for 5 minutes at room temperature. There was a final wash with 1ml of 1x BD Perm/Wash Buffer before the cells were resuspended in 100µl of diluted DNase incubated at 37^{o}C for an hour. This was followed by washing with 1ml of 1x BD Perm/Wash Buffer with the supernatant removed followed by resuspending the cells in 50µl of BD Perm/Wash containing diluted fluorescent anti-BrdU antibodies for 20 minutes at room temperature. The cells were then washed again with 1ml of 1x BD Perm/Wash Buffer with the supernatant removed and resuspended in 20µl of the 7-aminoactinomycin D (7-AAD) solution. 1ml of PBS containing 5mM of EDTA was added to each tube and the cells were then analyzed by fluorescence activated

cell sorting (FACS) at 20,000 events using quadrant plot analysis plot on a flow cytometry (Calibur) (Becton Dickinson, USA).

2.2.21 Flank and NOD-SCID/J Intracranial mouse tumor model

All animal-related procedures described in this study were approved by our IACUC. The NOD-SCID/J mice were allowed to acclimatize for 2 weeks in the specific pathogen free (SPF) room before the commencement of the experiment. The mouse was anesthetized with 50µl to 60µl of anesthesia (0.5ml ketamine, 0.5ml xylazine and 2.3ml sterile water) intra-peritoneally and was allowed 5-10 minutes for the anesthesia to take effect. For the MCF-7 subcutaneous injections, 6-week-old NOD-SCID mice were similarly allowed to acclimatize for 2 weeks before the start of the experiment. Each mouse was anesthetized before being injected subcutaneously into the right rear flank with 100µl of phosphate-buffered saline (PBS) alone (as a control) or containing 3 x 10^6 MCF7-vector or MCF7-parkin stable cells. Tumor formation in injected mice was monitored daily. Where visible tumor was formed, its length (L) and width (W) were measured, and the tumor volume, *i.e.* L x $W^2/2$, subsequently calculated. The anesthetized mouse was placed on the stage positioned in the centre of the stereotaxic frame with the head of the mouse immobilized through the positioning catch on the ears and mouth of the mouse anchored on the teeth grip. A fine scissors was used to make an incision on the head of the mouse to expose the location of bregma (intersection between the sagittal suture and the coronal suture) on the cranium of the mouse. The location of the coordinates of implantation was designated at +2mm, +1.5mm, -2.5mm with respect from the position of the bregma and the position was marked off. The Hamilton syringe was then flushed 5 times with

sterile PBS before 2µl of PBS containing 250,000 cells was drawn into the Hamilton syringe and the syringe was carefully positioned over the site of implantation. A burr drill operated at maximum speed was used to create a hole which is just large enough for the needle of the Hamilton syringe to pass through taking extreme care not to penetrate into the brain while drilling. Once the hole was created, the needle on the Hamilton syringe was lowered 2.5mm into the brain somewhere in the middle of the cerebral cortex and the cells were injected with the help of an auto-injector at the rate of 0.1µl/minute. After the injection had been completed, an additional 5 minutes of waiting time was used before the needle was retracted out of the cerebral cortex, this was to try to prevent any backflow or leakage of cells from the site of implantation. The head of the mouse was sutured up and its breathing, body temperature and color of eye and tail monitored for about 5 minutes before it was replaced back into its cage wrapped up with a layer of sterile tissue paper over the body to keep it warm. The mice were then observed daily for neurological deficits like ataxia and perfusion was performed on any first signs and indications of neurological deficits. The brains of the mice are then fixed in 4% paraformaldehyde for up to a maximum of 3 days before they are embedded in paraffin wax for sectioning purposes.

2.2.22 NOD-SCID/J Intracranial mouse survival assay

In order to determine if there are any differences in the survival rates of NOD-SCID mice implanted with parkin-expressing or vector-containing U-87MG cells, 3 groups of 12 mice were set up and 250,000 cells of each parkin-expressing (PK#7 or PK#19) and 1 vector control (Vector#22) cell types were stereotaxically implanted respectively in each group according to the method as described in

section 2.2.21. An additional PBS group was set up to as a solvent control group whereby the mice are just stereotaxically injected with PBS. The mice were monitored daily for onset of neurological deficits and ataxia for about 150 days and their survival rates were documented.

2.2.23 Microarray

Total RNA from the various U-87MG parkin expressing and vector control cells were extracted using the RNeasy Mini Kit (Qiagen, USA). The concentration and quality of the total RNA extracted was assessed by the NanoDrop ND-1000 machine (Thermo Scientific, USA) and the Bioanalyzer (Agilent, USA). After the quality of the RNA was ascertained, the GeneChip® WT cDNA Synthesis and Amplification Kit (Affymetrix, USA) was used to generate the first and second cycle cDNA synthesis and the cRNA synthesis through *in vitro* transcription amplification. After the second cycle cDNA synthesis and cRNA hydrolysis step, the GeneChip® WT Terminal Labeling Kit was used for the fragmentation and terminal labeling of the cDNA to generate targets compatible with the GeneChip arrays. After which, the targets were hybridized to the GeneChip® Human Gene 1.0 ST Array which constituted 28,000 gene-level probe sets.

300ng of total RNA were used for the experiments and the arrays were washed and stained using the FS450_0007 fluidics protocol and scanned using an Affymetrix 3000 7G scanner. The scanned images were inspected for hybridization efficiency and CEL files generated from GCOS (GeneChip Operating Software) were imported into Expression Console (EC) 1.1 software for array QC. The CEL data files were analyzed on Biotique XRAY using mixed ANOVA model with quantile normalization employed. The multiple test

correction was done using Benjamini-Hochberg false discovery rate of less than 0.005 and the display of results with fixed factor absolute fold change greater than 1.5 folds.

2.2.24 Bioinformatic analysis of microarray data

Bioinformatic analysis of the microarray data obtained in our study was performed with the help from Miss Felicia Ng, a bioinformatician at the Singapore Institute of Clinical Studies. CEL files from the Affymetrix Human Gene 1.0 ST Arrays were processed using the R statistical software and Bioconductor packages (R Dev Core Team, 2010; Gentleman et al., 2004). The *xps* package (Stratowa, 2010) was used to perform RMA normalization and filter probes with non-significant Detection Above Background (DABG) p-values (threshold set at 0.01). After that, an 'Expression Set' was created using the *Biobase* package (Gentleman et al., 2004) for further analysis in R. Raw and processed data are available on the GEO public database website (GSE29494) [Link: http://www.ncbi.nlm.nih.gov/geo/query/acc.cgi?token=dxstlywiiykyqvk&acc=GSE29494]. Differentially expressed genes between parkin samples (PK7, PK19, PK25) and vector samples (V8, V17, V22) were generated using the *samr* package with false discovery rate less than 0.001. Analysis of pathways and gene sets implicated by Parkin expression was carried out using MetaCore from GeneGo Inc. and Gene Set Enrichment Analysis (Subramaniam et al., 2005). To generate the Parkin signature, probes with log fold change 1.2 were selected and applied to downstream analysis. In order to quantify the extent of Parkin pathway activation, we adapted the Connectivity Map approach (Lamb et al, 2006). Briefly, the Connectivity Map is a pattern matching approach, based on the Kolmogorov

Smirnov statistic, to determine the concordance of the gene signature to gene expression levels in the clinical sample. Public GBM datasets with clinical data, in terms of survival length, were obtained from either the GEO database or the database website. The following datasets were used in the analysis: Rembrandt (http://caintegrator-info.nci.nih.gov/rembrandt) and Freije (GSE4412)(20). In the case of Rembrandt dataset, only survival ranges were available on the website. Hence, the lower limit of the range was used in this analysis. To generate the reference profiles, the datasets were processed using the mas5 algorithm, quantile normalized and median-centered. Expression values less than the threshold value of 50 were replaced with the threshold value. The Parkin gene signature was compared to each sample in the 2 reference profiles mentioned above and an activation score was calculated using the Connectivity Map approach to identify 2 groups of patients: Parkin (+) and Parkin (-) (18, 19). The calculation of the activation score and p-value are as described in Lamb et. al, 2006. In this study, a positive activation score (the Parkin(+) group) indicate that the sample is positively associated to the gene signature and vice versa. Kaplan Meier and Cox regression analysis of Parkin(+) and Parkin(-) group were done in R using the *survival* package.

CHAPTER 3

PARKIN MITIGATES THE RATE OF GLIOMA CELL PROLIFERATION IN *IN VITRO* AND *IN VIVO*

3.1 Overview

As mentioned in the introduction, much of the interest in characterizing the function of the parkin gene has been directed towards understanding its role in neurodegeneration by virtue of its original association with PD (Kitada et al., 1998). However, aberrant parkin function has also been linked to several other disorders including cancer (Cesari et al., 2003). Comparatively, the role of parkin in these disorders is less well characterized. In particular, despite a consistent association between parkin expression alterations and cancers, there was a paucity of reports (at the time when I first started the project) that demonstrates robustly the functional consequence of parkin expression restoration in parkin-deficient cancer cells. As a proof of concept that parkin can mitigate cancer growth, I have together with my colleague (i.e. Tay Shiam-Peng) examined the tumor-suppressing effects of restoring parkin in breast cancer cells, which have been reported to be otherwise highly deficient in parkin expression (Cesari et al., 2003). Using a battery of *in vitro* cancer cell assays and an *in vivo* NOD-SCID mouse model of tumor formation, we found that parkin over-expression in breast cancer cells can indeed slow down their rate of proliferation both *in vitro* and *in vivo* (Tay et al., 2010). With the support from this proof of concept study that parkin is capable of exerting tumor suppression, I went on to characterize the role of parkin in gliomagenesis and subsequently demonstrated that parkin expression is

similarly deficient in glioma cell lines and that its expression restoration mitigates cancer growth in glioma cells, the results of which are presented below.

3.2 Results

3.2.1 Ectopic parkin expression in parkin-deficient MCF-7 breast cancer cells mitigates their proliferation *in vitro* and *in vivo*.

Consistent with the finding by Cesari and colleagues (Cesari et al., 2003), our lab has demonstrated that parkin expression is significantly downregulated at both the transcript and protein levels in a variety of breast cancer cell lines, including MCF-7, as well as in primary human breast cancer samples (Tay et al., 2010). To examine the functional effects of restoring parkin expression in parkin-deficient breast cancer cells, we generated stable clones of MCF-7 cells expressing FLAG-tagged parkin (MCF-7-PK) or containing vector alone as a control (MCF-7-Vector). Three individual parkin-positive MCF-7 clones (#5, 7 and 11) were selected for our experiments to minimize clonal variation. Notably, all of these parkin-positive clones express parkin at a higher level than vector control or parental cells (Fig. 3.1A), but are otherwise similar morphologically. A simple population growth assay reveals that the proliferation rate of parkin-expressing MCF-7 cells is significantly reduced compared to control cells (Fig. 3.1B), suggesting that ectopic parkin expression in MCF-7 cells mitigates their growth. Since cancer cells are anchorage-independent and have the ability to form colonies in soft agar, we also examined whether ectopic parkin expression in MCF-7 cells compromise its ability to generate colonies in soft agar. We found that the number of soft agar colonies formed by parkin-expressing MCF-7 cells is

dramatically reduced and the size of these colonies also tends to be smaller compared to those generated by control MCF-7 cells (Fig. 3.1C).

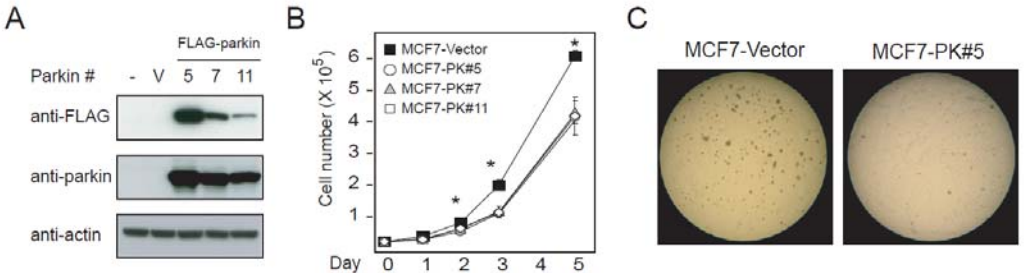

Figure 3.1 Over expression of parkin in MCF-7 cells mitigates their proliferation rate (A) Anti-FLAG and anti-parkin immunoblots of total lysates prepared from native MCF-7 cells (-), vector control (V) and the parkin-expressing stable clones (#5, 7 & 11). Equal loading of the different lysates was verified by anti-actin immunoblotting. (B) Graphical depiction of the percentage of cells undergoing cell proliferation, as measured by cell population number, in MCF-7 vector control and parkin-expressing stable cell lines. (C) Representative images showing apparent decreased ability of parkin-expressing MCF-7 cells in forming colonies in soft agar compared to MCF-7-vector control. These experiments were performed at least three times. (*$P < 0.05$, Student's *t*-test).

To extend our above findings, I examined the effects of parkin over expression on the ability of MCF-7 cells to generate solid tumor *in vivo*. A flank tumor model (n = 9 for each group), where NOD-SCID mice were injected subcutaneously with parkin expressing or control MCF-7 cells, or otherwise with PBS alone, was used for this purpose. Over a period of four weeks post-injection, I observed visible tumor formation that progressively increases in size in mice injected with control or parkin-expressing MCF-7 cells, but not in those injected with vehicle alone (Fig. 3.2A, not shown for PBS control). Consistent with our *in vitro* findings above, I found that parkin-positive clones tend to generate tumors of significantly smaller volume and mass *in vivo* compared to control cells (Fig. 3.2A-C). Taken together, our results demonstrate that ectopic parkin expression in parkin-deficient MCF-7 cells mitigate its proliferation both *in vitro* and *in vivo*, and strongly suggest a negative role for parkin in breast cancer cell proliferation.

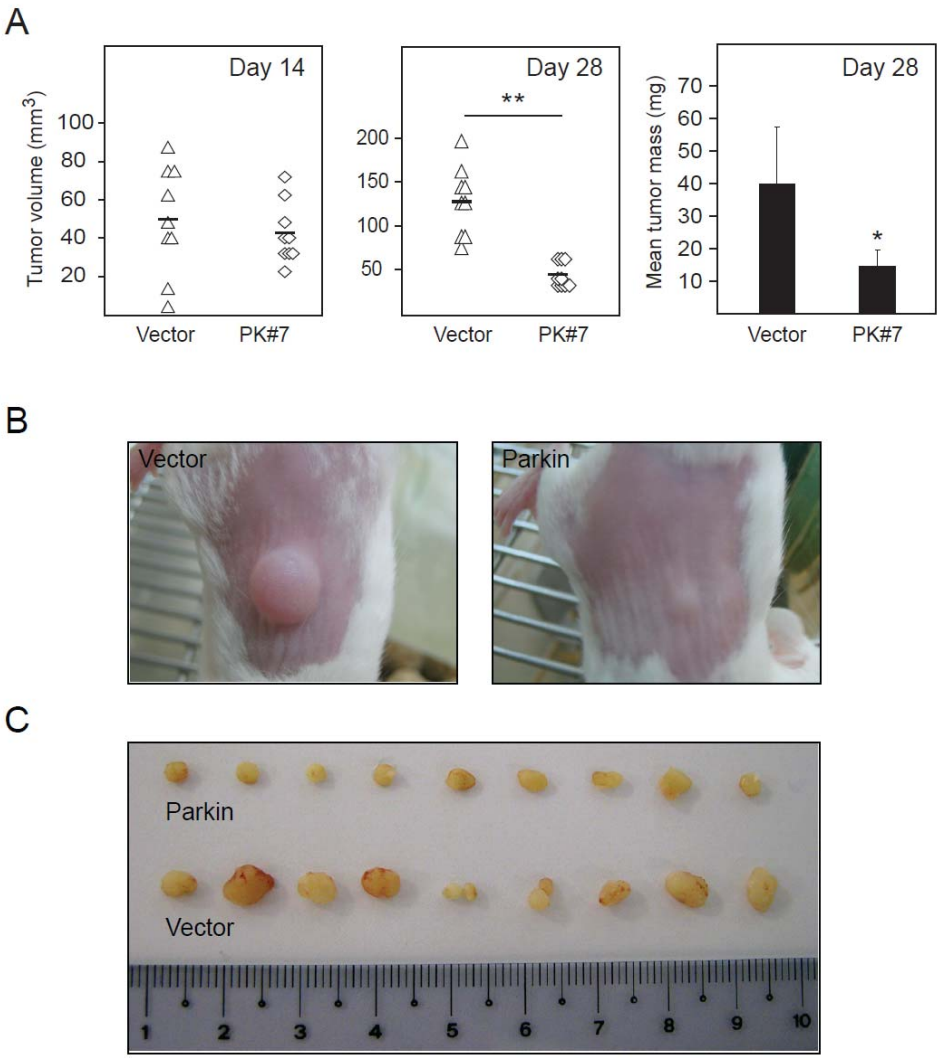

Figure 3.2 Parkin expression mitigates MCF-7 cancer cell growth *in vivo*. (A) Graph showing the volume (*left and middle panels*) and mass (*right panel*) of tumor generated by different cell types in NOD-SCID mice (n = 9) at day 14 and day 28. The experiment was duplicated with essentially the same result (*$P < 0.05$, **$P < 0.001$, Student's *t*-test). (B) Images showing the presence of macroscopic tumor in NOD-SCID mice at 21 days post-injection with MCF-7 vector control cells, in contrast to those injected with MCF-7 cells stably expressing parkin. (C) Images showing tumors resected from mice injected with MCF-7 vector control cells (*top panels*) or parkin-expressing MCF-7 cells (*bottom panels*).

3.2.2 Parkin expression is downregulated in various glioma cell lines

A recent genomic profiling study revealed discrete deletion on chromosome 6 involving the parkin gene in glioblastoma multiforme (Mulholland et al., 2006), the most malignant form of astrocytic gliomas. In addition, recent comprehensive genomic characterization of 206 glioblastomas revealed significantly recurrent focal alterations like homozygous deletions in the regions of parkin gene (McLendon et al., 2008). To examine if parkin expression is affected in glioma cells, I conducted a preliminary study on the abundance of parkin transcripts in several glioma cell lines using a semi-quantitative RT-PCR assay, and found apparent reduction in the level of parkin mRNA in all the glioma cell lines examined, including U-87MG, U-373, U-251 and T-98G compared to control HEK cells (Fig. 3.3A). Consistent with this, subsequent quantitative analysis of parkin mRNA expression using Real-time PCR reveals an average of 16-fold decrease in the levels of parkin transcripts in these glioma cell lines compared to control HEK cells (Fig. 3.3B). The dramatic reduction in parkin expression levels correlate well with the amount of parkin protein in extracts derived from the various glioma cell lines examined (Fig. 3.3C). Collectively, these results demonstrated that parkin expression is significantly down-regulated in glioma cells and suggest that aberrant parkin expression may be relevant to gliomagenesis.

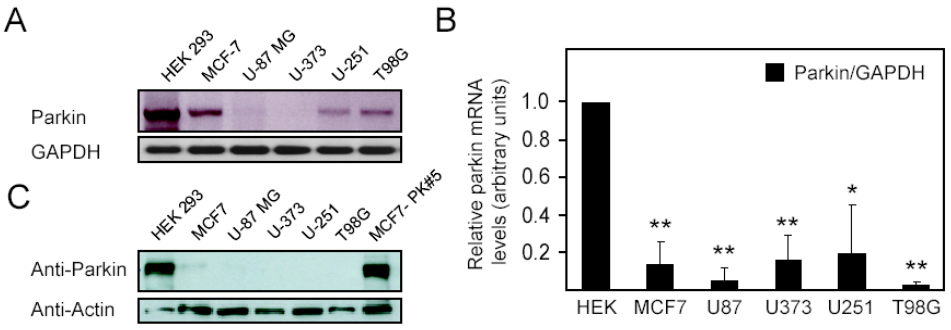

Figure 3.3 Parkin expression is down-regulated in various glioma cell lines. (A) Semi-quantitative RT-PCR results showing the relative expression levels of parkin transcripts in HEK, MCF-7 and several glioma cell lines. (B) Bar-graph depicting the real-time quantification of parkin mRNA levels in various glioma cell lines. The non tumor-derived HEK 293 and the tumor-derived MCF-7 cells were used as controls. (C) Representative anti-parkin immunoblot showing the relative expression of endogenous parkin protein in various glioma cell lines. The blot was stripped and reprobed with anti-actin to reflect loading variations. These experiments were performed at least three times. (*$P < 0.05$, **$P < 0.001$, Student's *t*-test).

3.2.3 Parkin is uniformly localized in the cytoplasm of various glioma cell lines

Besides expression downregulation, I wished to determine if there is any aberrant localization of parkin in the various glioma cell lines. Several groups including ours have previously demonstrated that mutation or stress-induced parkin solubility alteration and mislocalization in the cell can impair its function (Reviewed in Tan et al., 2009). However, no aberrant localization of parkin was observed. Indeed, immunocytochemical analysis reveals a largely uniform cytoplasmic distribution of parkin which is consistent throughout the various glioma cell lines examined (Fig. 3.4A-D). Although at times punctate, there is no obvious evidence of parkin aggregates in these cells (Fig. 3.4).

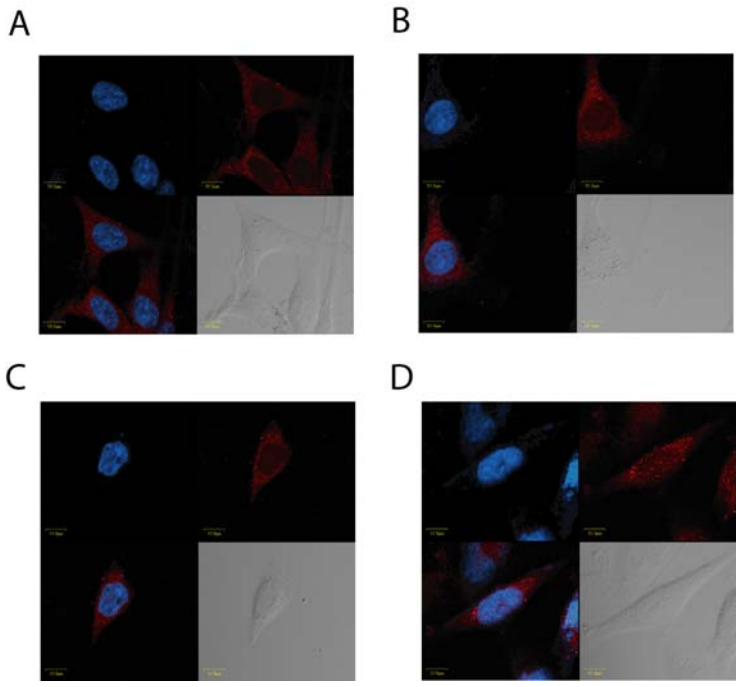

Figure 3.4 Parkin is uniformly localized in the cytoplasm in various glioma cell lines. Representative confocal images showing anti-parkin (red) staining and DAPI (anti-nuclei, blue) staining in various glioma cell lines (A) U-87MG (B) U-373 (C) U-251 (D) T-98G. Scale bar at 10μm on the lower left of each panel.

3.2.4 Ectopically-expressed parkin mitigates the rate of proliferation of parkin-deficient U-87MG glioma cells *in vitro*

In order to investigate the effects of parkin on glioma, stable clones of U-87MG stably expressing vector alone as a control (U-87MG-Vector) or containing FLAG-tagged parkin (U-87MG-PK) in a mammalian expression vector, pcDNA3 were generated (Fig. 3.5A). The glioma cell line, U-87MG cells was used for this purpose because it expresses parkin very poorly and is also a popular cell model for glioma studies. As in the case with MCF-7-parkin stable cells, three parkin-expressing U-87MG clones were chosen to minimize clonal variations. All the parkin-positive clones express parkin at a significantly higher level than vector control or parental cells (Fig. 3.5A), but are otherwise similar morphologically.

The respective rate of proliferation in the vector or parkin-expressing U-87MG cells were analyzed by means of a variety of proliferation assays. A simple cell count assay (via haemocytometer) revealed that the rate of proliferation in parkin-expressing U-87MG cells is significantly reduced compared to control cells (Fig. 3.5B), suggesting that ectopic parkin expression in U-87MG cells mitigate their growth. Consistent with this, there is also reduced incorporation of BrdU, a thymidine analogue, in parkin-expressing U-87MG cells compared to U-87MG vector control cells (Fig. 3.5C). Moreover, ectopic parkin expression in U-87MG cells compromise their ability to generate colonies in soft agar. It is also noteworthy that the size of the colonies formed by parkin-expressing U-87MG cells in soft agar is also comparatively smaller than those generated by U-87MG vector control cells (Fig. 3.5D). Taken together, my results above based on a wide spectrum of *in vitro* cancer cell assay strongly suggest that restoration of parkin levels in parkin-deficient glioma cells could exert an anti-proliferative effect on their growth.

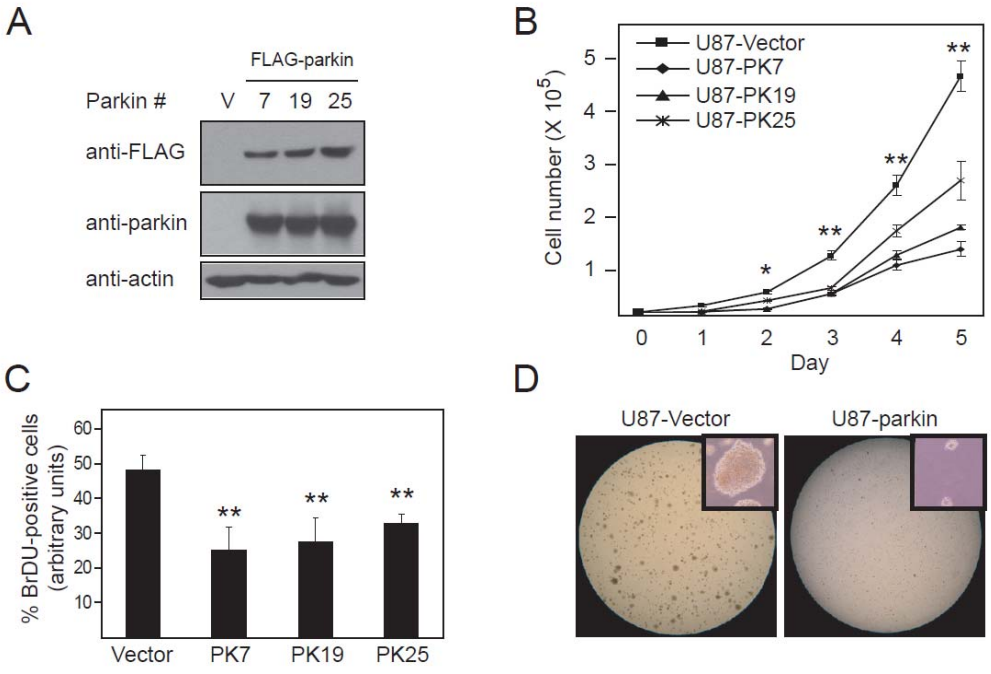

Figure 3.5 Over expression of parkin in U-87MG glioma cells mitigates their proliferation rates. (A) Anti-FLAG and anti-parkin immunoblots of total lysates prepared from U-87MG vector control (V) and parkin-expressing stable clones (#7, 19 & 25). Equal loading of the different lysates was verified by anti-actin immunoblotting (B-C) Bar-graph showing the percentage of cells undergoing cell proliferation in U-87MG vector control and parkin-expressing stable cell lines, as measured by (B) cell population, or (C) the BrdU assay. This experiment is repeated at least three times. (*$P < 0.05$, **$P < 0.001$, Student's *t*-test) (D) Representative images showing apparent decrease ability of parkin-expressing U-87MG cells in forming colonies on soft agar compared to U-87MG-vector control.

3.2.5 T415N mutant parkin expression in U-87MG glioma does not affect rate of cellular proliferation

In order to determine if the reduced rate of cellular proliferation observed above was attributed to parkin's catalytic activity, I created T415N mutant parkin stables and vector control (Fig. 3.6A & B) in U-87MG cell line and assessed their rate of cellular proliferation using the simple cell count assay. The T415N mutation is found on the C-terminal of parkin protein located in between IBR and RING2 domain has been demonstrated to be a "ligase-dead" or "catalytically null" parkin mutant (Fig. 3.6A) (Matsuda et al., 2006). There is no observable difference between the rate of cellular proliferation of T415N mutant parkin expressing U-87MG cells as compared to the vector control (Fig. 3.6C), suggesting that the catalytic activity of parkin is important for its tumor suppression property.

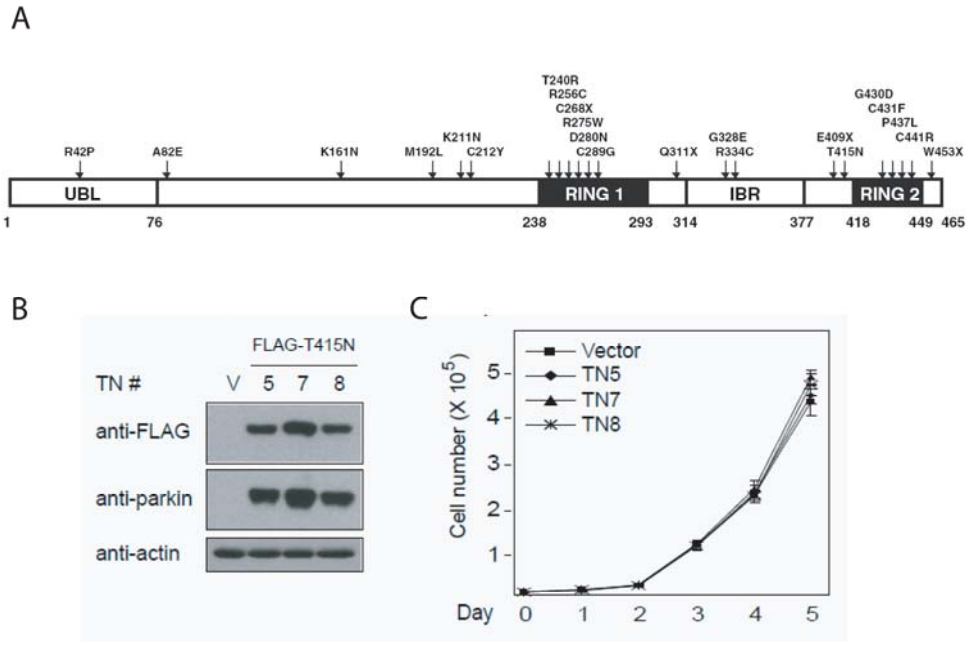

Figure 3.6 Over expression of T415N mutant parkin in U-87MG glioma cells do not affect their rate of cellular proliferation as compared to the vector control.
(A) Schematic representation of parkin protein illustrating the positions of the various point mutations of parkin (B) Anti-FLAG and anti-parkin immunoblots of total lysates prepared from U-87MG vector control (V) and T415N mutant parkin-expressing stable clones (#5, 7 & 8). Equal loading of the different lysates was verified by anti-actin immunoblotting (C) Line-graph showing the percentage of cells undergoing cell proliferation in U-87MG vector control and T415N mutant parkin-expressing stable cell lines. This experiment is repeated at least three times.

3.2.6 Parkin expression in U-87MG cells reduces their ability to generate tumor *in vivo*

Although I have shown that functional parkin is capable of suppressing glioma growth *in vitro*, there is a need to ascertain its ability to do so *in vivo*. Accordingly, I examined the effects of parkin over-expression on the ability of U-87MG cells to generate solid tumor *in vivo*. An intracranial glioma model (n = 5 for each group), which involved the injection of parkin-expressing or control U-87MG cells into the cerebral cortex of NOD-SCID mice, was used for this purpose. I have elected to use this model as unlike flank tumor model, the intracranial model better recapitulates the features of brain cancer. At four weeks

post-injection, I observed the appearance of macroscopic tumors in four out of five dissected brains of mice injected with vector control U-87MG cells, but none in those injected with parkin-expressing U-87MG cells (Fig. 3.7A) or vehicle alone (not shown). The formation of the macroscopic tumors was the end result of the growth of the tumor cells along the injection tract created when implanting the tumor cells. Consistent with this, the average weight of brains harvested from all five mice injected with parkin-expressing U-87MG cells is significantly reduced compared to those harvested from control mice (Fig. 3.7C). Further, histological examination of brain sections derived from these mice revealed that NOD-SCID mice injected with U-87MG vector control cells via the intra-cranial route developed visibly larger tumor in the brain at the end of the experimental period compared to those injected with U-87MG cells stably expressing parkin (Fig. 3.7B). Taken together, my results strongly support a negative role for parkin in glioma cell proliferation.

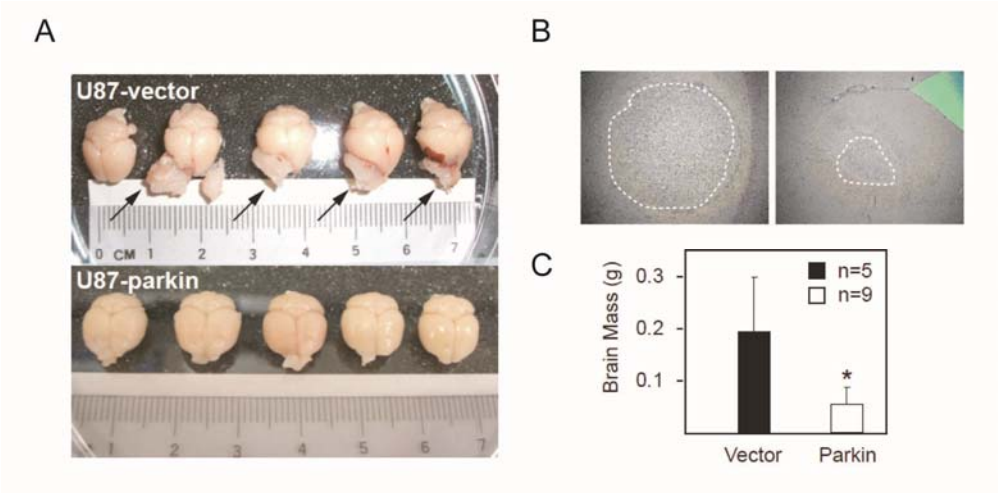

Figure 3.7 Parkin expression in U-87MG cells reduces their ability to generate tumor *in vivo*. (A, top) Digital images showing macroscopic glial tumors (arrows) that developed in the brains of NOD-SCID mice 4 weeks after being injected with U-87MG vector control cells via the intra-cranial route. (A, bottom) In contrast, mice injected with U-87MG cells stably expressing parkin show no obvious signs of macroscopic tumors.

(B) H&E stained sections showing that NOD-SCID mice injected with U-87MG vector control cells (left) via the intra-cranial route that do not exhibit macroscopic tumors developed visibly larger tumor in the brain after 4 weeks, compared to those injected with U-87MG cells stably expressing parkin, as indicated (right). (C) Masses of brains between NOD-SCID mice 4 weeks after being injected with U-87MG vector control cells and U-87MG cells stably expressing parkin. Images shown above are of the same magnification.

3.2.7 Parkin expression in U-87MG cells exhibit significantly improved survival of NOD-SCID mice as compared to U-87MG vector control

As an extension of the *in vivo* study, I repeated the above experiment but allowed injected mice from different groups (i.e. U-87MG-vector, U-87MG-parkin #7 and #19; n = 10 for each group) to live beyond four weeks to examine their respective survival profile. I found that whereas NOD-SCID mice harbouring glioma generated from U-87MG-vector control cells readily succumb to the tumor, those injected with U-87MG-parkin #7 exhibit significantly better survival (Fig. 3.8A). Curiously, the U-87MG-parkin #19 group showed a mortality curve that is between vector and U-87MG-parkin #7 groups, but with a profile tending towards and not significantly different from the vector group (Fig. 3.8A). At post-mortem analysis, I found that tumor derived from U-87MG-parkin #19 had lost much of its parkin expression over time, which likely accounted for its survival profile, whereas those derived from U-87MG-parkin #7 exhibit robust parkin expression even after prolonged periods *in vivo* (Fig. 3.8B). Thus, parkin expression appears to correlate inversely with cancer mortality.

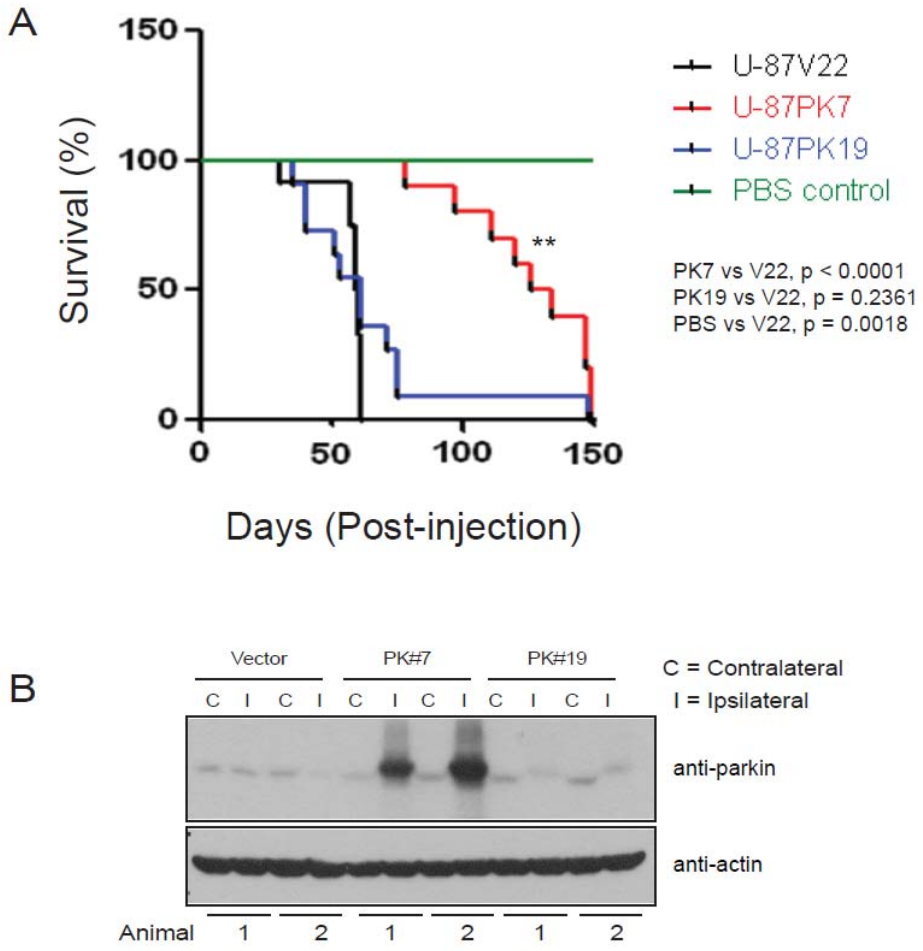

Figure 3.8 Parkin expression correlates inversely with cancer mortality in a mouse model of glioma. (A) Kaplan-Meier curves depicting the mortality of mice injected with U-87MG cells stably expressing vector (V22) or parkin (PK7 and PK19), as indicated. Mice injected with vehicle alone (PBS) act as control for the experiment. (B) Anti-parkin immunoblot of brain lysates prepared from 2 representative animals from each group. The blot was stripped and reprobed with anti-actin to reflect loading variations. "Ipsilateral" refers to tumor-harboring side of the brain while "Contralateral" refers to the non-injected side. Note that parkin expression is dramatically diminished in lysates derived from the ipsilateral brains of mice injected with U-87MG-parkin #19 compared to those injected with U-87MG-parkin #7.

3.3 Discussion

The main finding of my results chapter here is that functional parkin expression in otherwise parkin-deficient breast cancer and glioma cells exerts significant negative effects on their respective rate of proliferation. At the same

time, I also found that parkin expression may reduce glioma-associated mortality, at least in animal models. Taken together, my results are therefore consistent with the original suggestion by Cesari et al that parkin may act as a tumor suppressor.

Despite a consistent association between parkin expression alterations and cancers, the pace of research surrounding the role of parkin in cancer continues to lag far behind investigations that seek to understand its role in neurodegeneration (Veeriah et al., 2010). Indeed, only a few groups thus far have reported the functional consequence of parkin expression restoration in cancer cells. By means of a wide spectrum of proliferation assays that include population growth, anti-BrdU-staining, soft-agar colony formation as well as generation of solid tumors in NOD-SCID mice, I show here that parkin is a potent tumor suppressor. Perhaps to overcome this effect by parkin, cancer cells apparently devised ways to down-regulate parkin expression. Indeed, several groups have documented parkin gene alterations and concomitant reduction in parkin transcript abundance in a wide variety of cancers that includes breast, liver, non-small-cell lung and ovarian carcinoma (Cesari et al., 2003, Denison et al., 2003, Picchio et al., 2004, Wang et al., 2004). Here, I have added glioma cells to the list of parkin-deficient cancer cells. Notably, the localization of parkin in these cells is otherwise not grossly affected.

Although an apparent E3-independent activity of parkin that is relevant to cancer has been reported by da Costa et al (da Costa et al 2009), I found here that parkin catalytic activity is essential for its ability to suppress glioma cell proliferation. The RING2 catalytic missense mutant, T415N, completely abolishes the tumor suppressive effects of parkin on glioma cells. Interestingly, T415N is a disease-associated parkin mutant isolated from PD patients that has been

demonstrated to be devoid of catalytic activity (Matsuda et al., 2006, Chew et al., 2011). Supporting this finding, Veeriah and colleagues have identified for the first time several inactivating somatic parkin mutations in GBMs. Like PD-associated parkin mutations, the majority of cancer-associated parkin mutations are found on the RING catalytic box of the protein (Veeriah et al., 2010). Collectively, these results suggest that the expression level of parkin and its catalytic competency are both needed to keep the cell cycle in balance.

In view of reports suggesting that parkin may regulate the cell cycle by means of its ability to control the level of cyclin E, I next sought to determine if parkin can influence the cell cycle program of glioma cells, and if so, whether it involves cyclin E. Aspects on how parkin can potentially regulate glioma cell cycle will be discussed in the next chapter. Because my above results also reveal a potential relationship between parkin expression and survival of the outcome of glioma-bearing animals, I was interested to see if this relationship holds true for human glioma patients, which will be discussed in chapter 5.

CHAPTER 4

PARKIN MITIGATES CELL CYCLE PROGRESSION THROUGH REGULATION OF CELL CYCLE REGULATORY MACHINERY AND PI3K/AKT CELLULAR SURVIVAL PATHWAY

4.1 Overview

I have demonstrated in the previous chapter that parkin is capable of mitigating the rate of cellular proliferation of U-87MG glioma cells both *in vitro* (using the simple cell count, BrdU incorporation assay, soft-agar colony assay) as well as *in vivo* (using the non-obese diabetic-severe combined immunodeficiency [NOD-SCID] intra-cranial mouse model). The next step would be to determine i) at which stage of the cell cycle does parkin affects, ii) the cell cycle regulatory proteins that are involved and iii) the mechanism which is responsible for the reduced rate of proliferation in parkin-expressing relative to control U-87MG cells.

As mentioned in the introductory chapter, the cell cycle comprises of 4 stages namely the G1-phase, S-phase and G2/M-phase and progression through these phases are regulated by orderly sequential expression, activation and inhibition of cyclin-dependent kinase (CDK), cyclins and CDK inhibitors (CDKI). In the G1-phase following mitogenic stimulation, cyclin D are synthesized and they bind to CDK4 and CDK6 for activation, which allow for progression of cell cycle through the G1-phase. Towards the end of the G1-phase, cyclin E is induced and it binds with CDK2 to form a cyclin E/CDK2 complex which is essential for transition from G1-phase into S-phase. DNA synthesis during S-phase is

facilitated by an active cyclin A/CDK2 complex. After the DNA synthesis is completed, cyclin A would form a complex with CDK1 to enable the progression of cell cycle through the G2-phase. At the G2/M-phase transition, cyclin A would be degraded and cyclin B would be associated with CDK1 to form a complex which is required for progression through the mitosis stage. Notably, the expression of parkin was previously shown to attenuate the accumulation of cyclin E (Staropoli et al., 2003), which provides a mechanism by which parkin can promote cell cycle arrest at the G1-phase. It is also noteworthy that in gliomas, there is hyperactivation of the PI3K/Akt pathway frequently caused by PTEN mutations and also amplification of growth-promoting signaling cascades, for example through activating mutations in EGF receptors. A combination of dysregulated cell cycle and enhanced mitogenic signaling probably account for gliomagenesis.

Here, I demonstrated that parkin-mediated suppression of glioma growth is related to its ability to promote cell cycle arrest at the G1 phase. Surprisingly, the level of cyclin D1, but not cyclin E, is reduced in parkin-expressing glioma cells. Further, parkin expression also leads to a selective downregulation of Akt serine-473 phosphorylation. Supporting this, cells derived from parkin null mouse exhibit increased levels of cyclin D1 and Akt phosphorylation and divide significantly faster compared to their wild type counterparts, all of which are suppressed following the re-introduction of parkin into these cells. Taken together, my results have therefore shed light onto the mechanism underlying parkin-mediated suppression of glioma growth.

4.2 Results

4.2.1 Parkin expression in U-87MG cells mitigates cell cycle progression in asynchronized U-87MG cell line

As an initial approach to examine whether parkin expression affects the cell cycle profile of U-87MG cells, asynchronous parkin-expressing U-87MG cells together with their respective vector control were analyzed for their distribution in various stages of the cell cycle using propidium iodide. Consistent with their slower growth rate, the percentage of parkin-expressing U-87MG cells at the G1-phase is significantly higher than vector control cells. Reciprocating this phenomenon is a corresponding reduction in the number of parkin-expressing U-87MG cells entering the S-phase and subsequently the G2/M-phase as compared to vector control cells (Fig. 4.1).

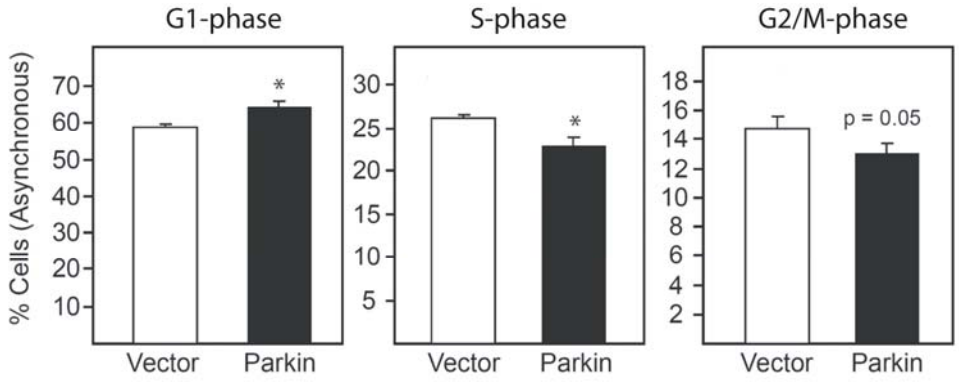

Figure 4.1 Parkin expression in U-87MG cells mitigates cell cycle progression in asynchronized U-87MG cell line. Percentage of asynchronous parkin expressing and vector control cells in the various stages of cell cycle progression, G1-phase, S-phase and G2/M-phase as measured by propidium iodide uptake via flow-cytometry. This experiment is repeated at last three times. n=3 (*$P < 0.05$, Student's *t*-test).

4.2.2 Parkin expression in U-87MG cells mitigates cell cycle progression in synchronized U-87MG cell line

A similar phenomenon as above was observed in cell cycle synchronous parkin-expressing U-87MG cells, which exhibit reduced tendency to enter both the S-phase and the G2/M-phase as compared to the vector control (Fig. 4.2A). This phenomenon is clearly related to the catalytic viability of parkin as mutant parkin (T415N)-expressing U-87MG stable cells fail to delay the entry of cells into the mitotic phase (Fig. 4.2B). Instead, these mutant parkin-expressing cells exhibit a tendency to be distributed in the S-phase and G2/M-phase as compared to their vector control counterparts (Fig. 4.2B).

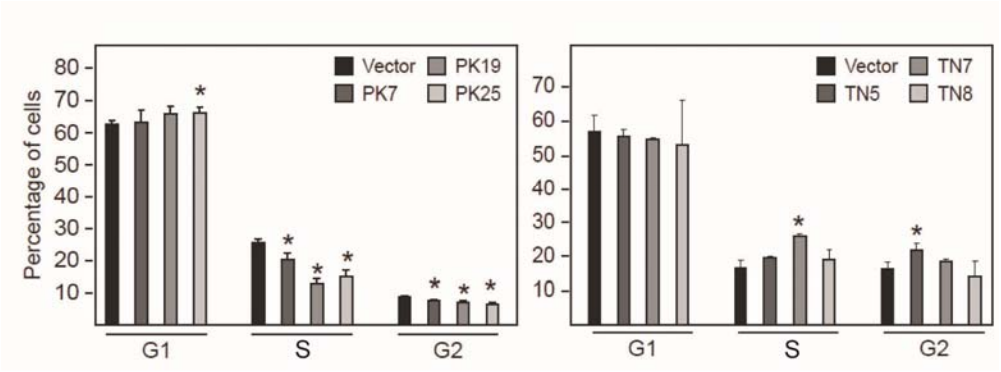

Figure 4.2. Parkin overexpression in U-87MG cells delays entry of synchronized U-87MG cells into mitotic phase. Bar graph showing the percentage of U-87MG-vector and U-87MG-wild type parkin-expressing cells (*left*) or U-87MG-vector and U-87MG-mutant parkin T415N cells (TN5, 7 & 8) (*right*) at different stages of the cell cycle as measured by flow cytometry. n=3 (**P* < 0.05, Student's *t*-test).

4.2.3 Parkin expression in U-87MG cells reduces cyclin D1 but not cyclin E levels

I next examined if enhanced cyclin E proteolysis may account for the cell cycle profile in U-87MG-Parkin cells. Surprisingly, I did not detect an apparent difference in the steady state level of cyclin E between parkin-expressing and control U-87MG cells (Fig. 4.3A). Instead, I found that the expression of cyclin

D1 (which, like cyclin E, is also involved in G1 to S transition), is dramatically repressed in parkin-expressing U-87MG cells (Fig. 4.3A). In contrast, cyclin D1 levels remain largely unaltered in U-87MG cells stably expressing the T415N mutant (Fig. 4.3B), which emphasizes the need for parkin to be functional for it to influence the progression of cell cycle. The presence of a doublet in the cyclin D1 immunoblot is due to the presence of phosphorylated forms of cyclin D1.

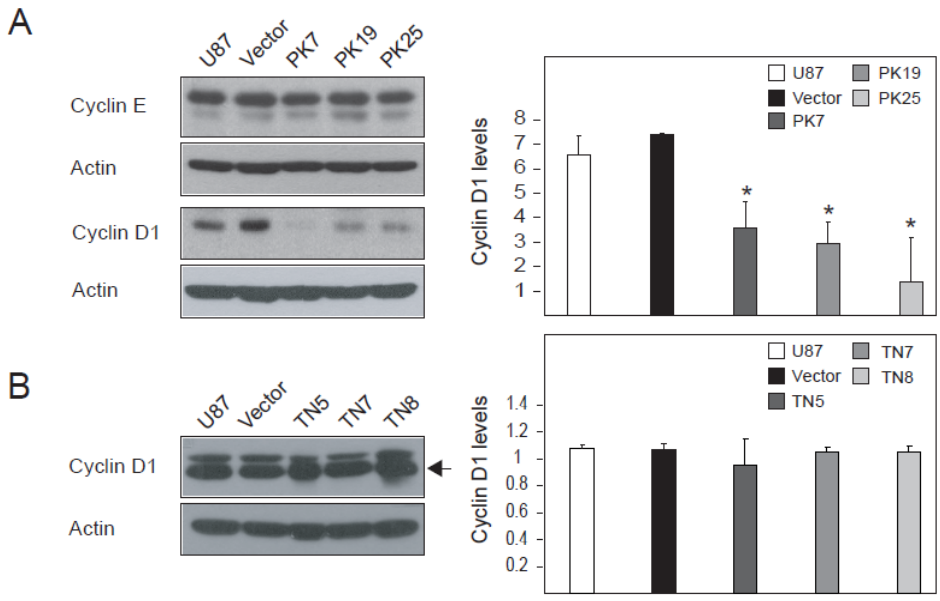

Figure 4.3. Parkin overexpression in U-87MG cells reduces the level of cyclin D1. (A) Immunoblots showing the levels of cyclin E and cyclin D1 in lysates prepared from native U-87MG cells (U-87MG), U-87-vector (Vector) and FLAG-parkin-expressing stable clones (PK7, 19 & 25). (B) As in (A) except parkin-expressing cells were replaced by mutant parkin-expressing (T415N) clones. The anti-cyclin D1 immunblots from three independent experiments were used to derive the relative densitometric units of cyclin D1 (normalized to respective actin level), which is presented as a histogram on the right. Equal loading of the different lysates was verified by anti-actin immunoblotting. All experiments were performed in triplicates.

Together, these results suggest that cyclin D1 expression, rather than cyclin E, possibly underlies parkin's ability to influence the cell cycle program of glioma cells.

4.2.4 Akt phosphorylation is elevated in glioma cells

As mentioned, over-activation of the PI3 kinase/Akt signaling pathway is a frequent feature of glioma cells. Consistent with this, PTEN-deficient U-87MG, U-373MG and U-251MG cells exhibit elevated levels of phosphorylated Akt compared to T-98G, a PTEN-expressing glioma cell line (Fig. 4.4).

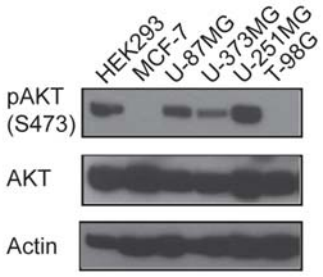

Figure 4.4. Phospho-Akt expression in various glioma cell lines. Immunoblots showing the levels of phoshorylated-Akt (S473) and total Akt in lysates prepared from various commercial cell lines. Three out of four glioma cell lines examined (U-87MG, U373MG & U251MG) exhibit enhanced phospho-Akt level.

4.2.5 Akt Ser-473 phosphorylation is significantly reduced in parkin-expressing glioma cells.

Notably, the complete activation of Akt requires phosphorylation at two amino acids positions namely serine-473 (Ser 473) and threonine-308 (Thr 308). To investigate whether exogenous parkin expression in U-87MG cells exerts any effect on Akt signaling, I immunoblotted lysates prepared from U-87MG parkin and U-87MG vector cells with phosphorylation-specific Akt antibodies and found that the levels of Akt phosphorylated at Ser-473 is significantly reduced in parkin-expressing U-87MG cells compared to control cells (Fig. 4.5). This phenomenon is not due to changes in Akt expression in the presence of parkin (Fig. 4.5), and is not observed when the experiment was repeated with U-87MG cells stably expressing parkin T415N mutant (Fig. 4.5), suggesting again that the catalytic activity of parkin is important and is required for its effect on Akt Ser-473 phosphorylation.

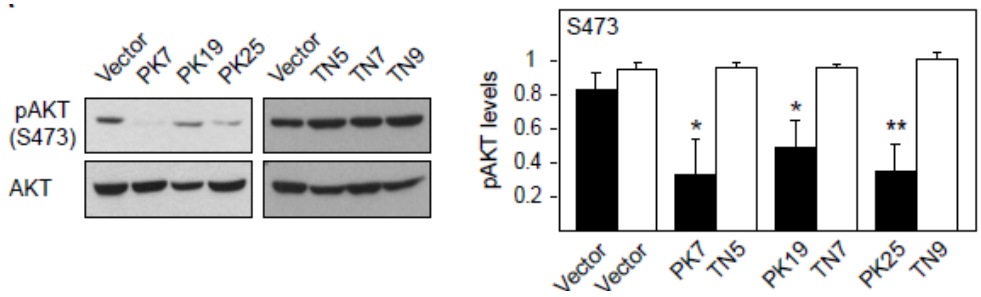

Figure 4.5. Phosphorylation of Akt at Ser-473 is significantly repressed in parkin-expressing U-87MG cells. Immunoblots showing the levels of phoshorylated-Akt (S473) and total Akt in lysates prepared from U-87MG-vector (Vector) and FLAG-parkin (PK7, 19 & 25) or FLAG-parkin T415N (TN5, 7 & 9)-expressing stable clones. The anti-Akt immunblots from three independent experiments were used to derive the relative densitometric units of phospho-Akt (normalized to respective total Akt level), which is presented as a histogram (right).

In contrast, phosphorylation of Akt in U-87MG cells at another site, Thr-308, appears to be unaffected by parkin overexpression (Fig. 4.6A). Consistent with this, the levels of activated phosphoinositide-dependent kinase (PDK) 1, an upstream effector of Akt Thr-308 phosphorylation, is not appreciably altered in parkin-expressing U-87MG cells (Fig. 4.6B).

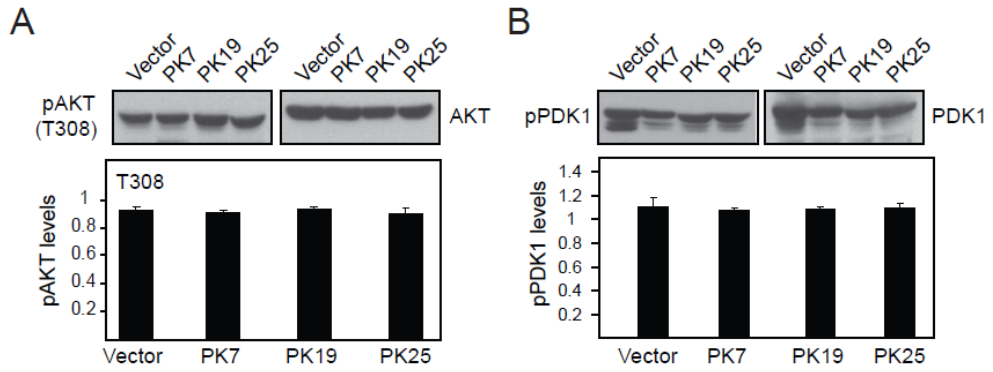

Figure 4.6. Phosphorylation of Akt at Thr-308 is unaffected in parkin-expressing U-87MG cells. (A) Immunoblots showing the levels of phoshorylated-Akt (T308) and total Akt in lysates prepared from U-87MG-vector (Vector) and FLAG-parkin (PK7, 19 & 25) expressing stable clones. The anti-Akt immunblots from three independent experiments were used to derive the relative densitometric units of phospho-Akt (normalized to respective total Akt level), which is presented as a histogram (right). (B) As in (A) except anti-phospho-PDK1 and anti-PDK1 were used to probe the immunoblots.

4.2.6 Parkin downregulates levels of phosphorylated-Akt (Ser 473) under epidermal growth factor (EGF)-stimulation

In gliomas, there is frequent amplification of EGF receptors, which leads to hyperactivation of its tyrosine kinase activity within the cell and thereby enhanced oncogenic signaling. As EGF signalling is known to promote Akt phosphorylation, I was interested to examine whether parkin suppression of Akt Ser-473 persists in the presence of EGF. I therefore looked at the extent of Akt Ser-473 phosphorylation in the presence or absence of EGF stimulation. Under serum-starved condition, the basal level of Ser-473 phosphorylated Akt in parkin-expressing U-87MG cells is expectedly reduced compared to control cells (Fig. 4.7). Upon EGF stimulation, a marked increase in Akt phosphorylation is observed in both control and parkin-expressing U-87MG cells, although the steady-state levels of Ser-473 phosphorylated Akt in U-87MG-Parkin cells remains low relative to U-87MG-Vector control cells (Fig. 4.7).

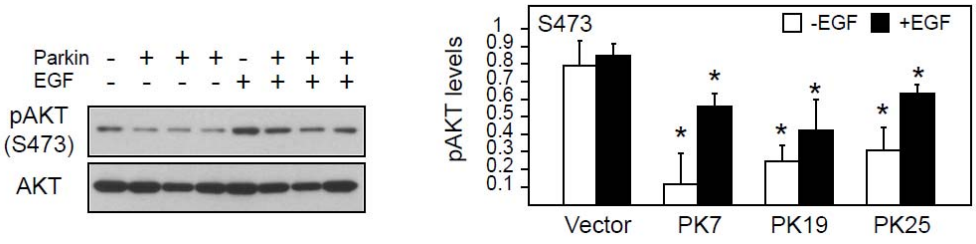

Figure 4.7 Parkin downregulates levels of phosphorylated-Akt (Ser 473) even under epidermal growth factor (EGF)-stimulated condition in U-87MG cell line (A) Anti-phosphorylated Akt (Ser 473) and anti-Akt immunoblots of total lysates prepared from U-87MG vector control (vector) and parkin-expressing stable clones (PK7, PK19 & PK25) under non EGF-stimulated and EGF-stimulated (30ng/ml, 2mins) conditions. (B) Bar-graph depicting densitometric readings of normalized levels of phosphorylated Akt (Ser 473) against unphosphorylated-Akt in various U-87MG vector control (Vector) and parkin-expressing stable cell lines (PK7, PK19 & PK25) These experiments were performed at three times. (*$P < 0.05$, Student's *t*-test).

Collectively, these results show that parkin-mediated effects on Akt phosphorylation works both in the absence or presence of growth factor stimulation. At the same time, the results also suggest that parkin-mediated suppression of glioma cell growth is in part contributed by its ability to regulate growth factor-dependent or independent PI3 kinase/Akt signaling pathway via the downregulation of Akt Ser-473 phosphorylation.

4.2.7 Parkin catalytic mutant T415N does not affect the levels of phosphorylated-Akt (Ser 473) under epidermal growth factor (EGF)-stimulated condition in U-87MG cell line

In order to determine if the catalytic activity of parkin is responsible for the downregulation of phosphorylated Akt upon EGF stimulation, mutant parkin (T415N) expressing U-87MG were assessed for their levels of phosphorylated Akt before and after EGF stimulation. As shown in figure 4.6, the levels of phosphorylated Akt at Ser 473 position were relatively unaffected between parkin expressing U-87MG cells as compared to the vector controls and they were at comparable levels before and after EGF stimulation.

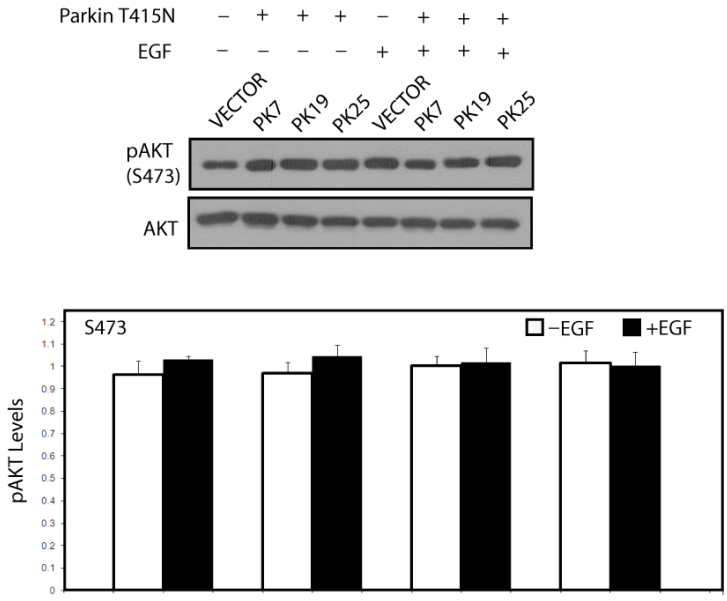

Figure 4.8 Parkin mutant T415N does not affect the levels of phosphorylated-Akt (Ser 473) under EGF-stimulated condition in U-87MG cell line (A) Anti-phosphorylated Akt (Ser 473) and anti-Akt immunoblots of total lysates prepared from U-87MG vector control (vector) and parkin-expressing stable clones (PK7, PK19 & PK25) under non EGF-stimulated and EGF-stimulated (30ng/ml, 2mins) conditions. (B) Bar-graph depicting densitometric readings of normalized levels of phosphorylated Akt (Ser 473) against unphosphorylated-Akt in various U-87MG vector control (Vector) and parkin-expressing stable cell lines (PK7, PK19 & PK25) These experiments were performed at three times. (*$P < 0.05$, Student's *t*-test).

4.2.8 Parkin null fibroblasts exhibit enhanced proliferation rate that is mitigated by parkin expression restoration

To further support the role of parkin as a suppressor of cellular proliferation, I analyzed the growth characteristics of mouse embryonic fibroblasts (MEFs) prepared from wild type and parkin null mice that were reported previously (Von Coelln et al., 2004). As expected, parkin null fibroblasts exhibit significantly enhanced rate of growth over time (Fig. 4.9A). Further, consistent with my results presented in Chapter 3, restoration of parkin expression in parkin -/- MEF (via the introduction of exogenous FLAG-tagged parkin) results in a

substantially slower growth rate. Thus, enhanced cellular proliferation in the absence of parkin appears to be quite a universal feature amongst dividing cells.

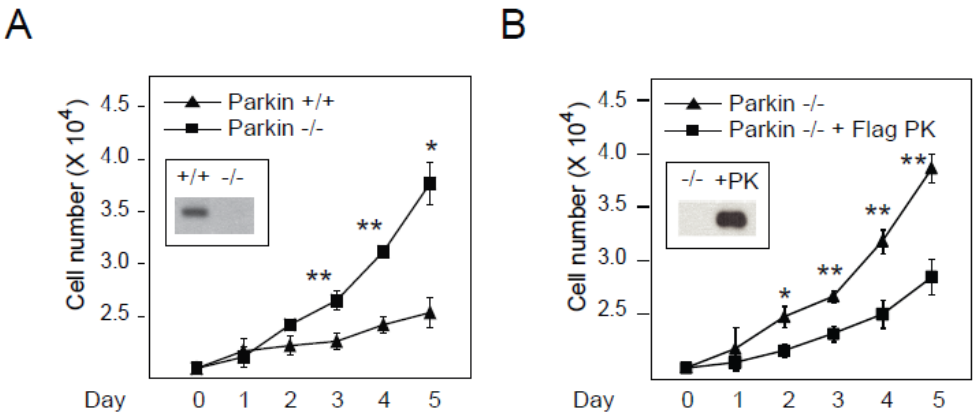

Figure 4.9. Restoration of parkin expression in parkin null fibroblasts reduces their proliferation rate. (A) Graphical depiction of the rate of cell growth of primary embryonic fibroblasts derived from wild type (parkin +/+) or parkin null mice (parkin -/-). (B) As in (a) except that data for parkin +/+ MEFs is replaced by parkin null MEFs ectopically expressing FLAG-parkin. (Inset in both graphs shows anti-parkin immunoblot).

4.2.9 Expression of cyclin D1 and phospho-Akt are upregulated in parkin null fibroblasts but is suppressed following parkin expression restoration.

Supporting my observations above, parkin -/- MEFs also show elevated levels of cyclin D1 and phospho-AKT (S473) (Fig. 4.10A). These observations were essentially duplicated in MEFs derived from a separate line of parkin null mice [generated by means of a targeted deletion of *parkin* exon 3 (Fujiwara et al., 2008)] (Fig. 4.10B), suggesting that my observations are not unique to a particular parkin KO line.

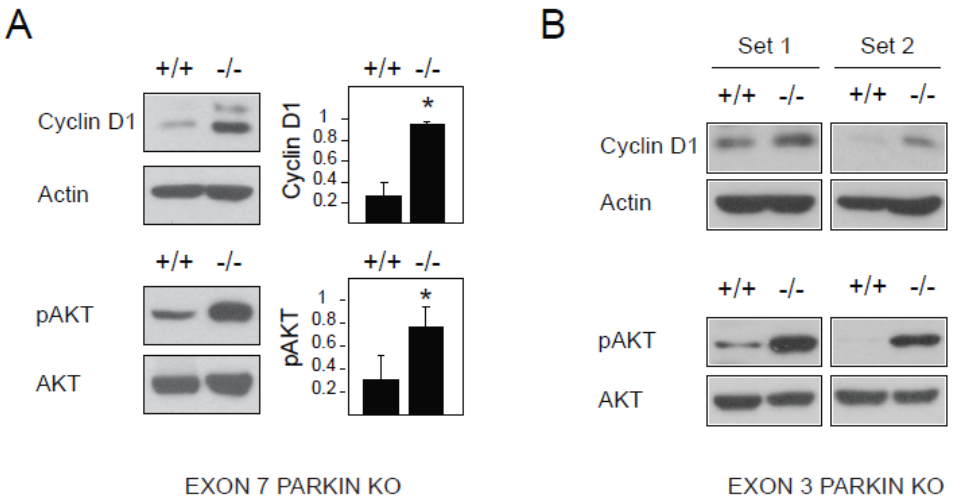

Figure 4.10. Parkin null MEFs exhibit enhanced expression of cyclin D1 and phospho-Akt (A) Immunoblots showing the levels of cyclin D1 (top) and phospho-Akt (S473) (bottom) in parkin +/+ and -/- MEFs. These experiments were repeated at least three times and the relative densitometric units of cyclin D1/actin and phospho-Akt/Akt in parkin +/+ and parkin -/- MEFs are presented as histogram alongside their respective immunoblots. (B) Immunoblots showing the levels of cyclin D1 (top) and phospho-Akt (S473) (bottom) in parkin +/+ and -/- immortalized MEFs derived from exon 3-deleted parkin mice (see text). These experiments were duplicated.

Importantly, restoration of parkin expression in parkin -/- MEF results in a significant reduction in the expression of cyclin D1 and phospho-AKT (S473) (Fig. 4.11).

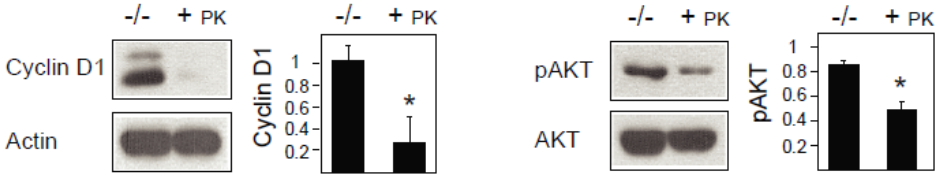

Figure 4.11. Parkin expression restoration in parkin -/- MEFs suppresses expression of cyclin D1 and phospho-Akt (A) Immunoblots showing the levels of cyclin D1 (top) and phospho-Akt (S473) (bottom) in parkin -/- MEFs ectopically expressing FLAG-parkin. These experiments were repeated at least three times and the relative densitometric units of cyclin D1/actin and phospho-Akt/Akt in parkin -/- and parkin -/- (+ FLAG-parkin) MEFs are presented as histogram alongside their respective immunoblots.

Taken together, my results support an inverse association between parkin function and cellular proliferation, and identified cyclin D1 and phospho-Akt (S473) as key common denominators of the functional relationship between parkin and cellular growth that is relevant to gliomagenesis.

4.3 Discussion

In the earlier chapter, I have shown that the expression of parkin in otherwise parkin-deficient glioma cells mitigate their rate of cellular proliferation. Here, I went on to determine if this parkin-induced suppression of glioma cell proliferation is due to its influence on the cell cycle program. My study presented in this chapter revealed that parkin is indeed capable of exerting a negative effect on the cell cycle program of U-87MG cells but curiously through the down-regulation of cyclin D1 instead of cyclin E expression

Previously, Staropoli and colleagues have shown that the deficiency of parkin potentiates the accumulation of cyclin E protein in cultured postmitotic neurons exposed to the glutamatergic excitotoxin kainate, suggesting that the cell cycle regulator, cyclin E, could be regulated by parkin in neurons (Staropoli et al., 2003). Further to this, expression of wild type parkin (but not mutant parkin lacking exon 3-4) was shown to degrade cyclin E in HEK293T cells (Ikeuchi et al., 2009). These lines of evidence suggest the ability of parkin to negatively regulate the levels of cyclin E and thereby promoting the cells to halt at the G1-phase. I therefore examined the levels of cyclin E in parkin-expressing glioma cells. Unexpectedly, my results suggest that cyclin E is not the critical player underlying parkin-mediated effects on glioma cells. However, it is noteworthy to highlight that we have previously observed no significant change in cyclin E

expression between parkin-deficient and parkin-expressing breast cancer cells (Tay et al., 2010). Moreover, cyclin E levels are also not appreciably altered in cells or tissues derived from parkin null mice relative to control (Fu et al., 2004).

Instead of cyclin E, cyclin D1 appears to be the important parkin-linked cell cycle factor in glioma cells. Supporting this, the level of cyclin D1 in parkin-expressing U-87MG cells is significantly reduced both at the level of mRNA transcript and protein. As cyclin D1 induction is considered a rate-limiting step in cell cycle progression through the G1 phase (Fu et al., 2004), its suppression by parkin is expected to impact on the rate of cellular proliferation, which is essentially what I have observed. Indeed, both parkin-expressing asynchronous and synchronous U-87MG cells exhibit a higher tendency to accumulate in the G1 phase. In contrast, glioma cells that express a catalytic mutant of parkin that does not exert any observable effects on cyclin D1 level did not show such a characteristic. Together, these findings suggest that parkin acts on cyclin D1 to regulate the cell cycle program in glioma cells.

I next went on to determine if parkin would affect any important pathways that have been implicated in the gliomagenesis. The PI3K/Akt survival pathway is one of the major survival pathways in gliomagenesis is in caused by frequent PTEN mutations in gliomas especially glioblastoma multiforme (GBM) which lead to the hyperactivation of the PI3K/Akt signaling pathway that promotes cell survival. Maximum activation of Akt requires T308 phosphorylation by PDK1 and S473 phosphorylation by PDK2, a kinase whose exact identity remains rather obscure although biochemical studies suggested mTOR complex 2 as a likely candidate (Hresko et al., 2005). Interestingly, the expression of wild type parkin reduced the levels of phosphorylated Akt specifically at serine 473 position but

not at threonine 308 position, suggesting that parkin acts on PDK2 instead of PDK1. Consistent with this, the levels of PDK1 in parkin-expressing glioma cells are comparable to their control counterparts. In addition, the catalytic activity of parkin was found to be required for this ability as catalytically inactive mutant parkin (T415N) does not reduce the level of phosphorylated Akt at serine 473 position.

One of the main factors that contribute to cancer cell growth is oncogenic signaling caused by mutated forms of receptor tyrosine kinase. EGFR gene amplification occurs in approximately 40% of all known GBM and this usually leads to enhanced EGF signaling and hyperactivation of its tyrosine kinase activity within the cell contributing to oncogenic signaling Even under EGF stimulation conditions, parkin-expressing U-87MG cells had reduced level of phosphorylated Akt (S473) as compared to the vector control. Notably, parkin exerts its effect on Akt S473 phosphorylation in quiescent cells as well as in those treated with EGF. This observation is in contrast to a previous report by Fallon and colleagues who demonstrated in COS-7 and HEK293 that parkin-mediated monoubiquitination of the adaptor protein Eps15 inhibits its ability to initiate receptor down-regulation and leads to enhanced EGF receptor signaling as well as downstream EGF-induced Akt signaling (Fallon et al., 2006). Similarly, we have also reported an apparent increase in Akt S473 phosphorylation in parkin-expressing MCF-7 cells compared to control (Tay et al., 2010). I am therefore puzzled by this discrepancy but noted that my current observation in U-87MG cells is reproducible in MEFs prepared from wild type and parkin null mice, suggesting that parkin-mediated effects on Akt signaling may be dependent on the cell type examined. Notwithstanding this, over-activation of Akt signaling is a

frequent feature of tumors including gliomas. That parkin can down-regulate Akt signaling in U-87MG cells would offer a mechanism underlying its tumor suppressor function. In addition, parkin expression in U-87MG cells was shown to down-regulate levels of phospho-GSK3β and total GSK3β proteins (results not shown).

Following these sets of exciting data, I wanted to have a more comprehensive view of how parkin would affect the global regulation of genes, I subjected parkin-expressing and vector control U-87MG cells through a series of microarray experiments and analysis. This is to determine if there were any subset of genes that might perhaps provide us with a clue as to what are the major set of genes regulated by parkin and if possible, to elucidate a set of genes which might perhaps be used as a key signature for potential early diagnosis of glioma cancer and prediction of survivability in patients. The outcomes of my analyses are presented in the next chapter.

CHAPTER 5

PARKIN PATHWAY ACTIVATION PREDICTS SURVIVAL OUTCOME OF GLIOMA PATIENTS

5.1 Overview

In the previous two chapters, I have presented results demonstrating that parkin is a negative regulator of glioma cell proliferation and that it exerts its tumor suppressing function directly through influencing components of the cell cycle machinery and indirectly through the down-regulation of the growth-promoting Akt pathway. However, as cancer development is a multi-step process involving a wide spectrum of factors, it is conceivable that parkin's effect on glioma growth is not limited to the above pathway and may involve other players. I was therefore naturally interested to know the global gene expression changes in glioma cells triggered by parkin. Because my in vivo data suggest that parkin expression may also help improve the survival outcome in animals with gliomas, I was at the same time curious to know if the same is true in human glioma patients and if there exists a "parkin signature pathway" that may help prognosticate cancer survival. Notably, current glioma prognostication usually relies on histo-pathological analysis. Such morphology-based investigation has its limitations as gliomas are increasingly recognized to be molecularly heterogeneous even within the same histological subgroup. A "parkin signature pathway" that can be used as a complementary prognostication tool to histo-pathological analysis will be of obvious clinical value.

Here, I subjected parkin-expressing and vector-control U-87MG cells to microarray analyses using Affymetrix chips and noted significant difference in global gene expression between the two types of cells. Among these, one gene that caught our attention is *VEGFR-2 (also known as KDR)*, whose expression is reduced by nearly 4-fold in U87-parkin compared to vector control. Separately, I found that parkin expression alone appears to correlate inversely with glioma mortality. As maximal and meaningful data mining from micro-array analyses requires expert help from a bioinformatician, I have sought help from Ms. Felicia Ng (a bio-informatician from the Singapore Institute for Clinical Sciences) to further analyze the micro-array data. Based on the changes in gene expression observed between control and parkin-expressing U-87MG cells, we were able to derive a parkin gene signature. Importantly, we show here that the parkin signature consistently stratified patient survival outcome in the 2 major independent datasets with diverse glioma variants, thereby strengthening the significance of the signature initially derived from limited cell line numbers. Taken together, my results strongly established a role for parkin in gliomagenesis, and further suggest that disease progression may be a manifest of parkin pathway inactivation.

5.2 Results

5.2.1 Parkin expression in U-87MG cells significantly affects global gene expression as compared to the vector control

To examine if exogenous parkin expression in otherwise parkin-deficient U-87MG glioma cells will lead to global gene expression changes, 3 parkin expressing U-87MG stables (PK7, PK19, PK25) and 3 respective vector controls (V8, V17, V22) (each in triplicates) were subjected to microarray array analysis using the Affymetrix GeneChip Human Gene 1.0 ST Array and subsequently analysed using the analysis software Biotique XRAY. The principal component analysis (PCA) plot revealed distinctive differential expression of subset of genes between the parkin expressing U-87MG cells and their respective vector control as segregated by the dotted line (Fig. 5.1).

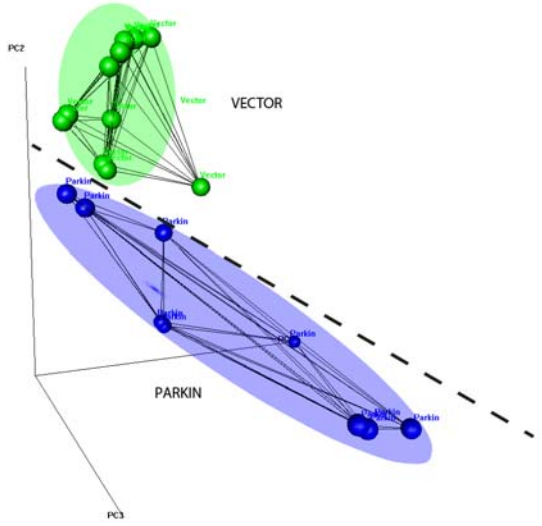

Figure 5.1 Principal component analysis (PCA) plot showing different transcriptional profile of genes between the parkin expressing U-87MG cells and their respective vector controls. Normalized transcriptional profiles of parkin expressing U-87MG (PK7, PK19, PK25) and vector controls (V8, V17, V22).

5.2.2 VEGFR-2 expression are significantly reduced in parkin-expressing glioma cells

A more detailed analysis of the above micro-array data reveals that the most significant alterations are a near 16-fold upregulation of the gene encoding Interleukin 13 receptor and a 10-fold repression of the gene encoding a transmembrane protein (Fig. 5.2). Notably, the expression of cyclin D1 transcript is reduced by about 2-fold in the presence of parkin over-expression (not shown in Fig. 5.2), which is consistent with the results presented in the previous chapter.

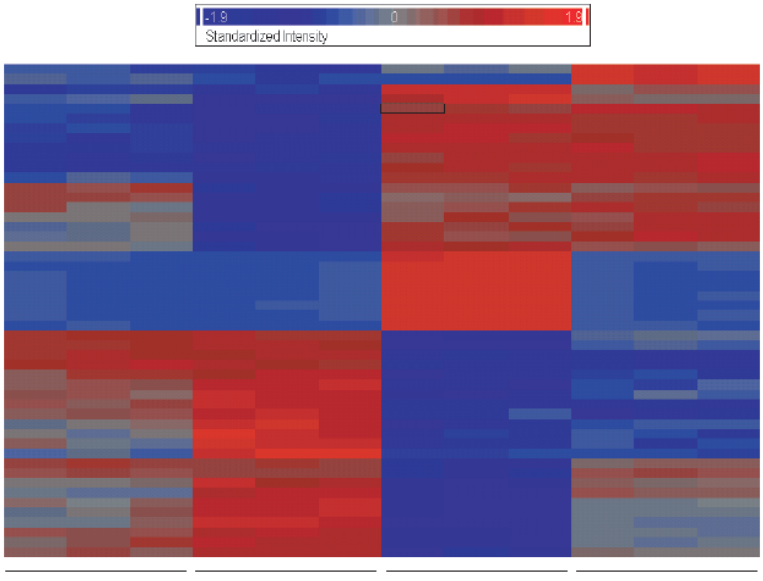

Fold Induction

15.6	NM000640_Interleukin 13 receptor
7.4	NM002422_Stromelysin 1
7.0	NM032797_Apoptosis-inducing factor
5.8	NM000576_Interleukin-1
5.8	NM003784_Serpin peptidase inhibitor
4.9	NM014365_Heat shock 22 kD protein 8
4.8	NM005226_Sphigosine-1 phosphate receptor 3
3.8	NM013231_Fibronectin leucine-rich transmembrane protein 2
3.5	NM004751_Glucosaminyl transferase 3
3.1	NM004079_Cathepsin S

Fold Repression

10.2	NM052913_Transmembrane protein 200A
9.2	NM001001522_Transgelin
5.0	NM152447_leucine-rich repeat & FNIII domain containing 5
4.7	**NM002253_Kinase insert domain receptor (VEGF2)**
4.2	NM020911_Plexin A4
3.9	NM020663_Ras homolog gene family
3.7	NM001613_Actin
3.5	NM002298_L-plastin
2.9	NM001500_GDP-mannose 4
2.7	NM006080_Sema domain

Figure 5.2 Parkin gene signature. Heatmap of the Parkin signature derived from the microarray dataset

However, one gene that immediately caught my attention is *VEGFR-2 (*also known as *KDR)*, whose expression is reduced by nearly 4-fold in U87-parkin compared to vector control (Fig. 5.3A). Aberrant VEGFR-2 expression is associated with a wide variety of cancers, including gliomas. Consistent with the microarray analyses result above, anti-VEGFR-2 immunoblotting revealed a significant reduction in parkin-expressing U87 cells, but not in those that expresses the T415N mutant, as compared to control cells (Fig. 5.3B). Moreover, VEGFR-2 level is elevated in parkin null MEFs (Fig. 5.3C) which decreases upon re-introduction of (exogenous FLAG-tagged) parkin (Fig. 5.3D).

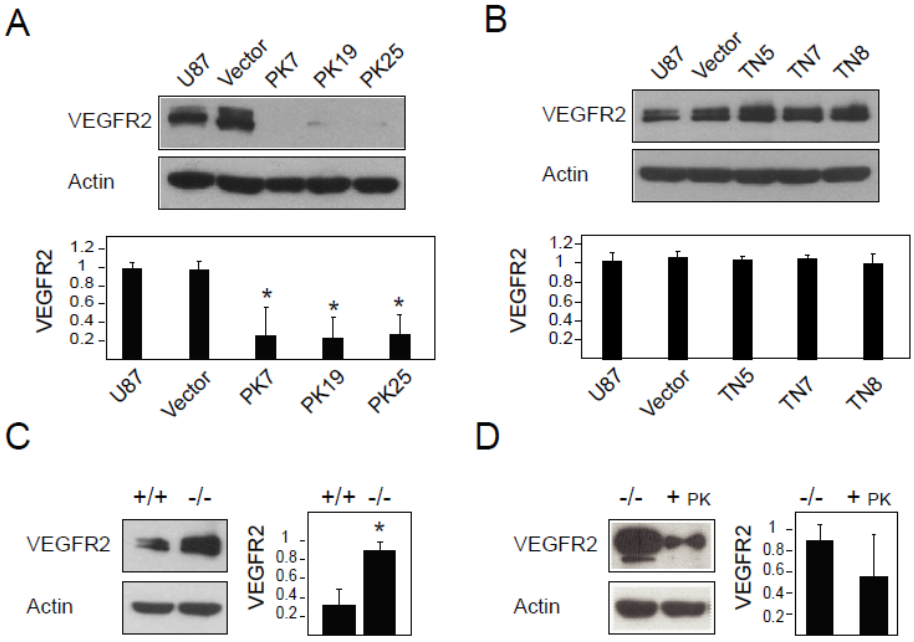

Figure 5.3 VEGFR-2 expression is downregulated in parkin-expressing U-87MG cells. (A) Immunoblots showing the levels of VEGFR2 in lysates prepared from native U-87MG cells (U87), U87-vector (Vector) and U87-FLAG-parkin (PK7, 19 & 25). The anti-VEGFR2 immunoblot from three independent experiments were used to derive the relative densitometric units of VEGFR2 (normalized to respective actin loading control level), which is presented as a histogram (bottom). (B) As in (A) except U87-FLAG-parkin (PK7, 19 & 25)-expressing cells were replaced by U87-FLAG-parkin T415N (TN5, 7 & 8)-expressing cells. (C-D) Immunoblots (left) and histogram (right) showing the levels of VEGFR2 in (C) parkin +/+ and -/- MEFs and parkin -/- and parkin -/- stably expressing FLAG-parkin (+PK) MEFs.

Thus, the expression of VEGFR-2, along with cyclin D1 and phospho-AKT (S473), all of which are known to enhance cellular proliferation, are significantly elevated in glioma cells and MEFs deficient in functional parkin.

5.2.3 Interleukin 13 receptor is significantly upregulated in parkin-expressing-U-87MG cells

As mentioned earlier, the top induced gene in parkin-expressing U-87MG cells is *interleukin 13 receptor-α2* (*IL-13Rα2*). It is noteworthy that IL-13Rα2 is commonly found to be overexpressed in human malignant glioma cell lines and primary tumor cell cultures. Importantly, cytotoxin against IL-13Rα2 was actually found to be highly selective in killing human GBM-derived cells *in vitro* while leaving normal cells including endothelial cells, immune cells and neuronal cells generally unaffected (Husain et al., 2003). This might present a potential mode of therapeutics in which expression of parkin could sensitize gliomas to IL-13Rα2 cytotoxin therapy against gliomas. I was therefore keen to examine if IL-13Rα2 protein expression is correspondingly upregulated in parkin-expressing U-87MG cells. As expected, anti- IL-13Rα2 immunoblotting of cell lysates prepared from the various stable U-87MG cell lines revealed a significant upregulation of the protein in parkin-expressing glioma cells relative to their vector counterparts (Fig. 5.4)

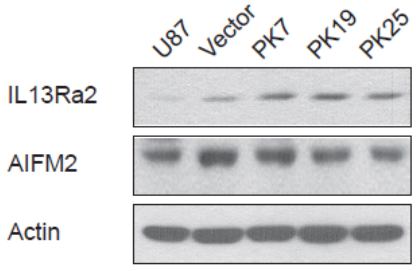

Figure 5.4 IL-13Rα2 expression is upregulated in parkin-expressing U-87MG cells. (A) Immunoblots showing the levels of VEGFR2 in lysates prepared from native U-87MG cells (U87), U87-vector (Vector) and U87-FLAG-parkin (PK7, 19 & 25).

5.2.4 Other notable gene expression changes in parkin-expressing-U-87MG cells

Besides VEGFR2 and IL-13Rα2, two other potentially important genes that were differentially regulated in parkin-expressing U-87MG cells relative to control include FK506 binding protein 5 (FKBP5) and transgelin. Previously, FKBP5 was found to be upregulated in gliomas and inhibition of FKBP5 expression was found to suppress cellular proliferation and overexpression of FKBP5 was found to enhance cell growth (Mikkelsen et al, 2008). In addition, FKBP5 was also found to be involved in the nuclear factor-kappa B (NF-κB) pathway activation in glioma cells through the regulation of expression of IKKα and phosphorylated NF-κB. The inhibition of FKBP5 was shown to sensitize both PTEN-positive and PTEN-negative cells rapamycin-resistance glioma cells to rapamycin treatment (Mikkelsen et al, 2008).

In good agreement with the microarray data, anti-FKBP5 immunoblotting revealed an obvious and significant reduction in the levels of FKBP5 in parkin-expressing glioma cells relative to vector control (Fig. 5.5 A-B). Again, parkin activity is needed here as U-87MG cells expressing the catalytic null parkin mutant failed to promote a reduction in FKBP5 expression (Fig. 5.5 C-D)

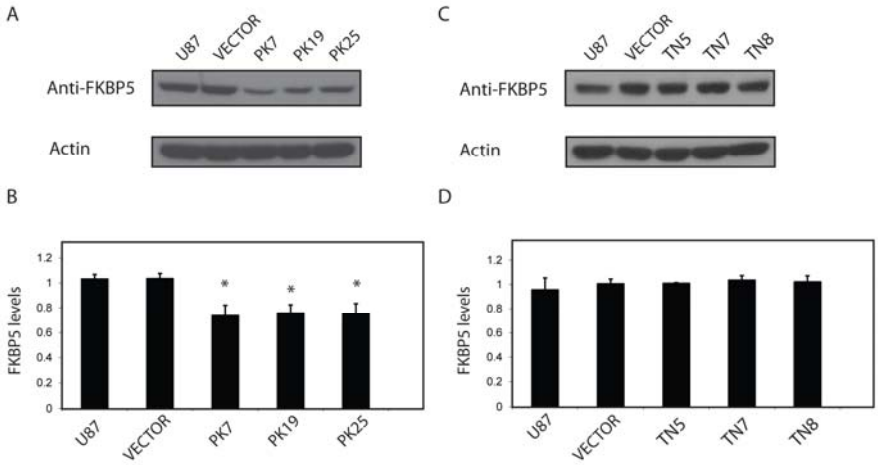

Figure 5.5 Parkin expression downregulates the levels of FKBP5 in U-87MG cell line as compared to the vector control. (A) Anti-FKBP5 immunoblots of total lysates prepared from native U-87MG (U87), U-87MG vector control (vector) and parkin-expressing stable clones (#7, 19 & 25). Equal loading of the different lysates was verified by anti-actin immunoblotting. (B) Bar-graph depicting densitometric readings of normalized FKBP5 levels in various U-87MG native, vector control and parkin-expressing stable cell lines. These experiments were performed three times. (*$P < 0.05$, Student's *t*-test) (C) Anti-FKBP5 immunoblots of total lysates prepared from native U-87MG (U87), U-87MG vector control (vector) and mutant parkin-expressing stable clones (#TN5, TN7 & TN8). Equal loading of the different lysates was verified by anti-actin immunoblotting. (D) Bar-graph depicting densitometric readings of normalized FKBP5 levels in various native U-87MG (U87), U-87MG vector control (vector) and mutant parkin-expressing stable clones (#TN5, TN7 & TN8).

5.2.5 Parkin expression downregulates levels of microRNA-21 (miR-21) and microRNA-155 (miR-155) in glioma cells

MicroRNAs (miRNAs) are a class of small, non-protein coding, endogenous RNAs that are important regulatory molecules in the regulation of gene expression by translation repression, mRNA cleavage and mRNA decay initiated by miRNA-guided rapid deadenylation. In addition to this, recent studies showed miRNAs to be involved in cell proliferation, cell signaling and apoptosis processes (Zhang et al, 2007). MicroRNA-21 (miR-21) was previously identified as an anti-apopototic factor in glioblastomas when it was demonstrated that knockdown of miR-21 in cultured glioblastoma cell lines triggered the caspase activation and associated apoptotic cell death (Chan et al, 2005). miR-21 was previously found to be overexpressed in grade II-IV astrocytomas (Conti et al, 2009) and was shown to promote glioma invasion by targeting matrix metalloproteinase regulators (Gabriely et al, 2008). Besides astrocytomas and glioblastomas, the overexpression of miR-21 was also demonstrated in a wide range of malignancies including breast, colon, gastric, lung, pancreas and prostate cancer (Volinia et al, 2006). Similarly, miR-155 was previously shown to be

overexpressed in a breast cancer (Iorio et al, 2005), lung cancer (Yanaihara et al, 2006), Hodgkin disease (Kluiver et al, 2005), primary mediastinal non-Hodgkin lymphoma (Kluiver et al, 2005) and a variety of lymphomas and leukemias which includes pediatric Burkitt lymphoma (Metzler et al, 2004), chronic lymphocytic leukemia (CLL) (Calin et al, 2005) and acute myeloid leukemia (AML) (Garzon et al, 2008).

Interestingly, the levels of miR-21 and miR-155 both appear to be affected by parkin. Indeed, the expression of parkin in U-87MG cells results in a significant downregulation of the levels of miR-21 by 1.6 folds (p-value < 0.001) as compared to the U-87MG vector controls, as revealed by the microarray data analysis. I have validated this finding by means of real-time PCR which recorded on the average of about 7-fold reduction in miR-21 expression in parkin expressing U-87MG cells as compared to the U-87MG vector controls (Fig. 5.6A). This value is in good agreement to that obtained through microarray.

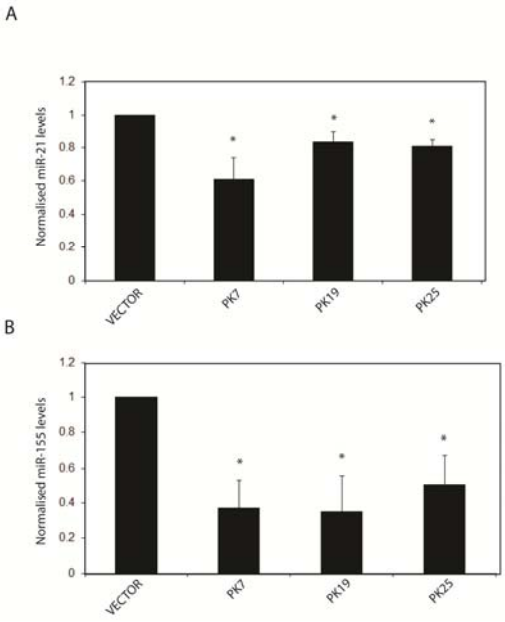

Figure 5.6 Parkin expression downregulates levels of microRNA-21 (miR-21) and microRNA-155 (miR-155) in U-87MG cell line as compared to the vector control as verified by Real-Time polymerase chain reaction (PCR). (A) Bar-graph depicting the normalised real-time quantification of miR-21 levels in U-87MG vector control (vector) and parkin-expressing stable clones (#7, 19 & 25). (B) Bar-graph depicting the normalised real-time quantification of miR-155 levels in U-87MG vector control (vector) and parkin-expressing stable clones (#7, 19 & 25). These experiments were performed three times. (**P* < 0.05, Student's *t*-test).

In a similar fashion, parkin expression in U-87MG cells also significantly reduced the levels of miR-155, in this case by 2.3 folds (p-value < 0.05) and 2.5 folds as revealed respectively by microarray analysis (not shown) and real time PCR (Fig. 5.6B). How parkin expression influences miR-21 and -155 expression is unclear at the moment. Future studies should help elucidate the mechanism involved.

5.2.6 Parkin expression correlates inversely with glioma mortality

I next sought to determine if parkin expression could portend prognosis in human glioma patients. For this purpose, I analyzed patient data from Rembrandt database (Madhaven et al., 2009) and found that that the mean expression of parkin is reduced in various glioma variants including astrocytomas, GBM and oligodendrogliomas (Fig. 5.7).

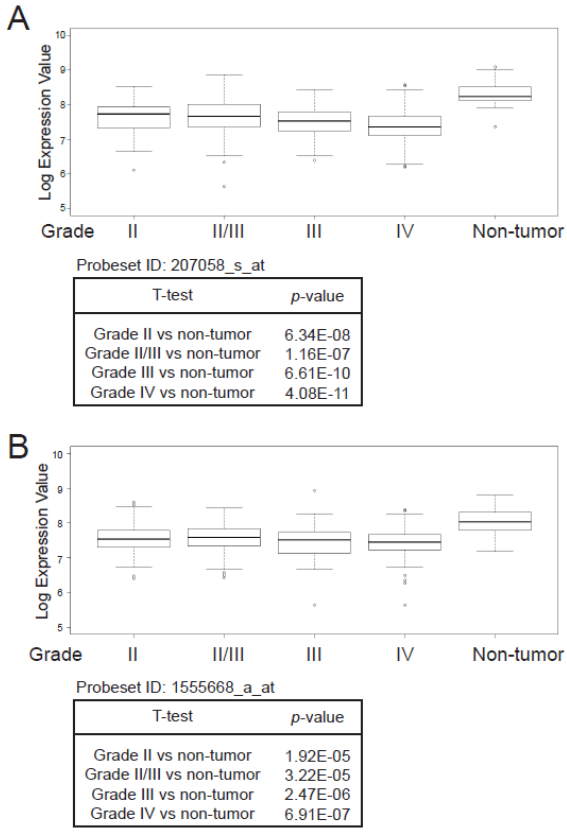

Figure 5.7 PARK2 expression is consistently low in all tumor grades when compared to 'non-tumor'. (A-B) Boxplots show the range of PARK2 log expression values for expressing probesets (A) 207058_s_at and (B) 1555668_a_at in the Rembrandt dataset.

Importantly, Kaplan-Meier analysis revealed that glioma patients with poor parkin expression exhibit significantly higher mortality (Fig. 5.8), which is in agreement with results derived from mouse model that I have presented in Chapter 3.

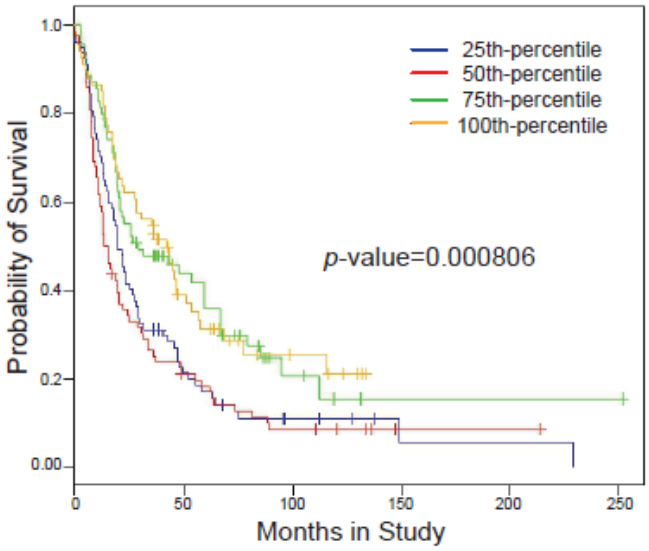

Figure 5.8 Low PARK2 expression portends poor prognosis. Kaplan-Meier plot showing that patients with high PARK2 expression have better survival prognosis compared to patients with low PARK2 expression.

My results thus suggest that parkin expression correlates inversely with cancer mortality and that pathways associated with parkin may affect survival outcome. The next step is to establish whether a parkin signature pathway could be derived from the microarray analysis data that might better interrogate the mortality of glioma patients.

5.2.7 Refining Microarray Data

The initial analysis of my microarray data was done using the Biotique XRAY software. As I was a novice at microarray analysis, I later sought the technical expertise from Ms. Felicia Ng (a bio-informatician from the Singapore Institute for Clinical Sciences) to further analyze the micro-array data. Our

microarray analysis results obtained were relatively consistent in terms of gene expression changes observed between control and parkin-expressing U-87MG cells. Notably, *VEGFR-2* (*KDR*) gene was also featured as a top downregulated gene in parkin-expressing glioma cells (Fig. 5.9)

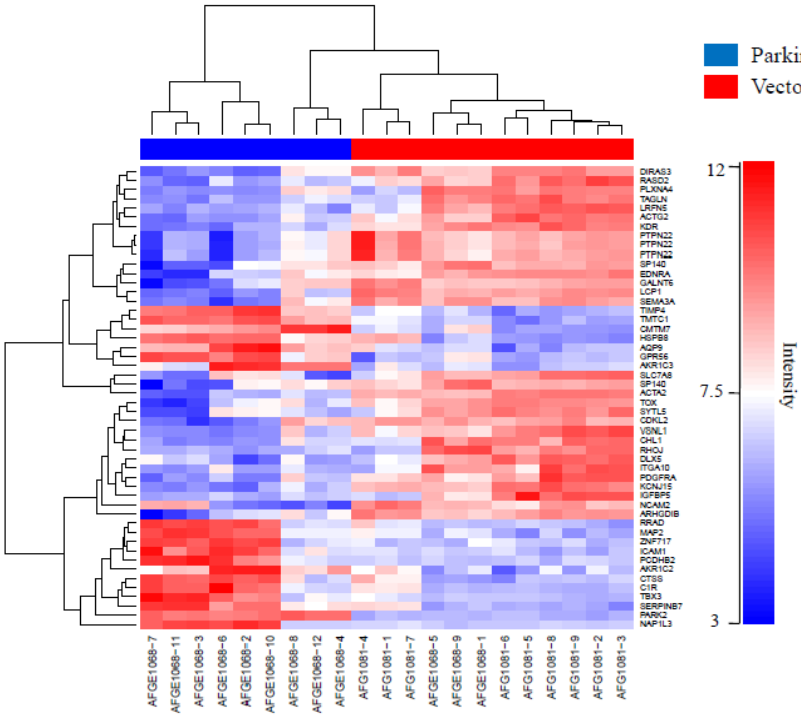

HuGene 1.0 ST v1 Identifier	Gene Symbol	Log FC	HuGene 1.0 ST v1 Identifier	Gene Symbol	Log FC
8130645	PARK2	4.67	8095080	PDGFRA	-1.62
8173917	NAP1L3	2.60	7963313	GALNT6	-1.68
8021623	SERPINB7	2.55	7944082	TAGLN	-1.84
8108683	PCDHB2	2.00	8067985	NCAM2	-1.90
7959102	HSPB8	1.91	7971461	LCP1	-1.94
7996081	GPR56	1.88	8058857	IGFBP5	-2.03
7960744	C1R	1.79	8100393	KDR	-2.10
7966690	TBX3	1.76	7974109	LRFN5	-2.22
7962058	TMTC1	1.72	7934906	ACTA2	-2.43
8088911	ZNF717	1.68	8042788	ACTG2	-2.47

Figure 5.9 Microarray analysis of gene expression changes in parkin expressing U-87MG cells are compared to their vector controls. (Top panel) Heatmap analysis of the differential gene expression between parkin expressing U-87MG and their respective vector control. (Bottom panel) Top 10 repressed or induced genes upon parkin over-expression. The log fold change difference is as shown. Gene symbol description can be found in table 5.1 below.

5.2.8 Parkin gene signature predicts survival outcome of human glioma patients

We next sought to (i) determine if differentially regulated genes between parkin-expressing and non-expressing U-87MG cells could stratify patient survival in public clinical glioma databases, and (ii) evaluate if this "parkin signature" could serve as a metric to stratify gliomas of distinct clinical grades effectively by examining its enrichment pattern in the datasets.

Recently, The Cancer Genome Atlas (TCGA) effort demonstrated that GBM can be molecularly sub-typed into groups distinguished by genetic aberrations and gene expression (Verhaal et al., 2010). These subtypes correlate with unique clinical profiles, illustrating that gene expression drives GBM disease progression and survival outcome. This provides a basis for our approach in evaluating gene expression perturbations arising from parkin-expressing and non-expressing U-87MG cells. We carried out the following: Using a larger collection of 802 probesets (top 20 ranking genes shown in Fig. 5.9), we determined by Gene Set Enrichment Analysis, the biological pathways enriched between parkin-expressing and non-expressing U-87MG cells. In particular, this 802-gene signature enriched for pathways in "programmed cell death" and "apoptosis" (Fig. 5.10). Next, we pared down this gene list with more stringent criteria and defined survival correlations using an adaptation of the "Connectivity Map" method (Lamb et al., 2006). While the Connectivity Map method was originally conceptualized to connect biological states of interest (represented by a gene signature) to the action of small molecule therapeutics (a database of reference profiles), our study attempts to make a connection between the biological state of parkin-expression to patient tumor expression profiles. A recent study (Ooi et al.,

2009) has shown that this method can be used effectively to score tumor expression profiles that correspond to the degree of oncogenic pathway activation.

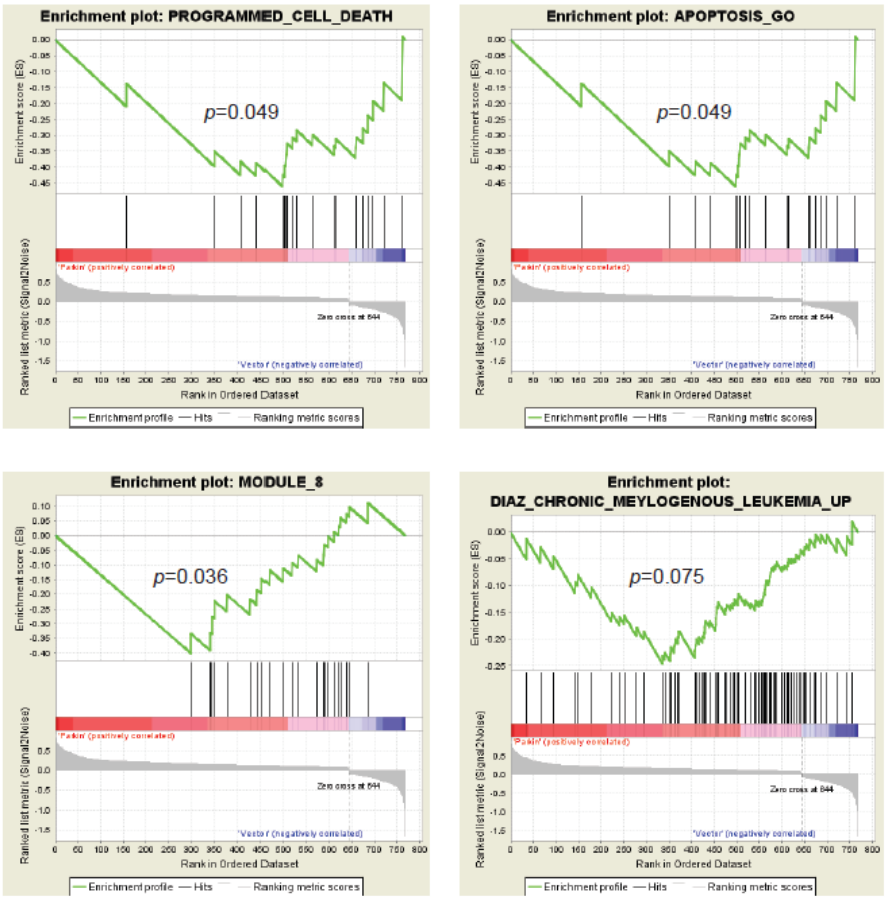

Figure 5.10. Parkin gene set enrichment and network analysis. Significantly enriched gene sets discovered using GSEA on the 802 differentially expressed probesets between Parkin-expressing and Vector samples.

Likewise, we have adapted the Connectivity Map methodology to score GBM expression profile databases based on the extent of pathway activation associated with the parkin signature. This strategy comprises 4 steps: (i) First, we defined a "parkin signature" – a set of genes exhibiting altered expression after specific perturbation of the parkin gene in our well-defined *in vitro* system, (ii) Second, we generated 2 databases of reference gene expression profiles from two major public clinical glioma databases – Rembrandt and Freije (Madhaven et al.,

2009, Freije et al., 2004), (iii) Third, using a non-parametric, rank-based pattern matching procedure, we mapped the parkin signature onto each patient gene expression profile and calculate activation scores based on the strength of association to the parkin signature, and finally (iv) the patients were sorted according to their pathway activation scores. Accordingly, we determined genes differentially regulated between parkin-expressing and non-expressing U-87MG cells, with FDR~0 and $\log_2$FC≥1.2, generating a "parkin signature" This signature consistently stratified patient survival in the 2 clinical databases (see table below and Fig. 5.11).

Dataset	# of probes	# of samples	(+)	(-)	total (+)(-)	%(+)(-)	Log Rank *p*-value	Hazard Ratio	Cox *p*-value	Hazard Ratio	Cox *p*-value
								Multivariate		Univariate	
Rembrandt	111	298	38	51	89	29.87	7.69E-09**	0.382 (0.192 - 0.759)	0.006*	0.215 (0.123 - 0.375)	5.7E-08**
FreijeA	61	85	8	7	15	17.65	0.00284*	0.143 (0.022 - 0.917)	0.04*	0.110 (0.02 - 0.586)	0.00976*

(+) represent patients with likeness to parkin signature; (-) represent patients with inverse gene expression relationship to parkin signature.

Of note, the parkin signature successfully assigned significant activation scores to 20-30% of patients, with the rest of patients showing no association. Further, in both databases, we observed that patients with a positive activation score (i.e. ROS+; strong concordance with parkin signature) tended to align with lower tumor grades and/or the oligodendroglioma histology, frequently associated with better prognosis (Caimcross et al., 1998). In contrast, patients with a negative activation score tended towards grade IV. Finally, we determined the prognostic power of the parkin signature using a Cox regression model. Our data indicate that the parkin signature is an independent predictor of glioma disease progression and survival, in addition to age and histology which are the current clinical indicators (Louis et al., 2007). Further, we observed that in both databases, the parkin signature predicted survival outcome better than histology alone. Taken together,

we provide strong evidence that parkin expression correlates inversely with glioma mortality and its pathway activation is predictive of survival outcome.

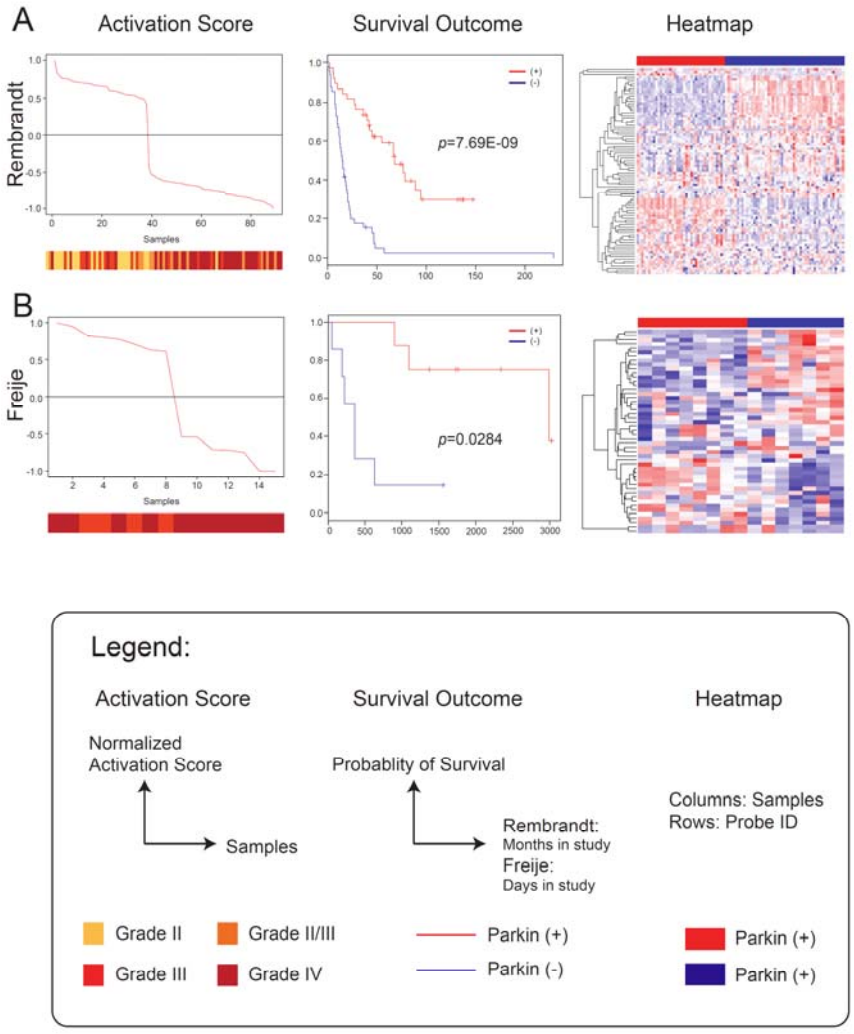

Figure 5.11 Parkin gene signature is predictive of survival outcome of human glioma patients. The 50-gene signature stratifies patient survival in 3 public glioma databases: (A) Rembrandt and (B) Freije. Activation scores denote ranking of gene signature likeness to clinical database gene expression, and patient survival is linked to this ranking. A positive score represents patients with similarity to parkin-overexpression, while a negative score denotes patients with inverse relation, i.e. similarity to vector-only cells. The tumor grade is scored for individual patients below the activation score chart. Survival data are plotted as Kaplan-Meier curves. (+), concordance of parkin-overexpression gene signature with patients' gene expression and consequently better survival; (-), inverse relation of parkin-overexpression (i.e. similarity to vector-only expression) with clinical database gene expression and consequently poorer survival. Heatmaps illustrate the expression patterns of genes in individual patients.

5.3 Discussion

In the previous chapter, parkin was shown to mitigate cell cycle progression of a representative glioma cell line, U-87MG, through the reduction of cyclin D1 and phosphorylated Akt (S473). Following these results, I wondered what would be the global subset of genes that could be regulated by expression of parkin in U-87MG cells. From the microarray analysis, the expression of parkin was found to differentially regulate 802 genes and from which cyclin D1 was also found to be transcriptionally downregulated by about 2 fold which correlated with the reduction in cyclin D1 levels as mentioned in the chapter 4. In addition, the angiogenic VEGFR2 was found to be downregulated by about 4.7-folds in parkin expressing U-87MG cells as compared U-87MG native and vector control cells. Although predominantly found on endothelial cells, VEGFR have also been detected on cancer cells including gliomas, suggesting a possible autocrine effect on their growth (Masood et al., 2001) Importantly, autocrine regulation of GBM cell cycle progression and viability through VEGF-VEGFR2 interplay involves co-activation of the PI3/Akt pathway (Knizetova et al., 2008) which parkin appears to regulate. Upon further examination, the protein level of VEGFR2 was also found to be consistently downregulated by about 3-folds in parkin expressing U-87MG cells as compared U-87MG native and vector control cells. Importantly, the expression of mutant form of parkin, T415N does not seem to reduce the levels of VEGFR2. This demonstrates that the reduction in the levels of VEGFR2 is dependent upon parkin's catalytic activity.

A number of other differentially expressed proteins and microRNAs like FKBP5, miR-21 and miR-155 were also identified from the microarray analysis. The transcript and protein levels of FKBP5 were found to be reduced as shown by

the microarray data analysis and immunoblotting. FKBP5 was previously found to be upregulated in gliomas and inhibition of FKBP5 expression was found to suppress cellular proliferation and overexpression of FKBP5 was found to enhance cell growth (Mikkelsen et al, 2008). Therefore, the reduction of FKBP5 through the expression of parkin would have profound effects on the rate of cellular proliferation, NF-κB signaling pathway and the sensitization of glioma cells towards activators of autophagy treatments. Further to this, a novel effect of parkin was discovered when it was shown to be able to downregulate the levels of miR-21 by about 1.6 folds and miR-155 by about 2.3 folds accordingly. The downregulation of miR-21 through the expression of parkin could potentially have triggered the caspase activation and associated apoptotic cell death in the gliomas cells (Chan et al, 2005) and reduced glioma invasion by targeting matrix metalloproteinase regulators (Gabriely et al, 2008). The downregulation of miR-155 could increase tumor protein 53-induced nuclear protein 1 (TP53INP1), a nuclear protein able to induce cell cycle arrest and apoptosis through caspase-3 activation (Gironella et al, 2007). Taken as a whole, the multi-mechanistic parkin is potentially able to downregulate VEGFR2, exerts it anti-proliferative effects through the mitigation of cyclin D1 and phosphorylated Akt at serine 473 protein levels. Concurrently, the presence of parkin could also reduce the levels of oncogenic microRNAs like miR-21 and miR-155 and the absence of parkin could facilitate evasion from apoptosis or prevent dephosphorylation of Akt.

In order to determine whether parkin expression correlates with glioma patient prognosis and survivability in a clinical setting, patient data from a public clinical glioma database, Rembrandt (Madhaven et al., 2009) were analyzed and we found that that the mean expression of parkin is reduced in various glioma

variants including astrocytomas, GBM and oligodendrogliomas. But more importantly, the low parkin expression correlates with poor prognosis, which is in agreement with results derived from our mouse model. From the analysis of the microarray data, we generated a "parkin signature" which we showed to be able to accurately predict survival outcome better than histology. And taken as a whole, we provide strong evidence that parkin expression correlates inversely with glioma mortality and its pathway activation is predictive of survival outcome.

CHAPTER 6

GENERAL DISCUSSION AND CONCLUSIONS

The objective of this project is to clarify and understand the role of parkin in gliomagenesis. Upon completion of this project, I have managed to obtain several evidences that strongly support a negative role for parkin in gliomagenesis. Importantly, I have also identified a signature pathway of parkin that is of potential prognostic value. The functional role of parkin in gliomagenesis was elucidated using both parkin expression and knockout studies in both *in vitro* and *in vivo* systems. From these model systems, I was able to demonstrate that parkin expression regulates the cell cycle program and growth-promoting signaling mechanisms of proliferating cells. When used to interrogate available human glioma database, I found that parkin activation pathway is also a predictor of the survival outcome of glioma patients. Taken together, the results presented in my thesis suggest that parkin is a key player in gliomagenesis, which is in addition to its established role in neurodegeneration. In this final chapter of my thesis, I will recap and evaluate the significance of my findings in perspective.

6.1 A role for parkin in gliomagenesis – From brain degeneration to brain cancer

Although a role for parkin in cancers may still come as a surprise to many, the 1.4Mb parkin gene is located within the common fragile site (CFS), FRA6E, a mutational hotspot on chromosome 6 that is frequently deleted in several tumor types including breast, ovarian, kidney and liver cancers (Cesari et al., 2003,

Denison et al., 2003, Picchio et al., 2004, Wand et al., 2004) FRA6E, along with other CFSs such as FRA3B, FRA16D and FRAXB, have been proposed to play a causal role in tumorigenesis and/or cancer progression (Druck et al., 1998) Notably, the FRA3B-associated *FHIT* and the FRA16D-associated *WWOX* genes are commonly deleted or altered in various tumor types. Further, several lines of evidence suggest that functionally, FHIT and WWOX act as tumor suppressors (Bednarek et al., 2001). The residence on FRA6E that the enormous parkin gene takes thus immediately suggests its potential association with cancers. Consistent with this, Cesari *et al* as well as a number of other groups have documented parkin gene alterations and concomitant reduction in parkin transcript abundance in a wide variety of cancers that includes breast, liver, non-small-cell lung and ovarian carcinoma (Tay et al., 2010, Fujiwara et al, 2008, Picchio et al., 2004, Denison et al., 2003). In addition, it was also shown that parkin was deleted in 2 out of 10 GBM patients' tumor samples and 4 out of 10 glioblastoma cell lines using high resolution microarray comparative genomic hybridization and molecular cytogenetic characterization techniques (Mulholland et al., 2006). Significant recurrent focal alterations involving homozygous deletions of parkin were also identified from 206 glioblastomas using three microarray platforms analyzed with multiple analytical algorithms (McLendon et al., 2008). More recently, Veeriah and colleagues have identified for the first time several inactivating somatic parkin mutations in GBMs and other malignancies and showed that cancer-causing parkin mutations impair its ability to promote cyclin E degradation (Veeriah et al., 2009). Collectively, these studies strongly implicate a role for parkin as a tumor suppressor that is relevant to gliomagenesis. Here, I have extended these findings by showing that parkin expression is deficient in several

glioma cell lines and that the restoration of parkin expression in these cells indeed retards their growth.

6.2 Parkin mitigates cell cycle progression at the G1-S phase transition through the downregulation of cyclin D1 level

My study showed that parkin negatively influences the cell cycle program of U-87MG cells but interestingly through the down-regulation of cyclin D1 instead of cyclin E expression. Staropoli and colleagues have previously shown that the deficiency of parkin potentiates the accumulation of cyclin E protein in cultured postmitotic neurons exposed to the glutamatergic excitotoxin kainate, suggesting that the cell cycle regulator, cyclin E, could be regulated by parkin in neurons (Staropoli et al., 2003). Veeriah and colleagues have also shown that somatic non-functional parkin mutations in cancer decrease parkin's E3 ligase activity, compromising its ability to ubiquitinate cyclin E and resulting in mitotic instability. Our results therefore differ from that reported by Veeriah and colleagues although we noted that they have used a different glioma cell line (i.e. T-98G) for their study. It is of importance to highlight that we have previously observed no significant change in cyclin E expression between parkin-deficient and parkin-expressing breast cancer cells (Tay et al., 20109). Moreover, cyclin E levels are also not significantly altered in cells or tissues derived from parkin null mice relative to control (Ko et al., 2005). On the other hand, the level of cyclin D1 in parkin-expressing U-87MG cells is significantly reduced both at the level of mRNA transcript and protein. As cyclin D1 induction is required for cell cycle progression through the G1 phase (Fu et al., 2004), its suppression by parkin is expected to impact on the rate of cellular proliferation, which is essentially what

we have observed. Indeed, both parkin-expressing asynchronous and synchronous U-87MG cells exhibit a cell cycle arrest at the G1 phase. In contrast, the expression of a catalytic inactive mutant of parkin (T415N) in glioma cells does not exert any observable effects on cyclin D1 level. Together, these findings suggest that functional parkin acts on cyclin D1 to regulate the cell cycle progression in glioma cells. Precisely how functional parkin regulates the expression of cyclin D1 is unclear to us at this present moment, although its apparent ability to down-regulate Akt phosphorylation may play a part here. Notably, the Akt pathway is known to enhance G1/S cell cycle progression through the inactivation of GSK3β, which results in increased cyclin D1 level (Liang et al, 2003).

6.3 Expression of catalytically active parkin selectively reduces levels of Akt phosphorylation at Ser 473 in U-87MG cells

Frequent PTEN mutations in gliomas which lead to the hyperactivation of the PI3K/Akt signaling pathway made the PI3K/Akt survival pathway one of the most important cell survival pathways in gliomas (Fan et al., 2010). Maximum activation of Akt requires both T308 phosphorylation by PDK1 and S473 phosphorylation by PDK2, a multi subunit kinase whose exact identity remains rather obscure although biochemical studies suggested mTOR complex 2 as a likely candidate (Hresko et al., 2005). Interestingly, parkin expression leads to a specific reduction in Akt S473 (but not T308) phosphorylation, suggesting that parkin acts on PDK2 instead of PDK1. Consistent with this, the levels of PDK1 in parkin-expressing glioma cells are comparable to their control counterparts. Again, the effect of parkin on Akt S473 phosphorylation requires its catalytic

activity, as this activation step of Akt is not compromised in T415N mutant parkin-expressing U-87MG cells. Notably, parkin exerts its effect on Akt S473 phosphorylation in quiescent cells as well as in those treated with EGF. This observation is in contrast to a previous report by Fallon and colleagues who demonstrated in COS-7 and HEK293 that parkin-mediated monoubiquitination of the adaptor protein Eps15 inhibits its ability to initiate receptor down-regulation and leads to enhanced EGF receptor signaling as well as downstream EGF-induced Akt signaling (Fallon et al., 2006). Similarly, we have also reported an apparent increase in Akt S473 phosphorylation in parkin-expressing MCF-7 cells compared to control (Tay et al., 2010). I therefore remain intrigued by this discrepancy but noted that my current observation in U-87MG cells is reproducible in MEFs prepared from wild type and parkin null mice, suggesting that parkin-mediated effects on Akt signaling may be dependent on the cell type examined. Notwithstanding this, over-activation of Akt signaling is a frequent feature of tumors including gliomas. That parkin can down-regulate Akt signaling in U-87MG cells would offer a mechanism underlying its tumor suppressor function.

6.4 Parkin expression reduces the levels of VEGFR2 and FKBP5 in U-87MG cells

The presence of parkin also clearly influences the expression of VEGFR2, one of the two high-affinity tyrosine kinase receptors involved in tumor neoangiogenesis. Although predominantly found on endothelial cells, VEGFR have also been detected on cancer cells including gliomas, suggesting a possible autocrine effect on their growth (Masood et al., 2001, Knizetova et al., 2008).

Importantly, autocrine regulation of GBM cell cycle progression and viability through VEGF-VEGFR2 interplay involves co-activation of the PI3k/Akt pathway (Knizetova et al., 2008), which parkin appears to regulate. It is interesting to note that the expression of VEGFR2 is dramatically reduced at both the mRNA and protein levels in parkin-expressing U-87MG relative to native or vector control cells.

FKBP5 was found previously to be upregulated in variety of gliomas and inhibition of FKBP5 expression was found to suppress cellular proliferation and overexpression of FKBP5 was found to increase cell growth (Mikkelsen et al, 2008). The transcript and protein levels of FKBP5 were reduced as indicated by the results from the microarray data analysis and immunoblotting. In addition, FKBP5 was found to be involved in the nuclear factor-kappa B (NF-κB) pathway activation in glioma cells through the regulation of expression of IKKα and phosphorylated NF-κB. The inhibition of FKBP5 was shown to sensitize both PTEN-positive and PTEN-negative cells rapamycin-resistance glioma cells to rapamycin treatment (Mikkelsen et al, 2008). Therefore, the reduction of FKBP5 would conceivably have negative effects on the rate of cellular proliferation and NF-κB signaling pathway.

Together, these results suggest that parkin-mediated suppression is not limited to a single pathway but potentially involves multiple intersecting pathways that converge to influence the cell cycle program in gliomas.

6.5 Parkin expression reduces the levels of oncogenic miR-21 and miR-155 in U-87MG cells

A novel discovery was made when parkin was found to be able to downregulate the levels of miR-21 and miR-155. The downregulation of miR-21 could possibly have triggered the caspase activation and associated apoptotic cell death in the gliomas cells (Chan et al, 2005) and reduced glioma invasion by targeting matrix metalloproteinase regulators (Gabriely et al, 2008). The downregulation of miR-155 could increase tumor protein 53-induced nuclear protein 1 (TP53INP1) to induce cell cycle arrest and apoptosis through caspase-3 activation (Gironella et al, 2007). Due to time limitation, I was not able to pursue the relationship between parkin and these micro-RNAs in depth but this topic is clearly of interest and will undoubtedly be a subject of our lab's future studies.

6.6 Parkin gene signature predicts survival outcome of human glioma patients

Although the findings above are interesting, I was cognizant that they were largely derived from a single glioma cell line, i.e. U-87MG. Whether the data is relevant to human gliomas was a concern. For this reason, I sought to determine if the data based on a limited cell line panel translated to significant clinical impact. The Cancer Genome Atlas (TCGA) efforts have recently highlighted the importance of gene expression in molecularly distinguishing GBM subtypes (Verhaak et al., 2010). These subtypes correlate with distinct genomic and clinical profiles, indicating that gene expression drives disease progression and survival outcome in GBM tumors. Similarly, Freije *et al*. defined survival stratification based on gene expression in glioma variants (Freije et al., 2004), thus

underscoring the significance of such molecular approaches. With the expert help from a bioinformatician, we thus analyzed 802 probe-sets differentially regulated between parkin-expressing and non-expressing U-87MG cells and identified several functional pathways by Gene Set Enrichment Analysis. We observed the following: (i) Parkin expression signature enriched for genes in "programmed cell death" and "apoptosis" functions; and (ii) In particular, we noted by network analysis that parkin expression repressed VEGFR-2 levels, leading to downregulation of the PI3K-AKT signaling axis, in agreement with my *in vitro* data. Recent work by TCGA highlighted the three major regulatory mechanisms in GBM growth: Receptor tyrosine kinase pathway/RAS/PI3K (AKT signaling), Rb signaling (G1/S progression) and p53 signaling pathways (senescence, apoptosis) (Atlas et al., 2008). These pathways are mutated in the majority of GBM patients (~80-90%). Further, significantly recurrent focal alterations not previously reported in GBMs, such as homozygous deletions in *PARK2*, emphasize that parkin may play a more central role in gliomagenesis that affects multiple downstream players.

To determine the clinical impact of this parkin signature, we utilized the "Connectivity Map" method (Lamb et al., 2006). Previous studies have proposed using gene expression signatures to predict the activity of oncogenic pathways in cancer (Ooi et al., 2009). Here, we hypothesized that the strength of concordance of the parkin signature to the individual patient's gene expression profile predicts the level of pathway activation which can subsequently be mapped to survival outcome. We pared down the gene list to 50 top-ranking candidates with more stringent criteria of $\log_2 FC \geq 1.2$ and FDR~0. This gene signature was then mapped onto publicly available clinical glioma databases – Rembrandt and Freije

(Madhaven et al., 2009, Freije et al., 2004). We successfully assigned parkin activation scores (with significant *p*-values between parkin+ and parkin- to reflect non-randomness of categories) to 20-30% of patients, while the remaining showed no difference. It is likely that this cohort of "parkin-zero" patients is a reflection of our filtering process. That is, we chose to examine two extreme scenarios of parkin+ and parkin- among only tumor patients/samples, and thus the most severe phenotypes; whereas no inclusion of normal brain tissue was used in the process. It is conceivable that with normal brain tissue as the comparator albeit their small numbers, more parkin-zero patients would have been assigned activation scores of significance. These remains to be investigated although we believe a more robust method to compare tumor and normal brain tissue would be to analyze their genomic aberrations (copy number, SNP). We show here that the parkin signature consistently stratified patient survival outcome in the 2 major independent datasets with diverse glioma variants, thereby strengthening the significance of the signature initially derived from limited cell line numbers. We noted that the signature was marginally insignificant in TCGA, possibly due to the fact that TCGA comprises only GBM specimens and thus less molecular heterogeneity. This trend was also observed by Yan *et al*. (Yan et al., 2011) in which their gene signature of interest displayed marginal significances in "all GBM" databases, TCGA (Atlas et al., 2008) and Murat (Murat et al., 2008). By inference, our data would seem to support a role for parkin as a metric to stratify gliomas of distinct clinical grades. We thus examined the patient tumor grades corresponding to their ranked parkin signature enrichment profiles in the 2 clinical databases. Interestingly, the parkin+ activation scores enriched for patients with lower, less aggressive tumor grades, or the oligodendroglioma histology which is typically

associated with better prognosis (Caimcross et al., 1998). In contrast, parkin- patients were mainly grade IV GBM. Our Cox regression model in the two clinical databases suggests that the parkin signature predicts for survival better than the current clinical indicator, histology. Our data therefore indicates that the parkin signature defines a role for molecular heterogeneity in contributing to survival outcome that cannot be fully accounted for by histology alone. This underscores the limitation of morphology-based pathological diagnoses which currently determine the type of glioma therapeutic regimens undertaken in the clinic. Thus, a re-examination of this 50-gene list including *PARK2*, could conceivably provide useful prognostic indicators to monitor disease progression.

6.7 Conclusions

The overall objective of my project is to understand and establish a role for parkin in gliomagenesis. This knowledge will enable us to better understand the role of parkin in cancer as a whole and whether its proposed anti-cancer function is relevant to glioma growth. At the moment, there are numerous reports relating parkin to cancer but few have provided a mechanism as to how parkin could suppress tumor formation. As stated in Chapter 1, my specific objectives were as follows:

I. To characterize the expression of parkin in glioma cells and examine the effects of parkin over-expression on the rate of glioma cell proliferation both *in vitro* and *in vivo*.

II. To dissect the mechanism underlying parkin-mediated tumor suppression (of glioma growth).

III. To validate the results obtained (from above aims) in human biopsy samples and/or glioma databases.

In relation to these objectives, I could now make the following conclusions:

I. Parkin deficiency is a characteristic of glioma cells and restoration of its expression mitigates glioma growth both in vitro and in vivo.

II. Parkin-mediated suppression of glioma growth is related to its ability to downregulate the VEGFR2-Akt-cyclin D1 pathway, although the entire spectrum of the parkin tumor suppression pathway is not restricted to these components and may involve other components such as FKBP and miR-21 and -155.

III. Importantly, parkin gene signature predicts survival outcome of human glioma patients, which validate the above findings derived from glioma cell lines.

Taken together, my Ph.D. work strongly established a role for parkin in gliomagenesis, and further suggests that disease progression may be a manifest of parkin pathway inactivation. A model summarizing my findings is provided below.

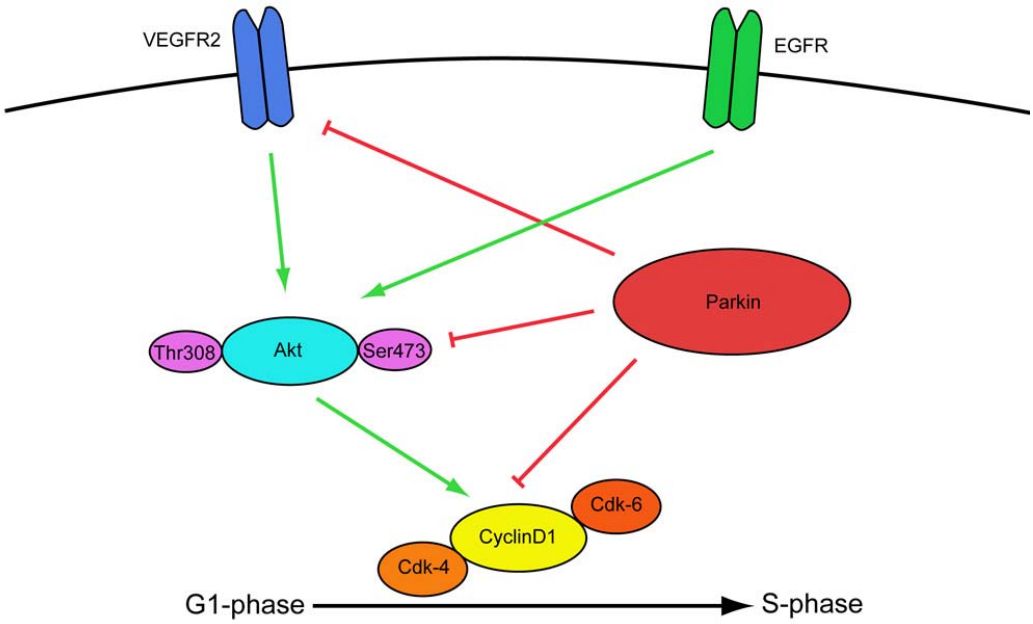

Figure 6.1 Proposed model of parkin's anti-proliferative effects in gliomas. Parkin downregulates the levels of VEGFR2 which leads to a reduction in the levels of phospho-Akt (S473) and this leads to reduce cell cycle progression through mitigation of cyclin D1.

6.8 Future Work

Parkin may participate in gliomagenesis through the VEGFR2-Akt-cyclin D1 pathway, however the precise mechanism for which parkin acts on this pathway is unknown. Future studies can be focused on whether parkin could interact and ubiquitinate these substrates directly and as a result reduce the levels of these proteins in the cell. Genetic studies focusing on the interaction of parkin with other oncogenes and tumor suppressor genes could also be investigated in various animal models like drosophila or mouse models to determine if parkin could indeed play a synergistic role with these cancer-causative genes.

CHAPTER 7

REFERENCES

Alves da Costa C, Sunyach C, Giaime E, West A, Corti O, Brice A, Safe S, Abou-Sleiman PM, Wood NW, Takahashi H, Goldberg MS, Shen J, Checler F. (2009) Transcriptional repression of p53 by parkin and impairment by mutations associated with autosomal recessive juvenile Parkinson's disease. Nat. Cell Biol. 11(11): 1370-1375.

Agirre X, Garate L, Artieda P, Heiniger A, Torres A, Minna JD, Prosper F. (2006) Abnormal methylation of the common PARK2 and PACRG promoter is associated with downregulation of gene expression in acute lymphoblastic leukemia and chronic myeloid leukemia. Int. J. Cancer 118(8):1945-53.

Ali S, Vollard AM, Widjaja S, Surjadi C, van de Vosse E, van Dissel JT. (2006) PARK2/PACRG polymorphisms and susceptibility to typhoid and paratyphoid fever. Clin Exp Immunol. 144(3):425-431.

Asangani IA, Rasheed SA, Nikolova DA, Leupold JH, Colburn NH, Post S, Allgayer H. (2008) MicroRNA-21 (miR-21) post-transcriptionally downregulates tumor suppressor Pdcd4 and stimulates invasion, intravasation and metastasis in colorectal cancer. Oncogene 27: 2128-2136.

Asthagiri AR, Pouratian N, Sherman J, Ahmed G, Shaffrey ME. (2007) Advances in brain tumor surgery. Neurol Clin 25: 975-1003.

Atlas, T.C.G. 2008. Comprehensive genomic characterization defines human glioblastoma genes and core pathways. Nature 455: 1061-1068.

Avraham E, Rott R, Liani E, Szargel R, Engelender S. (2007) Phosphorylation of Parkin by the cyclin-dependent kinase 5 at the linker region modulates its ubiquitin-ligase activity and aggregation. J Biol Chem. 282(17): 12842-12850.

Bachoo RM, Maher EA, Ligon KL, Sharpless NE, Chan SS, You MJ, Tang Y, DeFrances J, Stover E, Weissleder R. (2002) Epidermal growth factor receptor and Ink4a/Arf: Convergent mechanisms governing terminal differentiation and transformation along the neural stem cell to astrocyte axis. Cancer cell 1: 269-277.

Bansal K, Liang ML, Rutka JT. (2006) Molecular Biology of Human Gliomas. Technology in Cancer Res & Treatment. 5(3): 185-194.

Bartel DP. (2004) MicroRNAs: genomics, biogenesis, mechanism, and function. Cell 116: 281-197.

Batchelor TT, Sorensen AG, di Tomaso E, Zhang WT, Duda DG, Cohen KS, Kozak KR, Cahill DP, Chen PJ, Zhu M, Ancukiewicz M, Mrugala MM, Plotkin S, Drappatz J, Louis DN, Ivy P, Scadden DT, Benner T, Loeffler JS, Wen PY, Jain RK. (2007) AZD2171, a pan-VEGF receptor tyrosine kinase inhibitor, normalizes tumor vasculature and alleviates edema in glioblastoma patients. Cancer Cell 11: 83-95.

Baumann N, Pham-Dinh D. (2001) Biology of Oligodendrocytes and myelin in the mammalian central nervous system. Physio. Rev. 81(2): 871-927.

Beere HM, Wolf BB, Cain K, Mosser DD, Mahboubi A, Kuwana T, Tailor P, Morimoto RI, Cohen GM, Green DR. (2000) Heat-shock protein 70 inhibits apoptosis by preventing recruitment of procaspase-9 to the Apaf-1 apoptosome. Nat Cell Biol. 2: 469-475.

Bednarek AK, Keck-Waggoner CL, Daniel RL, Laflin KJ, Bergsagel PL, Kiguchi K, Brenner AJ, Aldaz CM. (2001) WWOX, the FRA16D gene, behaves as a suppressor of tumor growth. Cancer Res 61:8068-73.

Beroukhim R, Mermel CH, Porter D, Wei G, Raychaudhuri S, Donovan J, Barretina J, Boehm JS, Dobson J, Urashima M, Mc Henry KT, Pinchback RM, Ligon AH, Cho YJ, Haery L, Greulich H, Reich M, Winckler W, Lawrence MS, Weir BA, Tanaka KE, Chiang DY, Bass AJ, Loo A, Hoffman C, Prensner J, Liefeld T, Gao Q, Yecies D, Signoretti S, Maher E, Kaye FJ, Sasaki H, Tepper JE, Fletcher JA, Tabernero J, Baselga J, Tsao MS, Demichelis F, Rubin MA, Janne PA, Daly MJ, Nucera C, Levine RL, Ebert BL, Gabriel S, Rustgi AK, Antonescu CR, Ladanyi M, Letai A, Garraway LA, Loda M, Beer DG, True LD, Okamoto A, Pomeroy SL, Singer S, Golub TR, Lander ES, Getz G, Sellers WR, Meyerson M. (2010) The landscape of somatic copy-number alteration across human cancers. Nature 463(7283): 899-905.

Berse B, Brown LF, Van de Water L, Dvorak HF, Senger DR. (1992) Vascular permeability factor (vascular endothelial growth factor) gene is expressed differentially in normal tissues, macrophages, and tumors. Mol. Biol. Cell 3(2): 211-220.

Bignell GR, Greenman CD, Davies H, Butler AP, Edkins S, Andrews JM, Buck G, Chen L, Beare D, Latimer C, Widaa S, Hinton J, Fahey C, Fu B, Swamy S, Dalgliesh GL, Teh BT, Deloukas P, Yang F, Campbell PJ, Futreal PA, Stratton MR. (2010) Signatures of mutation and selection in the cancer genome. Nature. 463(7283): 893-898.

Bouwmeester T, Bauch A, Ruffner H, Angrand PO, Bergamini G, Croughton K, Cruciat C, Eberhard D, Gagneur J, Ghidelli S. (2004) A physical and functional map of the human TNF-alpha/NF-kappa B signal transduction pathway. Nat Cell Biol. 6, 97-105.

Caimcross, J.G., Ueki, K., Zlatescu, M.C., Lisle, D.K., Finkelstein, D.M., Hammond, R.R., Silver, J.S., Stark, P.C., Macdonald, D.R., Ino, Y., et al. (1998) Specific genetic predictors of chemotherapeutic response and survival in patients with anaplastic oligodendrogliomas. J Natl Cancer Inst 90: 1473-1479.

Calin GA, Dumitru CD, Shimizu M, Bichi R, Zupo S, Noch E, Aldler H, Rattan S, Keating M, Rai K, Rassenti L, Kipps T, Negrini M, Bullrich F, Croce CM. (2002) Frequent deletions and down-regulation of micro-RNA genes miR15 and miR16 at 13q14 in chronic lymphocytic leukemia. Proc. Natl. Acad. Sci. USA 99: 15524-15529.

Calin GA, Liu CG, Sevignani C, Ferracin M, Felli N, Dumitru CD, Shimizu M, Cimmino A, Zupo S, Dono M, Dell'Aquila ML, Alder H, Rassenti L, Kipps TJ, Bullrich F, Negrini M, Croce CM. (2004) MicroRNA profiling reveals distinct signatures in B-cell chronic lymphocytic leukemias. Proc. Natl. Acad. Sci. USA 101: 11755-11760.

Calin GA, Ferracin M, Cimmino A, et al. (2005) A microRNA signature associated with prognosis and progression in chronic lymphocytic leukemia. N. Engl. J. Med. 353: 1793-1801.

Schwartz AL, Ciechanover A. (2009) Targeting proteins for destruction by the ubiquitin system: implication for human pathobiology. Annu. Rev. Pharmacol. Toxicol. 49: 73-96.

Cesari R, Martin ES, Calin GA. (2003) Parkin, a gene implicated in the autosomal recessive juvenile parkinsonism, is a candidate tumor suppressor gene on chromosome 6q25-q27. Proc. Natl. Acad. Sci. 100(10): 5956-5961.

Chan JA, Krichevsky AM, Kosik KS. (2005) MicroRNA-21 is an antiapoptotic factor in human glioblastoma cells. Cancer Res 65: 6029-6033.

Cha S. (2006) Update on brain tumor imaging: from anatomy to physiology. Am J. Neuroradiol. 27: 475-487.

Chaudhry IH, O'Donovan DG, Brenchley PE, Reid H, Roberts IS. (2001) Vascular endothelial growth factor expression correlates with tumour grade and vascularity in gliomas. Histopathology 39: 409-415.

Chen W. (2007) Clinical applications of PET in the brain tumors. J Nucl Med 48: 1468-1481.

Chen ZJ, Fuchs SY. (2004) Ubiquitin-dependent activation of NF-kappaB: K63-linked ubiquitin chains: a link to cancer? Cancer Biol Ther 3:286-8.

Chen Y, Liu W, Chao T, Zhang Y, Yan X, Gong Y, Qiang B, Yuan J, Sun M, Peng X. MicroRNA-21 down-regulates the expression of tumor suppressor PDCD4 in human glioblastoma cell T98G. Cancer lett. 272: 197-205.

Cheung-Flynn J, Roberts PJ, Riggs DL, Smith DF. (2003) C-terminal sequences outside the tetratricopeptide repeat domain of FKBP51 and FKBP52 cause differential binding to Hsp90. J Biol Chem. 278, 17388-17394.

Chi AS, Wen PY. (2007) Inhibiting kinases in malignant gliomas. Expert Opin Ther Targets 11: 473-496.

Choi P, Snyder H, Petrucelli L, Theisler C, Chong M, Zhang Y, Lim K, Chung KK, Kehoe K, D'Adamio L, Lee JM, Cochran E, Bowser R, Dawson TM, Wolozin B. (2003) SEPT5_v2 is a parkin-binding protein. Brain Res Mol Brain Res. 117(2):179-89.

Chung KK, Zhang Y, Lim KL, Tanaka Y, Huang H, Gao J, Ross CA, Dawson VL, Dawson TM. (2001) Parkin ubiquitinates the alpha-synuclein-interacting

protein, synphilin-1: implications for the lewy body formation in Parkinson disease. Nat. Medicine 10: 1144-1150.

Citri, A., & Yarden, Y. (2006) EGF-ERBB signalling: Towards the systems level. Nat. Rev. Mol. Cell. Biol. 7(7): 505–516.

Clarke ID, Dirks PB. (2003) A human brain tumor-derived PDGFR-α deletion mutant is transforming. Oncogene 22: 722-733.

Conti A, Aguennouz M, La Torre D, Tomasello C. (2009) miR-21 and 221 upregulation and miR-181b downregulation in human grade II-IV astrocytic tumors. J. Neurooncol. 93: 325-332.

Copani A, Uberti D, Sortino MA, Bruno V, Nicoletti F, Memo M. (2001) Activation of cell-cycle associated proteins in neuronal death: a mandatory or dispensable path? Trends Neurosci. 24: 25-31.

Corti O, Hampe C, Koutnikova H, Darios F, Jacquier S, Prigent A, Robinson JC, Pradier L, Ruberg M, Mirande M, Hirsch E, Rooney T, Fournier A, Brice A. (2003) The p38 subunit of the aminoacyl-tRNA synthetase complex is a Parkin substrate: linking protein biosynthesis and neurodegeneration. Hum. Mol. Gen. 12: 1427-1437.

Costello JF, Berger MS, Huang HS, Cavenee WK. (1996) Silencing of p16/CDKN2 expression in human gliomas by methylation and chromatin condensation. Cancer Res. 56: 2405-2410.

Costello JF, Plass C, Arap W, Chapman VM, Held WA, Berger MS, Su Huang HJ, Cavenee WK. (1997) Cyclin-dependent kinase 6 (CDK6) amplification in human gliomas identified using two-dimensional separation of genomic DNA. Cancer Res. 57: 1250-1254.

Dai C, Celestino JC, Okada Y, Louis DN, Fuller GN, Holland EC. (2001) PDGF autocrine stimulation dedifferentiates cultured astrocytes and induces oligodendrogliomas and oligoastrocytomas from neural progenitors and astrocytes in vivo. Genes & Dev. 15: 1913-1925.

Dehvari N, Sandebring A, Flores-Morales A, Mateos L, Chuan YC, Goldberg MS, Cookson MR, Cowburn RF, Cedazo-Mínguez A. (2009) Parkin-mediated ubiquitination regulates phospholipase C-gamma1. J Cell Mol Med. 13(9B):3061-3068.

Denli AM, Tops BB, Plasterk RH, Ketting RF, Hannon GJ. (2004) Processing of primary microRNA by the Microprocessor complex. Nature 432: 231-235.

Denison SR, Wang F, Becker NA. (2003) Alterations in the common fragile site gene Parkin the ovarian and other cancers. Oncogene. 22(51): 8370-8378.

Denning G, Jean-Joseph B, Prince C, Durden DL, Vogt PK. (2007) A short N-terminal sequence of PTEN controls cytoplasmic localization and is required for the suppression of cell growth. Oncogene 26: 3930-3940.

Di Cristofano A, Pandolfi PP. The multiple roles of PTEN in tumor suppression. (2000) Cell 100: 387-390.

Di Rocco F, Carroll RS, Zhang J, Black PM. (1998) Platelet-derived growth factor and its receptor expression in human oligodendrogliomas Neurosurgery 42: 341-346.

Diederichs S, Haber DA. (2007) Dual role for argonautes in microRNA processing and posttranscriptional regulation of microRNA expression. Cell 131: 1097-1108.

Ding WX, Ni HM, Li M, Liao Y, Chen X, Stolz DB, Dorn Ii GW, Yin XM. (2010) Nix is critical to two distinct phases of mitophagy: reactive oxygen species (ROS)-mediated autophagy induction and Parkin-ubiqutin-p62-mediated mitochondria priming. J. Biol. Chem. 285: 27879–27890.

Dong Z, Ferger B, Paterna JC, et al. (2003) Dopamine-dependent neurodegeneration in rats induced by viral vector-mediated overexpression of the parkin target protein, CDCrel-1. Proc Natl Acad Sci U S A 100: 12438–12443.

Doss-Pepe EW, Chen L, Madura K. (2005) Alpha-synuclein and parkin contribute to the assembly of ubiquitin lysine 63-linked multiubiquitin chains. J Biol Chem 280: 16619–16624.

Druck T, Berk L, Huebner K. (1998) FHITness and cancer. Oncol Res 10:341-5.

Eriksson A, Siegbahn A, Westermark B, Heldin CH, and Claesson-Welsh L. (1992). PDGF α- and β-receptors activate unique and common signal transduction pathways. EMBO J. 11, 543–550.

Fallon L, Moreau F, Croft BG, Labib N, Gu WJ, Fon EA (2002) Parkin and CASK/LIN-2 associate via a PDZ-mediated interaction and are co-localized in lipid rafts and postsynaptic densities in brain. J Biol. Chem. 277(1): 486-491.

Fallon L, Belanger CM, Corera AT, Kontogiannea M, Regan-Klapisz E, Moreau F, Voortman J, Haber M, Rouleau G, Thorarinsdottir T, Brice A, van Bergen En Henegouwen PM, Fon EA. (2006) A regulated interaction with the UIM protein Eps15 implicates parkin in EGF receptor trafficking and PI(3)K-Akt signalling. Nat Cell Biol 8:834-42.

Farrer M, Chan P, Chen R, Tan L, Lincoln S, Hernandez D, Forno L, Gwinn-Hardy K, Petrucelli L, Hussey J, Singleton A, Tanner C, Hardy J, Langston JW. (2001) Lewy bodies and parkinsonism in families with parkin mutations. Ann Neurol. 50(3): 293-300.

Farrell CJ, Plotkin SR. (2007) Genetic causes of brain tumors: neurofibromatosis, tuberous sclerosis, von Hippel-Lindau, and other syndromes. Neurol Clin 25: 925-946.

Fisher JL, Schwartzbaum JA, Wrensch M, Wiemels JL. (2007) Epidemiology of brain tumors. Neurol Clin 25: 867-890.

Fishman PS, Olyer GA. (2002) Significance of parkin gene and protein in understanding Parkinson's disease. Curr Neurol Neurosci Rep 2(4): 296-302.

Fouladkou F, Landry T, Kawabe H, Neeb A, Lu C, Brose N, Stambolic V, Rotin D. (2008) The ubiquitin ligase Nedd4-1 is dispensable for the regulation of PTEN stability and localization. Proc. Natl. Acad. Sci. U. S. A. 105: 8585-8590.

Frederick L, Wang XY, Eley G, James CD. (2000) Diversity and frequency of epidermal growth factor receptor and mutations in human glioblastomas. Cancer Res. 60: 1383-1387.

Freije, W.A., Castro-Vargas, F.E., Fang, Z., Horvath, S., Cloughesy, T., Liau, L.M., Mischel, P.S., and Nelson, S.F. (2004) Gene expression profiling of gliomas strongly predicts survival. Cancer Res 64:6503-6510.

Frolov MV, Dyson, NJ. (2004) Molecular mechanisms of E2F-dependent activation and pRB-mediated repression. J. Cell Sci. 117: 2173-2181.

Fu, M., Wang, C., Li, Z., Sakamaki, T., and Pestell, R.G. (2004) Minireview: Cyclin D1: normal and abnormal functions. Endocrinology 145: 5439-5447.

Fueyo J, Gomez-Manzano C, Bruner JM, Saito Y, Zhang B, Zhang W, Levin VA, Yung WK, Kyritsis AP. (1996) Hypermethylation of the CpG island of p16/CDKN2 correlates with gene inactivation in gliomas. Oncogene 13: 1615-1619.

Fujiwara M, Marusawa H, Wang HQ, Iwai A, Ikeuchi K, Imai Y, Kataoka A, Nukina N, Takahashi R, Chiba T. (2008) Parkin as a tumor suppressor gene for hepatocellular carcinoma. Oncogene 27(46): 6002-11.

Fulci V, Chiaretti S, Goldoni M, Azzalin G, Carucci N, Tavolaro S, Castellano L, Magrelli A, Citarella F, Messina M, Maggio R, Peragine N, Santangelo S, Mauro FR, Landgraf P, Tuschl T, Weir DB, Chien M, Russo JJ, Ju J, Sheridan R, Sander C, Zavolan M, Guarini A, Foà R, Macino G. (2007) Quantitative technologies establish a novel microRNA profile of chronic lymphocytic leukemia. Blood. 109: 4944–51.

Furnari FB, Fenton T, Bachoo RM, Mukasa A, Stommel JM, Stegh A, Hahn WC, Ligon KL, Louis DN, Brennan C, Chin L, DePinho RA, Cavenee WK. (2008) Maliggnant astrocytic glioma: genetics, biology, and paths to treatment. Genes & Dev. 21: 2683-2710.

Gabriely G, Wurdinger T, Kesari S, Esau CC, Burchard J, Linsley PS, Krichevsky AM. (2008) MicroRNA 21 promotes glioma invasion by targeting matrix metalloproteinase regulators. Mol. Cell. Biol. 28: 5369-5380.

Gaidano G, Hauptschein RS, Parsa NZ. (1992) Deletions involving two distinct regions of 6q in B-cell non-Hodgkin lymphoma. Blood. 80(7): 1781-1787.

Galea-Lauri J, Richardson AJ, Latchman DS, Katz DR. (1996) Increased heat shock protein 90 (hsp90) expression leads to increased apoptosis in the

monoblastoid cell line U937 following induction with TNF-α and cycloheximide: a possible role in immunopathology. J. Immunol. 157: 4109-4118.

Gallia GL, Rand V, Siu IM, Eberhart CG, James CD, Marie SK, Oba-Shinjo SM, Carlotti CG, Caballero OL, Simpson AJ, Brock MV, Massion PP, Carson BS Sr, Riggins GJ. (2006) PIK3CA gene mutations in pediatric and adult glioblastoma multiforme. Mol. Cancer Res. 4: 709-714.

Garzon R, Volinia S, Liu CG et al. (2008) MicroRNA signatures associated with cytogenetics and prognosis in acute myeloid leukemia. Blood. 111: 3183-3189.

Garzon R, Calin GA, Croce CM. (2009) MicroRNAs in Cancer. Annu. Rev. Med. 60:167-179.

Geisler S, Holmstrom KM, Skujat D, Fiesel FC, Rothfuss OC, Kahle PJ, Springer W. (2010) PINK1/Parkin-mediated mitophagy is dependent on VDAC1 and p62/SQSTM1, Nat. Cell Biol. 12: 119–131.

Gilbert MR, Ruda R, Soffietti R. (2010) Ependymomas in adults. Curr. Neurol. Neurosci. Rep. 10(3): 240-247.

Gironella M, Seux M, Xie MJ, Cano C, Tomasini R, Gommeaux J, Garcia S, Nowak J, Yeung ML, Jeang KT, Chaix A, Fazli L, Motoo Y, Wang Q, Rocchi P, Russo A, Gleave M, Dagorn JC, Iovanna JL, Carrier A, Pébusque MJ, Dusetti NJ. (2007) Tumor protein 53-induced nuclear protein 1 expression is repressed by miR-155, and its restoration inhibits pancreatic tumor development, Proc. Natl. Acad. Sci. U. S. A. 104, 1617–16170.

Glenisson W, Castronovo V, Waltregny D. (2007) Histone deacetylase 4 is required for TGFbeta1-induced myofibroblastic differentiation. Biochim Biophys Acta. 1773(10): 1572-1582.

Göke R, Barth A, Schmidt A, Samans B, Lankat-Buttgereit. (2004) Programmed cell death protein 4 suppresses CDK1/cdc2 via induction of p21 (Waf1/Cip1). Am. J. Physio. Cell Physiol. 287: C1541-C1546.

Gualandi F, Morelli C, Pavan JV, Rimessi P, Sensi A, Bonfatti A, Gruppioni R, Possati L, Stanbridge EJ, Barbanti-Brodano G. (1994) Induction of

senescence and control of tumorigenicity in BK virus transformed mouse cells by human chromosome 6. Genes Chromosomes Cancer. 10(2):77-84.

Guan XY, Zhang HE, Zhou H, Sham JS, Fung JM, Trent JM. (2002) Characterization of a complex chromosome rearrangement involving 6q in a melanoma cell line by chromosome microdissection. Cancer Genet Cytogenet. 134(1):65-70.

Guha A, Feldkamp MM, Lau N, Boss G, Pawson A, (1997) Proliferation of human malignant astrocytomas is dependent on Ras activation. Oncogene 15: 2755-2765.

Guo P, Hu B, Gu W, Xu L, Wang D, Huang HJ, Cavenee WK, Cheng SY. (2003) Platelet-derived growth factor-B enhances glioma angiogenesis by stimulating vascular endothelial growth factor expression in tumor endothelia and by promoting pericyte recruitment. Am. J. Pathol. 162: 1083-1093.

Harper JW, Adami GR, Wei N, Keyomarsi K, Elledge SJ. (1993) The p21 Cdk-interacting protein Cip1 is a potent inhibitor of G1 cyclin-dependent kinases. Cell 75: 805-816.

Harper JW, Burton JL, Solomon MJ. (2002) The anaphase-promoting complex: it's not just for mitosis any more. Genes Dev. 16: 2179-2206.

Hawkins PT, Anderson KE, Davidson K, Stephens LR. (2006) Signalling through Class I PI3Ks in mammalian cells. Biochem. Soc. Trans. 34: 647-662.

Hedrich K, Kann M, Lanthaler AJ, Dalski A, Eskelson C, Landt O, Schwinger E, Vieregge P, Lang AE, Breakefield XO, Ozelius LJ, Pramstaller PP, Klein C. (2001) The importance of gene dosage studies: mutational analysis of the parkin gene in early-onset parkinsonism. Hum Mol Genet 10:1649 –1656.

Heldin, CH, Eriksson U, and Ostman A. (2002). New members of the platelet-derived growth factor family of mitogens. Arch. Biochem. Biophys. 398, 284–290.

Henson JW, Schnitker BL, Correa KM, von Deimling A, Fassbender F, Xu HJ, Benedict WF, Yandell DW, Louis DN. (1994) The retinoblastoma gene is involved in malignant progression of astrocytomas. Ann. Neurol. 36: 714-721.

Hermanson M, Funa K, Hartman M, Claesson-Welsh L, Heldin CH, Westermark B, Nister M. (1992) Platelet-derived growth factor and its receptors in human glioma tissue: Expression of messenger RNA and protein suggests the presence of autocrine and paracrine loops. Cancer Res. 52: 3213-3219.

Hershko A, Ciechanover, A. (1998) The ubiquitin system. Annu. Rev. Biochem. 67: 425-479.

Hochberg FH, Pruitt A. (1980) Assumptions in the radiotherapy of glioblastoma. Neurology 30: 907-911.

Holland EC, Varmus HE. (1998) Basic fibroblast growth factor induces cell migration and proliferation after glia-specific gene transfer in mice. Proc. Natl. Acad. Sci. USA 95(3): 1218-1223.

Holmes K, Roberts OL, Thomas AM, Cross MJ. (2007) Vascular endothelial growth factor receptor-2: Structure, function, intracellular signaling and therapeutic inhibition. Cell. Signal. 19: 2003-2012.

Hresko, R.C., and Mueckler, M. 2005. mTOR.RICTOR is the Ser473 kinase for Akt/protein kinase B in 3T3-L1 adipocytes. *J Biol Chem* 280:40406-40416.

Hristova VA, Beasley SA, Rylett RJ, Shaw GS. (2009) Identification of a novel Zn^{2+}-binding domain in the autosomal recessive juvenile Parkinson-related E3 ligase parkin. J Biol Chem. 284(22): 14978-14986.

Husain SR, Puri RK. (2003) Interleukin-13 receptor-directed cytotoxin for malignant glioma therapy: from bench to bedside. J Neurooncol 65(1):37-48.

Huynh DP, Scoles DR, Nguyen D, Pulst SM. (2003) The autosomal recessive juvenile Parkinson disease gene product, parkin, interacts with and ubiquitinates synaptotagmin XI. Hum Mol Genet. 12(20): 2587-2597.

Huynh DP, Nguyen DT, Pulst-Korenberg JB, Brice A, Pulst SM. (2007) Parkin is an E3 ubiquitin-ligase for normal and mutant ataxin-2 and prevents ataxin-2-induced cell death. Exp Neurol. 203(2): 531-541.

Ikeda F, Dikic I. (2008) Atypical ubiquitin chains: new molecular signals. EMBO Rep 9: 536-542.

Ikeuchi K, Marusawa H, Fujiwara M, Matsumoto Y, Endo Y, Watanabe T, Iwai A, Sakai Y, Takahashi R, Chiba T. (2009) Attenuation of proteolysis-mediated cyclin E regulation by alternatively spliced Parkin in human colorectal cancers. Int J Cancer. 125 (9): 2029-2035.

Imai Y, Soda M, Takahashi R. (2000) Parkin suppresses unfolded protein stress-induced cell death through its E3 ubiquitin-protein ligase activity. J. Biol. Chem. 275: 35661-35664.

Imai Y, Soda M, Inoue H, Hattori N, Mizuno Y, Takahashi R. (2001) An unfolded putative transmembrane polypeptide, which can lead to endoplasmic reticulum stress, is a substrate of Parkin. Cell 105:891–902.

Imai Y, Soda M, Hatakeyama S, Akagi T, Hashikawa T, Nakayama KI, Takahashi R. (2002) CHIP is associated with parkin, a gene responsible for Familial Parkinson's Disease and enhances its ubiquitin ligase activity. Molecular Cell 10: 55-67.

Imai Y, Inoue H, Kataoka A, Hua-Qin W, Masuda M, Ikeda T, Tsukita K, Soda M, Odama T, Fuwa T, Honda Y, Kaneko S, Matsumoto S, Wakamatsu K, Ito S, Miura M, Aosaki T, Tohara S, Takahashi R. (2007) Pael receptor is involved in dopamine metabolism in the nigrostriatal system. Neurosci Res. 59(4): 413-25.

Inoue S, Imamura A, Okazaki Y, Yokota H, Arai M, Hayashi N, Furukawa A, Itokawa M, Oishi M. (2007) Synaptotagmin XI as a candidate gene for susceptibility to schizophrenia. Am J Med Genet B Neuropsychiatr Genet. 144B(3): 332-340

Iorio MV, Ferracin M, Liu CG et al. (2005) MicroRNA gene expression deregulation in human breast cancer. Cancer Res 65: 7065-7070.

Ishii H, Dumon KR, Vecchione A, Trapasso F, Mimori K, Alder H, Mori M, Sozzi G, Baffa R, Huebner K, Croce CM. (2001) Effect of adenoviral transduction of the fragile histidine triad gene into esophageal cancer cells. Cancer Res 61:1578-84.

Ishii H, Dumon KR, Vecchione A, Fong LY, Baffa R, Huebner K, Croce CM. (2001) Potential cancer therapy with the fragile histidine triad gene: review of the preclinical studies. Jama 286:2441-9.

Jain RK, di Tomaso E, Duda DG, Leoffler JS, Sorensen AG, Batchelor TT. (2007) Angiogenesis in brain tumours. Nat Rev Neurosci 8: 610-622.

Jiang W, Cazacu S, Xiang C, Zenklusen JC, Fine HA, Berens M, Armstrong B, Brodie C, Mikkelsen T. (2008) FK506 binding protein mediates glioma cell growth and sensitivity to rapamycin treatment by regulating NF-kappaB signaling pathway. Neoplasia. 10(3):235-43.

Jackson EL, Garcia-Verdugo JM, Gil-Perotin S, Roy M, Quinones-Hinojosa A, VandenBerg S, Alvarez-Buylla A. (2006) PDGFR α-positive B cells are neural stem cells in the adult SVZ that form glioma-like growths in response to increased PDGF signaling. Neuron 51: 187-199.

Joch M, Ase AR, Chen CX, MacDonald PA, Kontogiannea M, Corera AT, Brice A, Séguéla P, Fon EA. (2007) Parkin-mediated monoubiquitination of the PDZ protein PICK1 regulates the activity of acid-sensing ion channels. Mol. Biol. Cell 18(8): 3105-3118.

KaelinWG Jr. (2007) The von Hippel-Lindau tumor suppressor protein and clear cell renal carcinoma. Clin Cancer Res. 13:680s-684s.

Kahle PJ, Neumann M, Ozmen L, Muller V, Jacobsen H, Schindzielorz A, Okochi M, Leimer U, van Der Putten H, Probst A, Kremmer E, Kretzschmar HA, Haass C. Subcellular localization of wild-type and Parkinson's disease-associated mutant alpha -synuclein in human and transgenic mouse brain. J Neurosci. 20(17): 6365-6373.

Kang S, Denley A, Vanhaesebroeck B, Vogt PK. (2006) Oncogenic transformation induced by the p110β, -γ and –δ isoforms of class I phosphoinositide 3-kinase. Proc. Natl. Acad. Sci. 103: 1289-1294.

Kanu OO, Mehta A, Di C, Lin N, Bortoff K, Bigner DD, Yan H, Adamson DC. (2009) Glioblastoma multiforme: a review of therapeutic targets. Expert Opin. Ther. Targets. 13(6): 701-718.

Keime-Guibert F, Chinot O, Taillandier L, Cartalat-Carel S, Frenay M, Kantor G, Guillamo JS, Jadaud E, Colin P, Bondiau PY, Meneï P, Loiseau H, Bernier V, Honnorat J, Barrié M, Mokhtari K, Mazeron JJ, Bissery A, Delattre JY. (2007) Radiotherapy for glioblastoma in the elderly. N Engl J Med 356: 1527-1535.

Kim MJ, Kim E, Ryu SH, Suh PG. (2000) The mechanism of phospholipase C-gamma1 regulation. Exp Mol Med. 32(3): 101-109.

Kim RH, Peters M, Jang Y, Shi W, Pintilie M, Fletcher GC, DeLuca C, Liepa J, Zhou L, Snow B, Binari RC, Manoukian AS, Bray MR, Liu FF, Tsao MS, Mak TW. (2005) DJ-1, a novel regulator of the tumor suppressor PTEN. Cancer Cell 7:263-273.

Kitada T., Asakawa S., Hattori N. (1998) Mutations in the parkin gene cause autosomal recessive juvenile parkinsonism. Nature. 392(6676): 605-608.

Kluiver J, Poppema S, de Jong D, et al. (2005) BIC and miR-155 are highly expressed in Hodgkin, primary mediastinal and diffuse large B cell lymphomas. J. Pathol. 207: 243-249.

Knizetova, P., Ehrmann, J., Hlobilkova, A., Vancova, I., Kalita, O., Kolar, Z., and Bartek, J. (2008) Autocrine regulation of glioblastoma cell cycle progression, viability and radioresistance through the VEGF-VEGFR2 (KDR) interplay. Cell Cycle 7:2553-2561.

Knobbe CB, Reifengerger G. (2003) Genetic alterations and aberrant expression of genes related to the phosphatidyl-inositol-3'-kinase/protein kinase B (Akt) signal transduction pathway in glioblastomas. Brain Pathol. 13: 507-518.

Ko HS, von Coelln R, Sriram SR, Kim SW, Chung KK, Pletnikova O, Troncoso J, Johnson B, Saffary R, Goh EL, Song H, Park BJ, Kim MJ, Kim S, Dawson VL, Dawson TM. (2005) Accumulation of the authentic parkin substrate aminoacyl-tRNA synthetase cofactor, p38/JTV-1, leads to catecholaminergic cell death. J. Neurosci. 25(35): 7968-7978.

Ko HS, Kim SW, Sriram SR, Dawson VL, Dawson TM. (2006) Identification of far upstream element-binding protein-1 as an authentic Parkin substrate. J. Biol. Chem. 281(24): 16193-16196.

Krichevsky AM, Gabriely G. (2009) miR-21: a small multi-faceted RNA. J Cell Mol Med. 13(1): 39-53.

Kumar S, Sarkar A, Sundar D. (2009) Controlling aggregation propensity in A53T mutant of alpha-synuclein causing Parkinson's disease. Biochem Biophys Res Commun. 387(2):305-309.

Lacey KR, Jackson PK, Stearns T. (1999) Cyclin-dependent kinase control of centrosome duplication. Proc. Natl. Acad. Sci. U.S.A. 96: 2817-2822.

Lamb, J., Crawford, E.D., Peck, D., Modell, J.W., Blat, I.C., Wrobel, M.J., Lerner, J., Brunet, J.P., Subramanian, A., Ross, K.N., et al. (2006) The Connectivity Map: using gene-expression signatures to connect small molecules, genes, and disease. Science 313:1929-1935.

Lee EJ, Gusev Y, Jiang J, Nuovo GJ, Lerner MR, Frankel WL, Morgan DL, Postier RG, Brackett DJ, Schmittgen TD. Expression profiling identifies microRNA signature in pancreatic cancer. Int. J. Cancer 120: 1046-1054.

Lemasters JJ. (2005) Selective mitochondrial autophagy, or mitophagy, as a targeted defense against oxidative stress, mitochondrial dysfunction, and aging. Rejuvenation Res. 8: 3–5.

Le Naour F, Misek DE, Krause MC, Deneux L, Giordano TJ, Scholl S, Hanash SM. (2001) Proteomics-based identification of RS/DJ-1 as a novel circulating tumor antigen in breast cancer. Clin Cancer Res 7:3328-3335.

Letessier A., Garrido-Urbani S., Ginestier C., Fournier G., Esterni B., Birnbaum D., Lopez M., Chaffanet M. (2007) Correlated break at *PARK2/FRA6E* and loss of AF-6/Afadin protein expression are associated with poor outcome in breast cancer. Oncogene. 11; 26(2):298-307.

Leu JI, Pimkina J, Frank A, Murphy ME, George DL. (2009) A small molecule inhibitor of inducible heat shock protein 70. Mol Cell. 36(1): 15-27

Levine AJ, Hu W, Feng Z. (2006) The p53 pathway: What questions remain to be explored? Cell Death Differ. 13: 1027-1036.

Lewis J, Devin A, Miller A, Lin Y, Rodriguez Y, Neckers L, Liu ZG. (2000) Disruption of hsp90 function results in degradation of the death domain kinase, receptor-interacting protein (RIP), and bloackage of tumor necrosis factor-induced nuclear factor-κB activation. J. Biol. Chem. 275: 10519-10526.

Li CJ, Vassilev A, DePamphilis ML. (2004) Role for Cdk1 (cdc2)/cyclin A in preventing the mammalian origin recognition complex largest subunit (Orc1) from binding to chromatin during mitosis. Mol. Cell. Biol. 24: 5875-5886.

Ligon KL, Alberta JA, Kho AT, Weiss J, Kwaan MR, Nutt CL, Louis DN, Stiles CD, Rowitch DH. (2004) The oligodendroglial lineage marker OLIG2 is universally expressed in diffuse gliomas. J. Neuropathol. Exp. Neurol. 63: 499-509.

Lim KL, Dawson VL, Dawson T. (2003) Molecular Biology of Parkin. Landes Bioscience Chapter 13:Eds. Kahle P and Haass C.

Lim KL, Chew KC, Tan JM, Wang C, Chung KK, Zhang Y, Tanaka Y, Smith W, Engelender S, Ross CA, Dawson VL, Dawson TM. (2005) Parkin mediates nonclassical, proteasomal-independent ubiquitination of synphilin-1: implications for Lewy body formation. J. Neurosci. 25(8): 2002-2009.

Lim KL, Dawson VL, Dawson T. (2006) Parkin-mediated lysine 63-linked polyubiquitination: a link to protein inclusions formation in Parkinson's and other conformational diseases? Neurobiol. Aging 27(4): 524-529.

Lim KL, Tan JM. (2005) Understanding the role of parkin in Parkinson’s disease. SGH Proceedings 14(1): 59-67.

Lim KL, Tan JM. (2007) Role of the ubiquitin proteasome system in Parkinson's disease. BMC Biochem 8 Suppl 1:S13.

Lim MK, Kawamura T, Ohsawa Y, Ohtsubo M, Asakawa S, Takayanagi A, Shimizu N. (2007) Parkin interacts with LIM Kinase 1 and reduces its cofilin-phosphorylation activity via ubiquitination. 313(13): 2858-2874.

Lincoln S, Wiley J, Lynch T, Langston JW, Chen R, Lang A, Rogaeva E, Sa DS, Munhoz RP, Harris J, Marder K, Klein C, Bisceglio G, Hussey J, West A, Hulihan M, Hardy J, Farrer M. (2003) Parkin-proven disease: common founders but divergent phenotypes. Neurology 60(10): 1605-1610.

Liu DX, Greene LA. (2001) Regulation of neuronal survival and death by E2F-dependent gene repression and derepression. Neuron 32: 425-438.

Liu M, Aneja R, Sun X, Xie S, Wang H, Wu X, Dong JT, Li M, Joshi HC, Zhou J. (2008) Parkin regulates Eg5 expression by Hsp70 ubiquitination-dependent inactivation of c-Jun NH2-terminal kinase. J Biol Chem. 283(51): 35783-35788.

Lokker NA, Sullivan CM, Hollenbach SJ, Israel MA, Giese NA. (2002) Platelet-derived growth factor (PDGF) autocrine signaling regulates survival and mitogenic pathways in glioblastoma cells: Evidence that the novel PDGF-C and PDGF-D ligands may play a role in the development of brain tumors. Cancer Res. 62: 3729-3735.

Looyenga BD, Furge KA, Dykema KJ, Koeman J, Swiatek PJ, Giordano TJ, West AB, Resau JH, Teh BT, Mackeigan JP. (2011) Chromosomal amplification of leucine-rich repeat kinase-2 (LRRK2) is required for oncogenic MET signaling in papillary renal and thyroid carcinomas. Proc Natl Acad Sci U S A. Jan 10

Louis DN. (1994) The p53 gene and protein in human brain tumors. J. Neuropathol. Exp. Neurol. 53: 11-21.

Louis DN, Ohgaki H, Wiestler OD, Cavenee WK, Burger PC, Jouvet A, Scheithauer BW, Kleihues P. (2007) The 2007 WHO classification of tumours of the central nervous system. IARC Press, Lyon, France.

Lu J, Getz G, Miska EA, Alvarez-Saavedra E, Lamb J, Peck D, Sweet-Cordero A, Ebert BL, Mak RH, Ferrando AA, Downing JR, Jacks T, Horvitz HR, Golub TR. (2005) MicroRNA expression profiles classify human cancers, Nature 435: 834–838.

Lücking CB, Dürr A, Bonifati V, Vaughan J, De Michele G, Gasser T, Harhangi BS, Meco G, Denèfle P, Wood NW, Agid Y, Brice A. (2000) Association between early-onset Parkinson's disease and mutations in the parkin gene. N Engl J Med. 342(21): 1560-1567.

Lui WO, Pourmand N, Patterson BK, Fire A. (2007) Patterns of known and novel small RNAs in human cervical cancer. Cancer Res. 2007; 67: 6031–6043.

Kutay H, Bai S, Datta J, Motiwala T, Pogribny I, Frankel W, Jacob ST, Ghoshal K. (2006) Downregulation of miR-122 in the rodent and human hepatocellular carcinomas. J Cell Biochem. 99: 671–678.

Madhankumar AB, Slagle-Webb B, Wang X, Yang QX, Antonetti DA, Miller PA, Sheehan JM, Connor JR. (2009) Efficacy of interleukin-13 receptor-targeted liposomal doxorubicin in the intracranial brain tumor model. Mol Cancer Ther. 8(3):648-654.

Madhavan, S., Zenklusen, J.C., Kotliarov, Y., Sahni, H., Fine, H.A., and Buetow, K. (2009) Rembrandt: helping personalized medicine become a reality through integrative translational research. Mol Cancer Res 7:157-167.

Ma T, Van Tine BA, Wei Y, Garrett MD, Nelson D, Adams PD, Wang J, Qin J, Chow LT, Harper JW. (2000) Cell cycle-regulated phosphorylation of p220(NPAT) by cyclin E/Cdk2 in Cajal bodies promotes histone gene transcription. Gene Dev. 14: 2298-2313.

Maher EA, Brennan C, Wen PY, Durso L, Ligon KL, Richardson A, Khatry D, Feng B, Sinha R, Louis DN, Quackenbush J, Black PM, Chin L, DePinho RA. (2006) Marked genomic differences characterize primary and secondary glioblastoma subtypes and identify two distinct molecular and clinical secondary glioblastoma entities. Cancer Res. 66: 11502-11513.

Masood, R., Cai, J., Zheng, T., Smith, D.L., Hinton, D.R., and Gill, P.S. (2001) Vascular endothelial growth factor (VEGF) is an autocrine growth factor for VEGF receptor-positive human tumors. Blood 98:1904-1913.

Matsushima-Nishiu M, Unoki M, Ono K, Tsunoda T, Minaguchi T, Kuramoto H, Nishida M, Satoh T, Tanaka T, Nakamura Y. (2001) Growth and gene expression profile analyses of endometrial cancer cells expressing exogenous PTEN. Cancer Res. 61:3741-3749.

Matsumine H, Yamamura Y, Kobayashi T, Nakamura S, Kuzuhara S, Mizuno Y. (1998) Early onset parkinsonism with diurnal fluctuation maps to a locus for juvenile parkinsonism. Neurology 50(5): 1340-1345.

Matsuo Y, Kamitani T. (2010) Parkinson's disease-related protein, alpha-synuclein, in malignant melanoma PLoS One. 5(5): e10481.

McBride HM. (2008) Parkin mitochondria in the autophagosome. J. Cell Biol. 183: 757–759.

McLendon R, Friedman A, Bigner D, Van Meir EG, Brat DJ, Mastrogianakis GM, Olson JJ, Mikkelsen T, Lehman N, Aldape K, Yung WK, Bogler O, Weinstein JN, VandenBerg S, Berger M, Prados M, Muzny D, Morgan M, Scherer S, Sabo A, Nazareth L, Lewis L, Hall O, Zhu Y, Ren Y, Alvi O, Yao J, Hawes A, Jhangiani S, Fowler G, San Lucas A, Kovar C, Cree A, Dinh H, Santibanez J, Joshi V, Gonzalez-Garay ML, Miller CA, Milosavljevic A, Donehower L, Wheeler DA, Gibbs RA, Cibulskis K, Sougnez C, Fennell T, Mahan S, Wilkinson J, Ziaugra L, Onofrio R, Bloom T, Nicol R, Ardlie K, Baldwin J, Gabriel S, Lander ES, Ding L, Fulton RS, McLellan MD, Wallis J, Larson DE, Shi X, Abbott R, Fulton L, Chen K, Koboldt DC, Wendl MC, Meyer R, Tang Y, Lin L, Osborne JR, Dunford-Shore BH, Miner TL, Delehaunty K, Markovic C, Swift G, Courtney W, Pohl C, Abbott S, Hawkins A, Leong S, Haipek C, Schmidt H, Wiechert M, Vickery T, Scott S, Dooling DJ, Chinwalla A, Weinstock GM, Mardis ER, Wilson RK, Getz G, Winckler W, Verhaak RG, Lawrence MS, O'Kelly M, Robinson J, Alexe G, Beroukhim R, Carter S, Chiang D, Gould J, Gupta S, Korn J, Mermel C, Mesirov J, Monti S, Nguyen H, Parkin M, Reich M, Stransky N, Weir BA, Garraway L, Golub T, Meyerson M, Chin L, Protopopov A, Zhang J, Perna I, Aronson S, Sathiamoorthy N, Ren G, Yao J, Wiedemeyer WR, Kim H, Kong SW, Xiao Y, Kohane IS, Seidman J, Park PJ, Kucherlapati R, Laird PW, Cope L, Herman JG, Weisenberger DJ, Pan F, Van den Berg D, Van Neste L, Yi JM, Schuebel KE, Baylin SB, Absher DM, Li JZ, Southwick A, Brady S, Aggarwal A, Chung T, Sherlock G, Brooks JD, Myers RM, Spellman PT, Purdom E, Jakkula LR, Lapuk AV, Marr H, Dorton S, Choi YG, Han J, Ray A, Wang V, Durinck S, Robinson M, Wang NJ, Vranizan K, Peng V, Van Name E, Fontenay GV, Ngai J, Conboy JG, Parvin B, Feiler HS, Speed TP, Gray JW, Brennan C, Socci ND, Olshen A, Taylor BS, Lash A, Schultz N, Reva B, Antipin Y, Stukalov A, Gross B, Cerami E, Wang WQ, Qin LX, Seshan VE, Villafania L, Cavatore M, Borsu L, Viale A, Gerald W, Sander C, Ladanyi M, Perou CM, Hayes DN, Topal MD, Hoadley KA, Qi Y, Balu S, Shi Y, Wu J, Penny R, Bittner M, Shelton T, Lenkiewicz E, Morris S, Beasley D, Sanders S, Kahn A, Sfeir R, Chen J, Nassau D, Feng L, Hickey E, Barker A, Gerhard DS, Vockley J, Compton C, Vaught J, Fielding P, Ferguson ML, Schaefer C, Zhang J, Madhavan S, Buetow KH, Collins F, Good P, Guyer M, Ozenberger B, Peterson J, Thomson E. (2008) Comprehensive genomic characterization defines human glioblastoma genes and core pathways. Nature455(7216): 1061-8.

McNally RS, Davis BK, Clements CM, Accavitti-Loper MA, Mak TW, Ting JP. (2010) DJ-1 enhances cell survival through the binding of cezanne, a negative regulator of NF-{kappa}B. J. Biol. Chem. Epub ahead of print.

Meng F, Henson R, Wehbe-Janek H, Ghoshal K, Jacob ST, Patel T. (2007) MicroRNA-21 regulates expression of the PTEN tumor suppressor gene in human hepatocellular cancer. Gastroenterology 133: 647-658.

Mengesdorf T, Jensen PH, Mies G, Aufenberg C, Paschen W. (2002) Down-regulation of parkin protein in transient focal cerebral ischemia: A link between stroke and degenerative disease? Proc Natl Acad Sci U S A 99:15042-7.

Metzler M, Wilda M, Busch K, et al. (2004) High expression of precursor microRNA-155/BIC RNA in children with Burkitt lymphoma. Genes Chrom. Cancer 39: 167-169.

Migliore L, Coppede F. (2002) Genetic and environmental factors in cancer and neurodegenerative diseases. Mutat Res 512: 135–153.

Millikin D, Meese E, Vogelstein B, Witkowski C, Trent J. (1991) Loss of heterozygosity for loci on the long arm of chromosome 6 in human malignant melanoma. Cancer Res. 51(20): 5449-53.

Mintz A, Gibo DM, Madhankumar AB, Debinski WJ. (2003) Molecular targeting with recombinant cytotoxins of interleukin-13 receptor alpha2-expressing glioma. J Neurooncol. 64(1-2):117-23.

Mira MT, Alcais A, Nguyen VT, Moraes MO, Di Flumeri C, Vu HT, Mai CP, Nguyen TH, Nguyen NB, Pham XK, Sarno EN, Alter A, Montpetit A, Moraes ME, Moraes JR, Dore C, Gallant CJ, Lepage P, Verner A, Van De Vosse E, Hudson TJ, Abel L, Schurr E. (2004) Susceptibility to leprosy is associated with PARK2 and PACRG. Nature 427:636-40.

Moore DJ, West AB, Dikeman DA, Dawson VL, Dawson TM. (2008) Parkin mediates the degradation-independent ubiquitination of Hsp70. J. Neurochem. 105: 1806-1819.

Moore DJ. (2008) The biology and pathobiology of LRRK2: implications for Parkinson's disease. Parkinsonism Relat. Disord. 14 Suppl 2: S92-8.

Morrison RS, Yamaguchi F, Bruner, JM, Tang M., Mckeehan W, Berger MS. (1994) Fibroblast growth factor receptor gene expression and

immunoreactivity are elevated in human glioblastoma multiforme. Cancer Res. 54: 2794-2799.

Mosser DD, Caron AW, Bourget L, Meriin AB, Sherman MY, Morimoto RI, Massie B. (2000) The chaperone function of Hsp70 is required for protection against stress-induced apoptosis. Mol. Cell. Biol. 20: 7146-7159.

Mukhopadhyay D, Riezman H. (2007) Proteasome-independent functions of ubiquitin in endocytosis and signaling. Science 315: 201-205

Mulholland PJ, Fiegler H, Mazzanti C, Gorman P, Sasieni P, Adams J, Jones TA, Babbage JW, Vatcheva R, Ichimura K, East P, Poullikas C, Collins VP, Carter NP, Tomlinson IP, Sheer D. (2006) Genomic profiling identifies discrete deletions associated with translocations in glioblastoma multiforme. Cell Cycle 5:783-91.

Murat, A., Migliavacca, E., Gorlia, T., Lambiv, W.L., Shay, T., Hamou, M.F., de Tribolet, N., Regli, L., Wick, W., Kouwenhoven, M.C., et al. (2008) Stem cell-related "self-renewal" signature and high epidermal growth factor receptor expression associated with resistance to concomitant chemoradiotherapy in glioblastoma. J Clin Oncol 26: 3015-3024.

Murray A, Hunt T. (1993) The Cell Cycle. Oxford University Press, Cambridge, UK.

Nagakubo D, Taira T, Kitaura H, Ikeda M, Tamai K, et al. (1997) DJ-1, a novel oncogene which transforms mouse NIH3T3 cells in cooperation with ras. Biochem Biophys Res Commun 231: 509–513.

Nagy Z. (2000) Cell cycle regulatory failures in neurons: causes and consequences. Neurobiol. Aging 21: 761-769.

Nakada M, Okada Y, Yamashita J. (2003) The role of matrix metalloproteinases in glioma invasion. Front. Biosci. 8: e262-e269.

Nakahara T, Gotoh L, Motomura K, Kawanami N, Ohta E, Hirano M, Uchimura H. (2001) Acute and chronic haloperidol treatments increase parkin mRNA levels in the rat brain. Neurosci. Lett. 306: 93-96.

Nakahara T, Kuroki T, Ohta E, Kajihata T, Yamada H, Yamanaka M, Hashimoto K, Tsutsumi T, Hirano M, Uchimura H. (2003) Effects of the

neurotoxic dose of methamphetamine on gene expression of parkin and Pael-receptors in the rat striatum. Parkinsonism Relat. Disord. 9: 213-219.

Nakayama KI, Nakayama K. Ubiquitin ligases: cell-cycle control and cancer. (2009) Nature Rev. Cancer 6: 369-381.

Nam EJ, Yoon H, Kim SW, Kim H, Kim YT, Kim JH, Kim JW, Kim S. MicroRNA expression profiles in serous ovarian carcinoma. (2008) Clin Cancer Res. 14: 2690–2695.

Narendra DP, Tanaka A, Suen DF, Youle RJ. (2008) Parkin is recruited selectively to impaired mitochondria and promotes their autophagy. J. Cell Biol. 183: 795–803.

Narendra DP, Jin SM, Tanaka A, Suen DF, Gautier CA, Shen J, Cookson MR, Youle RJ. (2010) PINK1 is selectively stabilized on impaired mitochondria to activate Parkin, PLoS Biol. 8. e1000298.

Narita Y, Nagane M, Mishima K, Huang HJ, Furnari FB, Cavenee WK. (2002) Mutant epidermal growth factor receptor signaling down-regulates p27 through activation of the phosphatidylinositol 3-kinase/Akt pathway in glioblastomas. Cancer Res. 62: 6764-6769.

Negrini M, Sabbioni S, Possati L, Rattan S, Corallini A, Barbanti-Brodano G, Croce CM. (1994) Suppression of tumorigenicity of breast cancer cells by microcell-mediated chromosome transfer: studies on chromosomes 6 and 11. Cancer Res 54:1331-6.

Nikiforova MN, Tseng GC, Steward D, Diorio D, Nikiforov YE. MicroRNA expression profiling of thyroid tumors: biological significance and diagnostic utility. J. Clin. Endocrinol. Metab. 93: 1600-1608.

Notaridou M, Quaye L, Dafou D, Jones C, Song H, Høgdall E, Kjaer SK, Christensen L, Høgdall C, Blaakaer J, McGuire V, Wu AH, Van Den Berg DJ, Pike MC, Gentry-Maharaj A, Wozniak E, Sher T, Jacobs IJ, Tyrer J, Schildkraut JM, Moorman PG, Iversen ES, Jakubowska A, Medrek K, Lubiński J, Ness RB, Moysich KB, Lurie G, Wilkens LR, Carney ME, Wang-Gohrke S, Doherty JA, Rossing MA, Beckmann MW, Thiel FC, Ekici AB, Chen X, Beesley J, Gronwald J, Fasching PA, Chang-Claude J, Goodman MT, Chenevix-Trench G, Berchuck A, Pearce CL, Whittemore AS, Menon U, Pharoah PD, Gayther SA, Ramus SJ. (2010) Common alleles in candidate

susceptibility genes associated with risk and development of epithelial ovarian cancer. Int J Cancer. 128(9): 2063-2074.

Nozaki M, Tada M, Kobayashi H, et al. (1999) Roles of the functional loss of p53 and other genes in astrocytoma tumorigenesis and progression. Neuro-Oncology. 1(2): 124-137.

O'Connell RM, Taganov KD, Boldin MP, Cheng G, Baltimore D. (2007) MicroRNA-155 is induced during the macrophage inflammatory response. Proc. Natl. Acad. Sci. U. S. A. 104: 1604–1609.

Olsen JH, Friis S, Frederiksen K, McLaughlin JK, Mellemkjaer L, Moller H. (2005) Atypical cancer pattern in patients with Parkinson's disease. Br J Cancer 92: 201-205.

Olzmann JA, Li L, Chudaev MV, Chen J, Perez FA, Palmiter RD, Chin LS. (2007) Parkin-mediated K63-linked polyubiquitination targets misfolded DJ-1 to aggresomes via binding to HDAC6. J Cell Biol. 178(6): 1025-1038.

Ooi, C.H., Ivanova, T., Wu, J., Lee, M., Tan, I.B., Tao, J., Ward, L., Koo, J.H., Gopalakrishnan, V., Zhu, Y., et al. (2009) Oncogenic pathway combinations predict clinical prognosis in gastric cancer. *PLoS Genet* 5:e1000676.

Ovcharenko D, Kelnar K, Johnson C, Leng N, Brown D. Genome-scale microRNA and small-interfering RNA screens identify small RNA modulators of TRAIL-induced apoptosis pathway. Cancer Res. 67: 10782-10788.

Pandey P, Saleh A, Nakazawa A, Kumar S, Srinivasula SM, Kumar V, Weichselbaum R, Nalin C, Alnemri ES, Kufe D, Kharbanda S. (2000) Negative regulation of cytochrome c-mediated oligomerization of Apaf-1 and activation of procaspase-9 by heat shock protein 90. EMBO J. 19: 4310-4322.

Papagiannakopoulos T, Shapiro A, Kosik KS. (2008) MicroRNA-21 targets a network of key tumor-suppressive pathways in glioblastoma cells. Cancer Res 68: 8164-8172.

Periquet M, Corti O, Jacquier S, Brice A. (2005) Proteomic analysis of parkin knockout mice: alterations in energy metabolism, protein handling and synaptic function. J Neurochem. 95: 1259–1276.

Picchio M.C., Martin E.S., Cesari R. (2004) Alterations of the tumor suppressor gene Parkin in non-small cell lung cancer. Clin. Cancer Res. 10(8): 2720-2724.

Pickard BS, Malloy MP, Clark L, Lehellard S, Ewald HL, Mors O, Porteous DJ, Blackwood DH, Muir WJ. (2005) Candidate psychiatric illness genes identified in patients with pericentric inversions of chromosome 18. Psychiatr Genet. 15(1):37-44

Pickart CM. Ubiquitin in chains. (2000) Trends Biochem Sci 25:544-8.

Plun-Favreau H, Lewis PA, Hardy J, Martins LM, Wood NW. (2010) Cancer and neurodegeneration: between the devil and the deep blue sea. PLoS Genet. 6(12): e1001257.

Poulogiannis G, Mcintyre RE, Dimitriadi M, Apps JR, Wilson CH, Ichimura K, Luo F, Cantley LC, Wyllie AH, Adams DJ, Arends MJ. (2010) *PARK2* deletions occur frequently in sporadic colorectal cancer and accelerate adenoma development in *Apc* mutant mice. Proc Natl Acad Sci U S A. 107(34):15145-50.

Prinjha, RK, Shapland CE, Hsuan, JJ, Totty NF, Mason IJ, Lawson D. (1994) Cloning and sequencing of cDNAs encoding the actin cross-linking protein transgelin defines a new family of actin-associated proteins, Cell Motility and the Cytoskeleton. 28, 243-255.

Rabenhorst U, Beinoraviciute-Kellner R, Brezniceanu ML, Joos S, Devens F, Lichter P, Rieker RJ, Trojan J, Chung HJ, Levens DL, Zörnig M. (2005) Overexpression of the far upstream element binding protein 1 in hepatocellular carcinoma is required for tumor growth. Hepatology 50(4): 1121-1129.

Ravagnan L, Gurbuxani S, Susin SA, Maisse C, Daugas E, Zamzami N, Mak T, Jaattela M, Penninger JM, Garrido C, Kroemer G. (2001) Heat-shock protein 70 antagonizes apoptosis-inducing factor. Nat. Cell Biol. 3: 839-843.

Reifenberger G, Reifenberger J, Ichimura K, Meltzer PS, Collins VP. (1994) Amplification of multiple genes from chromosomal region 12q13-14 in human

malignant gliomas: Preliminary mapping of the amplicons shows preferential involved of CDK4, SAS and MDM2. Cancer Res. 54: 4299-4303.

Ren Y, Zhao J, Feng J. (2003) Parkin binds to alpha/beta tubulin and increases their ubiquitination and degradation. J. Neurosci. 23(8): 3316-3324.

Ren Y, Jiang H, Yang F, Nakaso K, Feng J. (2009) Parkin protects dopaminergic neurons against microtubule-depolymerizing toxins by attenuating microtubule-associated protein kinase activation. J. Biol. Chem. 284(6): 4009-4017.

Rich JN, Reardon DA, Peery T, Dowell JM, Quinn JA, Penne KL, Wikstrand CJ, Van Duyn LB, Dancey JE, McLendon RE, Kao JC, Stenzel TT, Ahmed Rasheed BK, Tourt-Uhlig SE, Herndon JE 2nd, Vredenburgh JJ, Sampson JH, Friedman AH, Bigner DD, Friedman HS. (2004) Phase II trial of gefitinib in recurrent glioblastoma. J Clin Oncol 22: 133-142.

Sakata E, Yamaguchi Y, Kurimoto E, Kikuchi J, Yokoyama S, Yamada S, Kawahara H, Yokosawa H, Hattori N, Mizuno Y, Tanaka K, Kato K. (2003) Parkin binds the Rpn10 subunit of 26S proteasomes through its ubiquitin-like domain. EMBO Rep. 4: 301-306.

Sathornsumetee S, Hjelmeland AB, Keir ST, et al. (2006) AAL881, a novel small molecule inhibitor of RAF and vascular endothelial growth factor receptor activities, blocks the growth of malignant glioma. Cancer Res 66: 8722–8730.

Sato S, Fujita N, Tsuruo T. (2000) Modulation of Akt kinase activity by binding to Hsp90. Proc. Natl. Acad. Sci. USA 97: 10832-10837.

Sarbassov DD, Ali SM, Sabatini DM. (2005) Growing roles for the mTOR pathway. Curr. Opin. Cell Biol. 17: 596-603.

Saunders-Pullman R, Barrett MJ, Stanley KM, Luciano MS, Shanker V, Severt L, Hunt A, Raymond D, Ozelius LJ, Bressman SB. (2010) LRRK2 G2019S mutations are associated with an increased cancer risk in Parkinson disease. Mov Disord. 25(15): 2536-2541.

Serrano M, Hannon GJ, Beach D. (1993) A new regulatory motif in cell-cycle control causing specific inhibition of cyclin D/CDK4. Nature 366: 704-707.

Schlaepfer DD, Broome MA, Hunter T. (1997) Fibronectin-stimulated signaling from a focal adhesion kinase-c-Src complex: Involved of Grb2, p130Cas, and Nck adaptor proteins. Mol. Cell. Biol. 17: 1702-1713.

Shen WH, Balajee AS, Wang J, Wu H, Eng C, Pandolfi PP, Yin Y. (2007) Essential role for nuclear PTEN in maintaining chromosomal integrity. Cell 128: 157-170.

Sherr CJ, McCormick F. (2002) The RB and p53 pathways in cancer. Cancer Cell 2: 103-112.

Shih AH, Dai C, Hu X, Rosenblum MK, Koutcher JA, Holland EC. (2004) Dose-dependent effects of platelet-derived growth-B on glial tumorigenesis. Cancer Res. 64: 4783-4789.

Shimura H, Hattori N, Kubo S, Mizuno Y, Asakawa S, Minoshima S, Shimuzu N, Iwai K, Chiba T, Tanaka K. et al. (2000) Familial parkinson disease gene product, parkin, is a ubiquitin-protein ligase. Nat. Genet. 25: 302–305.

Shimura H, Schlossmacher MG, Hattori N, Frosch MP, Trockenbacher A, Schneider R, Mizuno Y, Kosik KS, Selkoe DJ. (2001) Ubiquitination of a new form of alpha-synuclein by parkin from human brain: implications for Parkinson's disease. Science 293: 263-269.

Shinkaruk S, Bayle M, Lain G, Deleris G. (2003) Vascular endothelial cell growth factor (VEGF), an emerging target for cancer chemotherapy. Curr. Med. Chem.-Anti-Cancer Agents. 3: 95-117.

Shiota M, Kusakabe H, Izumi Y, Hikita Y, Nakao T, Funae Y, Katsuyuki M, Iwao H. (2010) Heat Shock Cognate Protein 70 is essential for Akt signalling in endothelial function. Arterioscler. Thromb. Vasc. Biol. 30: 491-497.

Smith WW, Pei Z, Jiang H, Moore DJ, Liang Y, West AB, Dawson VL, Dawson TM, Ross CA. (2005). Leucine-rich repeat kinase 2 (LRRK2) interacts with parkin, and mutant LRRK2 induces neuronal degeneration. Proc. Natl. Acad. Sci. U.S.A. 102(51): 18676–18681.

Smith DI, Zhu Y, McAvoy S, Kuhn R. (2006) Common fragile sites, extremely large genes, neural development and cancer. Cancer Lett 232:48-57.

Sriram SR, Li X, Ko HS, Chung KK, Wong E, Lim KL Dawson VL, Dawson TM. (2005) Familial-associated mutations differentially disrupt the solubility, localization, binding and ubiquitination properties of parkin. Hum. Mol. Genet. 14: 2571-2586.

Srivastava S, Zou ZQ, Pirollo K, Blattner W, Chang EH. (1990) Germ-line transmission of a mutated p53 gene in a cancer-prone family with Li-Fraumeni syndrome. Nature. 348: 747-749.

Staropoli JF, McDermott C, Martinat C, Schulman B, Demireva E, Abeliovich A. (2003) Parkin is a component of an SCF-like ubiquitin ligase complex and protects postmitotic neurons from kainate excitotoxicity. Neuron 37:735-49.

Stommel JM, Kimmelman AC, Ying H, Nabioullin R, Ponugoti AH, Wiedemeyer R, Stegh AH, Bradner JE, Ligon KL, Brennan C, Chin L, DePinho RA. (2007) Coactivation of receptor tyrosine kinases affects the response of the tumor cells to target therapies. Science 318: 287-290.

Stummer W, Pichlmeier U, Meinel T, Wiestler OD, Zanella F, Reulen HJ. (2006) Fluorescence-guided surgery with 5-aminolevulinic acid for resection of malignant glioma: a randomised controlled multicenter phase III trial. Lancet Oncol 7: 392-401.

Stupp R, Mason WP, van den Bent MJ, Weller M, Fisher B, Taphoorn MJ, Belanger K, Brandes AA, Marosi C, Bogdahn U, Curschmann J, Janzer RC, Ludwin SK, Gorlia T, Allgeier A, Lacombe D, Cairncross JG, Eisenhauer E, Mirimanoff RO. (2005) Radiotherapy plus concomitant and adjuvant temozolomide for glioblastoma. N Engl J Med 352: 987-996.

Tan JM, Wong ES, Dawson VL, Dawson TM, Lim KL. (2007) Lysine 63-linked polyubiquitin potentially partners with p62 to promote the clearance of protein inclusions by autophagy. Autophagy 4: 251-253.

Tan JM, Wong ES, Kirkpatrick DS, Pletnikova O, Ko HS, Tay SP, Ho MW, Troncoso J, Gygi SP, Lee MK, Dawson VL, Dawson TM, Lim KL. (2008) Lysine 63-linked ubiquitination promotes the formation and autophagic

clearance of protein inclusions associated with neurodegenerative diseases. Hum Mol Genet. 17(3): 431-439.

Tay SP, Yeo CWS, Chai C, Chua PJ, Tan HM, Ang AXY, Yip DLH, Sung JX, Tan PH, Bay BH, Wong SH, Tang C, Tan JMM, Lim KL. (2010) Parkin enhances the expression of cyclin-dependent kinase 6 and negatively regulates the proliferation of breast cancer cells. J. Biol. Chem. 285(38): 29231-29238.

Tetzlaff MT, Liu A, Xu X, Master SR, Baldwin DA, Tobias JW, Livolsi VA, Baloch ZW. (2007) Differential expression of miRNAs in papillary thyroid carcinoma compared to multinodular goiter using formalin fixed paraffin embedded tissues. Endocr Pathol. 18: 163–173.

Tran N, McLean T, Zhang X, Zhao CJ, Thomson JM, O'Brien C, Rose B. (2007) MicroRNA expression profiles in head and neck cancer cell lines. Biochem Biophys Res Commun. 358: 12–17.

Trent JM, Stanbridge EJ, McBride HL, Meese EU, Casey G, Araujo DE, Witkowski CM, Nagle RB. (1990) Tumorigenicity in human melanoma cell lines controlled by introduction of human chromosome 6. Science 247:568-71.

Tsai YC, Fishman PS, Thakor NV, Oyler GA. (2003) Parkin facilitates the elimination of expanded polyglutamine proteins and leads to preservation of proteasome function. J. Biol. Chem. 278: 22044-22055.

Um JW, Chung KC. (2006) Functional modulation of parkin through physical interaction with SUMO-1. J. Neurosci. Res. 84: 1543-1554.

Vanacore N, Spila-Alegiani S, Raschetti R, Meco G. (1999) Mortality cancer risk in parkinsonian patients: a population-based study. Neurology 52: 395-398.

Veeriah S, Taylor BS, Meng S, Fang F, Yilmaz E, Vivanco I, Janakiraman M, Schultz N, Hanrahan AJ, Pao W, Ladanyi M, Sander C, Heguy A, Holland EC, Paty PB, Mischel PS, Liau L, Cloughesy TF, Mellinghoff IK, Solit DB, Chan TA. (2010) Somatic mutations of the Parkinson's disease-associated gene PARK2 in glioblastoma and other human malignancies. Nat. Genet. 42(1): 77-82.

Verhaak, R.G., Hoadley, K.A., Purdom, E., Wang, V., Qi, Y., Wilkerson, M.D., Miller, C.R., Ding, L., Golub, T., Mesirov, J.P., et al. (2010) Integrated

genomic analysis identifies clinically relevant subtypes of glioblastoma characterized by abnormalities in PDGFRA, IDH1, EGFR, and NF1. Cancer Cell 17:98-110.

Vivanco I, Sawyers CL. (2002) The phosphatidylinositol 3-Kinase Akt pathway in human cancer. Nat Rev Cancer 2: 489-501.

Vives-Bauza C, Zhou C, Huang Y, Cui M, de Vries RL, Kim J, May J, Tocilescu MA, Liu W, Ko HS, Magrane J, Moore DJ, Dawson VL, Grailhe R, Dawson TM, Li C, Tieu K, Przedborski S. (2010) PINK1-dependent recruitment of Parkin to mitochondria in mitophagy, Proc. Natl Acad. Sci. USA 107: 378–383.

Volinia S, Calin GA, Liu CG, Ambs S, Cimmino A, Petrocca F, Visone R, Iorio M, Roldo C, Ferracin M, Prueitt RL, Yanaihara N, Lanza G, Scarpa A, Vecchione A, Negrini M, Harris CC, Croce CM. (2006) A microRNA expression signature of human solid tumors defines cancer gene targets. Proc. Natl. Acad. Sci. USA 103: 2257-2261.

Vousden KH, Lu X. (2002) Live or let die: The cell's response to p53. Nat. Rev. Cancer. 2: 594-604.

Vousden KH, Prives C. (2009) Blinded by the light: the growing complexity of p53. Cell. 137(3): 413-431.

Wang C, Tan JM, Ho MW, Zaiden N, Wong SH, Chew CL, Eng PW, Lim TM, Dawson TM, Lim KL. Alterations in the solubility and intracellular localization of parkin by several familial Parkinson's disease-linked point mutations. J. Neurochem. 93: 422-431.

Wang F, Denison S, Lai JP. (2004) Parkin gene alterations in hepatocellular carcinoma. Genes Chromo. Cancer. 40(2): 85-96.

Wang H, Zhang W, Huang HJ, Liao WS, Fuller GN. (2004) Analysis of the activation status of Akt, NFκB, and Stat3 in human diffuse gliomas. Lab. Invest. 84: 941-951.

Wen PY, Yung WK, Lamborn KR, Dahia PL, Wang Y, Peng B, Abrey LE, Raizer J, Cloughesy TF, Fink K, Gilbert M, Chang S, Junck L, Schiff D, Lieberman F, Fine HA, Mehta M, Robins HI, DeAngelis LM, Groves MD, Puduvalli VK, Levin V, Conrad C, Maher EA, Aldape K, Hayes M, Letvak L, Egorin MJ, Capdeville R, Kaplan R, Murgo AJ, Stiles C, Prados MD. (2006)

Phase I/II study of imatinib mesylate for recurrent malignant gliomas: North American Brain Tumor Consortium Study 99-08. Clin Cancer Res 12: 4899-4907.

Wen PY, Schiff D, Kesari S, Drappatz J, Gigas D, Doherty L. (2006) Medical management of patients with brain tumors. J Neurooncol 80: 313-332.

Wen PY, Kesari S. (2008) Malignant gliomas in adults. N Engl J Med. 359(5): 492-507.

West AB, Maidment NT. (2004) Genetics of Parkin-linked disease. Hum Genet. 114(4): 327-336.

West AB, Kapatos G, O'Farrell C, Gonzalez-de-Chavez F, Chiu K, Farrer MJ, Maidment NT. (2004b) N-myc regulates parkin expression. J. Biol. Chem. 279(28): 28896-28902.

West, A.B., Dawson, V.L., and Dawson, T.M. (2005) To die or grow: Parkinson's disease and cancer. Trends Neurosci 28:348-352

West AB, Dawson VL, Dawson TM. (2007) The role of parkin in Parkinson's disease. Parkinson's disease: genetics and pathogenesis. New York: Informa Healthcare USA, Inc.; p199–218.

Westphal M, Hilt DC, Bortey E, Delavault P, Olivares R, Warnke PC, Whittle IR, Jääskeläinen J, Ram Z. (2003) A phase 3 trial of local chemotherapy with biodegradable carmustine (BCNU) wafers (Gliadel wafers) in patients with primary malignant glioma. Neuro Oncol 5: 79-88.

Willmarth NE, Albertson DG, Ethier SP. (2004) Chromosomal instability and lack of cyclin E regulation in hCdc4 mutant human breast cancer cells. Breast Cancer Res 6:R531-9.

Wong HR, Menendez IY, Ryan MA, Denenberg AG, Wispe JR. (1998) Increased expression of heat shock protein-70 protects A549 cells against hypoxia. Am. J. Physiol. 275: L836-L841.

Wong AJ, Ruppert JM, Bigner SH, Grzeschik CH, Humphrey PA, Bigner DS, Vogelstein B. (1992) Structural alterations of the epidermal growth factor receptor gene in human gliomas. Proc. Natl. Acad. Sci. 89: 2965-2969.

Wu M, Xu LG, Li X, Zhai Z, Shu HB. (2002) AMID, an apoptosis-inducing factor-homologous mitochondrion-associated protein, induces caspase-independent apoptosis. J Biol Chem. 277(28):25617-23.

Xiao A, Yin C, Yang C, Di Cristofano A, Pandolfi PP, Van Dyke T. (2005) Somatic induction of Pten loss in a preclinical astrocytoma model reveals major roles in disease progression and avenues for target discovery and validation. Cancer Res. 65: 5172-5180.

Yamaguchi F, Saya H, Bruner JM, Morrison RS. (1994) Differential expression of two fibroblast growth factor-receptor genes is associated with malignant progression in human astrocytomas. Proc. Natl. Acad. Sci. USA 91: 484-488.

Yan, X., Ma, L., Yi, D., Yoon, J.G., Diercks, A., Foltz, G., Price, N.D., Hood, L.E., and Tian, Q. (2011) A CD133-related gene expression signature identifies an aggressive glioblastoma subtype with excessive mutations. Proc Natl Acad Sci U S A 108: 1591-1596.

Yanaihara N, Caplen N, Bowman E, et al. (2006) Unique microRNA molecular profiles in lung cancer diagnosis and prognosis. Cancer Cell 9: 189-198.

Yang F, Jiang Q, Zhao J, Ren Y, Sutton MD, Feng J. (2005) Parkin stabilizes microtubules through strong binding mediated by three independent domains. J. Biol. Chem. 284(6): 17154-17162.

Yang Y, Nishimura I, Imai Y, Takahashi R, Lu B. (2003) Parkin suppresses dopaminergic neuron-selective neurotoxicity induced by Pael-R in Drosophila. Neuron 37: 911–924.

Yokota T, Sugawara K, Ito K, Takahashi R, Ariga H, Mizusawa H. (2003) Down regulation of DJ-1 enhances cell death by oxidative stress, ER stress, and proteasome inhibition. Biochem. Biophys. Res. Commun. 312:1342-8.

Young GS. (2007) Advanced MRI of adult brain tumors. Neurol. Clin. 25: 947-973.

Zhang B, Pan X, Cobb GP, Anderson TA. (2007) MicroRNA as oncogenes and tumor suppressors. Dev. Biol. 302, 1-12.

Zhang Y, Gao J, Chung KK, Huang H, Dawson VL, Dawson TM. (2000) Parkin functions as an E2-dependent ubiquitin protein ligase and promotes the degradation of the synaptic vesicle-associated protein, CDCrel-1. Proc. Natl. Acad. Sci. USA 97:13354-13359.

Zhang Y, Zhang N, Dai B, Liu M, Sawaya R, Xie K Huang S. (2008) FoxM1B transcriptionally regulates vascular endothelial growth factor expression and promotes the angiogenesis and growth of glioma cells. Cancer Res 68: 8733–8742.

Zhu S, Wu H, Wu F, Nie D, Sheng S, Mo YY. MicroRNA-21 targets tumor suppressor genes in invasion and metastasis. Cell Res. 18:350-359.

PUBLICATIONS

1. Yeo WS. Ng SL, Chai C, Koh G, Ang BT, Takahashi R, Tang C, Lim KL et al. (2011) Parkin pathway activation mitigates glioma cell proliferation and predicts patient survival. Cancer Res. May 2012.

2. Tay, S.P., Lim, G.G., Yeo, W.S., Lim, K.L. (2011) Parkin and Parkinson's disease In "Parkinson's disease." Ed. Abdul Q. Rana *InTech Publisher*

3. Tay SP, Calvin WS Yeo, Chai C, Chua PJ, Tan HM, Ang AXY, Yip DLH, Sung JX, Tan PH, Bay BH, Wong SH, Tang C, Tan JMM, Lim KL. (2010) Parkin enhances the expression of cyclin-dependent kinase 6 and negatively regulates the proliferation of breast cancer cells. J. Biol. Chem. 285(38): 29231-29238.